HELSINKI UNIVERSITY OF TECHNOLOGY
Department of Electrical and Communications Engineering

MEASUREMENTS FOR MODELLING OF WIDEBAND NONLINEAR POWER AMPLIFIERS FOR WIRELESS COMMUNICATIONS

Gilda Gabriela Gámez González

Master's Thesis that has been submitted for official examination for the degree of Master of Science in Espoo, Finland on September 27th, 2004.

Supervisor Professor Timo Laakso

Instructor M.Sc. Viktor Nässi

Author:	Gilda Gabriela Gámez González
Title of the Thesis:	Measurements for modelling of wideband nonlinear power amplifiers for wireless communications
Date:	September 27th, 2004 **Pages:** 117
Department:	Department of Electrical and Communications Engineering
Professorship:	Signal Processing
Supervisor:	Professor Timo Laakso
Instructor:	Viktor Nässi

Power amplifier linearity is an important topic in today's communication systems, especially in wireless communications where amplifier distortion affects transmissions not only in the used channel but in adjacent ones. Generally, a power amplifier is more efficient when it is operated at high power levels. However, this results in distortion of the output signal. Therefore, highly linear power amplifiers are required for efficient wireless communications.

The objective of this thesis is to provide the basis for performing accurate measurements of power amplifiers in order to obtain enough reliable data helpful to model their nonlinearity. The objective was achieved by performing practical measurements with different types of signals from which diverse modelling parameters were obtained. Single- and two-tone signals were used to test the amplifier. In addition, a multisine signal, example of high peak-to-average ratio signal, was chosen to perform multi-tone signal measurements.

It was demonstrated how the frequency-dependent and frequency-independent behavior of the amplifier can be accurately modelled based on the single-tone signal measurements performed in this thesis. Furthermore, the exactness of the measurements was analyzed and it was determined that highly accurate measurements are a complicated process that involves numerous factors. Moreover, it was shown that amplifier measurements have a very wide usability. Mainly, the contribution of this thesis is represented by a full set of measurement results that can be used for future modelling of amplifiers.

Keywords: Amplifier, nonlinearity, measurement, network analyzer, spectrum analyzer, modelling parameter, two-tone signal, multisine signal.

Tekijä:	Gilda Gabriela Gámez González		
Työn nimi:	Laajakaistaisten epälineaaristen tehovahvistimien mittaaminen matkaviestinjärjestelmissä mallintamista varten		
Päivämäärä:	27. syyskuuta 2004	**Sivumäärä:**	117
Osasto:	Sähkö- ja tietoliikennetekniikan osasto		
Professuuri:	Signaalinkäsittelytekniikka		
Työn valvoja:	Professori Timo Laakso		
Työn ohjaaja:	Viktor Nässi		

Tehovahvistimen lineaarisuus on tärkeä aihe nykyajan tietoliikennejärjestelmissä. Erityisen tärkeää se on matkaviestinjärjestelmissä, joissa vahvistimen epälineaarisuus vaikuttaa tiedonsiirtoon lähetyskanavan lisäksi myös viereisissä kanavissa. Yleisesti tehovahvistimen hyötysuhde on parempi, kun sitä käytetään korkealla teholla. Tämä kuitenkin aiheuttaa vääristymää lähtösignaaliin.

Tämän diplomityön tavoitteena on luoda perusta tarkkojen tehovahvistinmittausten suorittamiseen, joita voidaan käyttää tehovahvistimien mallintamiseen. Tavoite saavutettiin suorittamalla mittauksia erityyppisillä signaaleilla, joista saatiin erilaisia mallinnusparametreja. Yksi- ja kaksitaajuussignaaleja käytettiin vahvistimien testaamiseen. Lisäksi monitaajuusmittauksissa käytettiin monisinisignaalia, joka on esimerkki signaalista jolla on korkea huippu- ja keskiarvotehon suhde.

Työssä osoitettiin, kuinka vahvistimen taajuusriippuva ja taajuusriippumaton käyttäytyminen voidaan tarkasti mallintaa suoritettujen mittausten avulla. Mittausten tarkkuus analysoitiin ja sen pohjalta todettiin, että erittäin tarkkojen mittausten tekeminen on monimutkainen prosessi, johon lukuisat tekijät vaikuttavat. Lisäksi osoitettiin että vahvistinmittauksilla on erittäin laaja käytettävyys. Työn tulokset on esitetty täydellisten mittaustulosten muodossa, joita voidaan jatkossa käyttää vahvistimien mallintamiseen.

Avainsanat: Vahvistin, epälineaarisuus, mittaus, piirianalysaattori, spektrianalysaattori, mallinnusparametri, kaksiäänisignaali, monisinisignaali.

Autor:	Gilda Gabriela Gámez González
Título de la Tesis:	Mediciones para el modelado de amplificadores de potencia no lineales de banda ancha para comunicaciones inalámbricas
Fecha:	27 de septiembre de 2004 **Páginas:** 117
Departamento:	Departamento de Ingeniería Eléctrica y Comunicaciones
Profesorado:	Procesamiento de Señales
Supervisor:	Profesor Timo Laakso
Instructor:	Viktor Nässi

La linealidad de amplificadores de potencia es muy importante en los sistemas de comunicación actuales, especialmente en comunicaciones inalámbricas donde la distorsión de los amplificadores afecta las transmisiones tanto en el canal en uso como en canales adyacentes. En general, un amplificador es más eficiente cuando es operado a altos niveles de potencia. No obstante, esto produce distorsión en la señal de salida. Por lo tanto, amplificadores de potencia altamente lineales son requeridos para comunicaciones inalámbricas eficientes.

El objetivo de esta tesis es proporcionar las bases para realizar medidas precisas de amplificadores de potencia que den como resultado información útil para su modelado. Este objetivo fue alcanzado mediante mediciones utilizando diferentes tipos de señales de las cuales se obtuvieron diversos parámetros. Señales de uno y dos tonos fueron usadas para probar el amplificador. Asimismo, una señal multi-seno, ejemplo de señales con alta relación pico a promedio, fue seleccionada para realizar mediciones de señales multi-tono.

Fue demostrado cómo el comportamiento dependiente e independiente de frecuencia del amplificador puede ser correctamente modelado en base a las mediciones de señal de un tono realizadas en esta tesis. Asimismo, se analizó la exactitud de los resultados y se determinó que las mediciones de alta precisión son procesos complicados que involucran numerosos factores y que las mediciones de amplificadores tienen un amplio campo de aplicación. La aportación principal de esta tesis es la serie de resultados obtenidos que pueden ser utilizados para modelar amplificadores de potencia.

Palabras clave: Amplificador, no-linearidad, medición, analizador de red, analizador de espectro, dato para modelado, señal de dos tonos, señal multi-seno.

Acknowledgement

To my grandfather, Rafael, for his million advices. To my mother, Gilda, (no words to express my love and gratitude). To my father, Jorge, for his continuous support. To Ina for make me feel that there are people missing and loving me back in my country. To the González-Martínez and González-Moreno families. And, over all, deeply to my late grandmother, Eve$^{(\dagger)}$, who educated and made of all of us a honest and united family.

To my academic father, Prof. Timo Laakso, for supervising and guiding my thesis and to my technical instructor, Viktor Nässi, for his always willing and useful help. To Prof. Pertti Vainikainen and Prof. Sven-Gustav Häggman for facilitating the cooperation with the Communications and Radio Communications Laboratories and to Viktor Sibakov, Rauno Kytönen, Jarmo Kivinen and Viatcheslav "Slava" Golikov for their advice in the practical part of the thesis.

To Peter Jantunen, because of his patience, personal support and for checking my whole thesis. To Mei Yen Cheong, for her friendship, advice and support on my working time, to Edgar Ramos for being my friend and helping me with the spanish translations and to Stefan Werner for his comments on this research.

To the planning officer Anita Bisi for listening patiently all my concerns during my master's studies. To the nice secretaries Anne, Mirja and Marja, for always assisting me with a smile.

To Katri, Niko, Heikki and their families, for making my time in Finland nice, comfortable and for teaching me to understand Finnish people's behavior. To my friends in Finland Enrique, Carmen and Karina for giving me a sense of family in this country. To Nadia for her friendship and continuous advices on my personal life. To all my Mexican and foreign friends who give color to my life and to my working mates for making the long (and short) working days easy-going.

THANK YOU.

Agradecimientos

A mi abuelito, Rafael, por sus millones de consejos. A mi mamá, Gilda, (no hay palabras para expresar mi cariño y gratitud). A a mi papá, Jorge, por su apoyo de siempre. A Ina por hacerme sentir que hay personas que me extrañan y quieren en mi país. A las familias González-Martínez y González-Moreno. Y, sobre todo, profundamente a mi abuelita Eve$^{(\dagger)}$, quien nos educó e hizo de todos nosotros una familia honesta y unida.

A mi padre académico, Prof. Timo Laakso, por supervisar y guiar mi tesis y a mi instructor técnico, Viktor Nässi, por su siempre dispuesta y útil ayuda. A los profesores Pertti Vainikainen y Sven-Gustav Häggman por facilitar la cooperación con los laboratorios de Comunicaciones y Radio Comunicaciones y a Viktor Sibakov, Rauno Kytönen, Jarmo Kivinen y Viatcheslav "Slava" Golikov por sus consejos en la parte práctica de esta tesis.

A Peter Jantunen, por su paciencia, apoyo personal y por revisar mi trabajo durante todo el proceso. A Mei Yen Cheong, por su amistad, consejos y apoyo en mi tiempo de trabajo, a Edgar Ramos por ser mi amigo y ayudarme con las traducciones a español y a Stefan Werner por sus comentarios en esta investigación.

A la coordinadora Anita Bisi, por escuchar pacientemente todas mis preocupaciones durante mis estudios de maestría. A las simpáticas secretarias Anne, Mirja y Marja por siempre ayudarme con una sonrisa.

A Katri, Niko, Heikki y sus familias, por hacer mi tiempo en Finlandia agradable, cómodo y por enseñarme a entender el comportamiento de la gente finlandesa. A mis amigos en Finlandia: Enrique, Carmen y Karina por darme el sentimiento de una familia en este país. A Nadia, por su amistad y continuos consejos en mi vida personal. A todos mis amigos mexicanos y extranjeros que dan color a mi vida y a mis colegas por hacer llevaderos los largos (y cortos) días de trabajo.

GRACIAS.

Contents

Appendices

List of Acronyms

μs	microsecond
3G	Third-generation (cell-phone technology)
AC	Alternating Current
ACPR	Adjacent Channel Power Ratio
AM-AM	Amplitude Modulation to Amplitude Modulation
AM-PM	Amplitude Modulation to Phase Modulation
APC	Amphenol Precision Connector
APC-2.4	2.4 mm Amphenol Precision Connector
APC-3.5	3.5 mm Amphenol Precision Connector
Att.	Attenuation
AWG	Arbitrary Waveform Generator
BW	Bandwidth
C	Celsius / Centigrade
CIR	Carrier-to-Interference Ratio
cm.	centimeter
CNR	Carrier-to-Noise Ratio
CP	Compression Point
DANL	Displayed Average Noise Level
dB	decibel
dBc	decibel (referenced to the carrier power)
dBm	decibel (referenced to one milliwatt)
DC	Direct Current
deg	degree
DUT	Device Under Test
e.g.	exempli gratia (Latin: for example)
EER	Envelope Elimination and Restoration
EIKA	Extended Interaction Klystron Amplifier

etc.	et cetera (Latin: and so forth)
et al.	et alii / et alia (Latin: and others)
FDM	Frequency Division Multiplexing
FET	Field Effect Transistor
FIR	Finite Impulse Response
GaN	Gallium Arsenide
GHz	Giga Hertz
HMM	Harmonic Mixing Mode
Hz	Hertz
i.e.	id est (Latin: that is)
I/Q	In-phase / Quadrature
IBO	Back-off referred to input level
IF	Intermediate Frequency
IFFT	Inverse Fast Fourier Transform
IM	Intermodulation
IMD	Intermodulation Distortion
IMP	Intermodulation Product
IMP3	Third Intermodulation Product
in.	inch
IP	Intercept Point
J	Joule
K	Kelvin
kHz	kilohertz
kW	kilowatt
LINC	Linear Amplification using Nonlinear Components
LSE	Least Squares Estimator
max.	maximum
MHz	MegaHertz
MIMR	Multi-tone Intermodulation Ratio
MS	MegaSample
MSK	Minimum Shift Keying
mW	milliwatt
mV	millivolt
NLWM	Nonlinearity With Memory
NPR	Noise Power Ratio

ns	nanosecond
NWA	Network Analyzer
OBO	Back-off referred to output level
OFDM	Orthogonal Frequency Division Multiplexing
PA	Power Amplifier
PAR	Peak-to-Average Ratio
PDF	Probability Density Function
PHEMT	Pseudomorphic High Electron Mobility Transistor
ppm	parts per million
PSK	Phase Shift Keying
PWM	Pulse-Width Modulation
QAM	Quadrature Amplitude Modulation
QBL	Quasi-band-limited Pulses
QPSK	Quaternary Phase Shift Keying
RF	Radio Frequency
rms	root-mean-square
SA	Spectrum Analyzer
sec.	second
SG	Signal Generator
SMA	Sub-Miniature A
SNR	Signal-to-Noise Ratio
S-parameter	Scattering parameter
SR	Sampling Rate
SSPA	Solid State Power Amplifier
SWR	Standing Wave Ratio
T	Temperature
THRU	Through (from Through Response Calibration)
TRW	Travelling Wave Resonator
TWT	Travelling Wave Tube
TWTA	Travelling Wave Tube Amplifier
W	Watt
V	Volt
VSG	Vector Signal Generator
WLSE	Weighted Least Squares Estimator
ZMNL	Zero-Memory Nonlinearity

List of Symbols

α	Complex constant
η	Power efficiency
ξ	Unknown parameter
π	Pi (≈ 3.1416)
τ	Time delay
τ_s	Operating noise figure / Noise sensitivity
ϕ	Phase shift
ω_C	Angular frequency of the carrier signal
ω_M	Angular frequency of the modulating signal
ω	Angular frequency
Φ	Phase
Ω	Ohm
$^\circ$	Degree
1 dB CP	One dB Compression Point
$2Tone_{max.sep.}$	Two tones maximum separation
A	Amplitude
A_M	Amplitude of the modulating signal
B	Bandwidth of a system
C_{ID}	Difference between the CIR and the intrinsic CNR
CNR_I	CNR caused by the system noise
$CNR_{N\&IMD}$	CNR including noise and IMD effects
$d[R]$	R-data point
$\mathbf{D}$	R-points data set
f	Frequency
f	Fundamental frequency
F	Noise factor
f_0	Center frequency

f_b	Basic frequency
f_c	Carrier frequency
f_{IMP}	Frequency of the intermodulation product
fm	Frequency of a baseband signal
f_{off}	Offset frequency
g	A function
IN	Input
IP2	Second order Intercept Point
IP3	Third order Intercept Point
k	Constant factor
K	Power gain
K_ϕ	Phase shift constant
m	Positive integer (excluding zero)
$M(t)$	Modulating signal
$M_s(t)$	Multisine signal
$MaxIMP$	Maximum Intermodulation Product
n	Positive integer (excluding zero)
N	Order of the nonlinearity
N_f	Noise figure
OBO_{1dBCP}	Back-off referred to output level and 1 dB CP
OBO_{sat}	Back-off referred output level and saturation level
OUT	Output
$p(\xi)$	Prior PDF (summarizing ξ knowledge before any data is observed)
$p(\mathbf{D} \mid \xi)$	Conditional PDF (summarizing a priori knowledge of $\mathbf{D}$ conditioned on knowing ξ)
$p(\mathbf{D}; \xi)$	Probability density function of D, which depends on ξ
p-p	Peak-to-peak
P	Power
P_B	Bandwidth power
P_{IMR}	Intermodulation Distortion Ratio
P_{IN}	Input power
$P_{IN,avg}$	Average input signal power
P_{IP3}	Power of the third-order intercept point

P_n	Noise power
P_{OUT}	Output power
$P_{OUT,A1}$	Output power in one input tone
$P_{OUT,avg}$	Average output signal power
$P_{OUT,max}$	Maximum output power
r_n	Noise ratio
R	Positive integer (excluding zero)
S	Scattering parameter
sat.	saturation level
SNR_{input}	Input Signal-to-Noise Ratio
SNR_{output}	Output Signal-to-Noise Ratio
t	Time
T	Absolute temperature
T_a	Actual temperature
T_e	Effective input noise temperature
T_n	Noise temperature
T_o	Operating temperature
Vcc	Voltage at the common collector
Vdc	Direct current voltage
$x(t)$	Input signal
$y(t)$	Output signal
Z	Boltzmann constant ($\approx 1.38 \times 10^{-23}$ J/°K)

List of Figures

List of Tables

Chapter 1

Introduction

Nowadays communications are full of activities that require fast flow of high amount of information. Moreover, it is not just necessary to communicate, but to use a variety of services available at any time and anywhere. Actually, any communication network brings problems itself, from the infrastructure point of view, such as the use of nonlinear components (e.g. amplifiers). Therefore, new technology brings with it clear advantages, such as mobility and faster communication links, but designers of new models and systems should also be aware of the possible drawbacks that may come with it.

1.1 Motivation

The nonlinearity of an amplifier affects the information being transmitted. This happens because the waveform of the transmitted signal gets distorted and might result in lost or incomprehensible information at the receiver. In general, amplifier nonlinearities are observed when high power levels are applied to them, which is usually done in order to obtain high power efficiency. This produces a conflict between clear transmission and transmitted power, which will determine the efficiency of the transmitter system. Likewise, the more efficient is an amplifier, the smallest is the battery and the cheapest is the cooling system. This leads to more extended speech time and cheaper and smaller communication devices, which are the key factors that drive power amplifier development [1].

On the other hand, the amount of users that a network can handle depends on its capacity and coverage [2, 3]. Therefore, the increase of users in a network bring along the need of higher power levels (specifically for downlink power control) at the network's base stations, which means more problems with the amplifier nonlinearities.

Furthermore, wireless communications evolve into more complex transmission schemes, such as the ones using Orthogonal Frequency Division Multiplexed (OFDM) signals. This kind of advanced modulation schemes, makes communications more sensible to nonlinear distortion, due to the large dynamic range of the transmitted signal [4]. In order to operate an amplifier at a high efficiency rate, the bias of the amplifier should be set near to the saturation zone. However, when an amplifier is used in this efficient way, the high peaks of a multi-tone input signal are clipped at the output of the amplifier. Thus, the problem of amplifier nonlinearity has a major effect on signals with high PAR, such as multisine and OFDM signals.

Moreover, there is a need to assess and alleviate power amplifier nonlinearity by using compensation methods based on amplifier models. Recent methods to model [5] and alleviate [6] this nonlinearity effect are being developed. These and other techniques can be based on practical measurements in order to make the attenuation of the nonlinearity more accurate. In other words, there is a need to perform measurements of power amplifiers, from which data to design accurate models that characterize the nonlinearities can be obtained. Furthermore, the proposed new models and compensating techniques can be tested by similar measurements, where the nonlinear amplifier's performance is evaluated.

1.2 Objective

The main objective of this thesis is to provide the basis to perform accurate measurements of power amplifiers that give as a result enough reliable data to characterize their nonlinearity. In order to achieve this, different types of practical measurements should be performed. Moreover, the data obtained is intended for designing models and compensation techniques in order to alleviate the amplifier's nonlinear characteristics.

For ease of analysis it is convenient to divide the nonlinear effects of power amplifiers into frequency-independent or frequency-dependent nonlinearities. Therefore, measurements to characterize frequency-independent and frequency-dependent nonlinearities should be performed. Single- and two-tone tests are used for this purpose. Furthermore, the effects of a multi-tone signal applied to a nonlinear power amplifier will be measured.

Measurements should be done carefully to obtain accurate data that is useful for modelling and compensation techniques. Therefore, a clear procedure is needed, including the suggested equipment to use, setup systems for each specific measurement and the parameters to be measured. Finally, the accuracy of the measurements, as well as a way to prove the usefulness of the performed measurements, should be analyzed.

1.3 Outline of the thesis

The organization of the contents of this thesis is presented in Figure 1.1. In Chapters 2 to 4, background and basic theory are reviewed. Later on, Chapters 5 to 7 present my contribution and understanding on measurements to obtain reliable data for modelling of power amplifiers nonlinearity.

Chapter 2 gives a brief introduction on general concepts related to amplifiers: how they work, their classification, and linearity and distortion in power amplifiers. Chapter 3 summarizes the parameters for modelling the distortion of power amplifiers obtained from single-, two- and multi-tone tests and gives an introduction to multisine and OFDM signals. Chapter 4 concludes the theoretical part of this thesis by including an overview of modelling and parameter estimation methods, which provide principles for planning the measurements.

In Chapter 5, planning aspects that should be considered before measurements are commented and the suggested proceedings and setup systems for making measurements are described. These measurements include: single-, two- and multi-tone tests. Furthermore, the results of the measurements and the parameters obtained for modelling purposes are presented in Chapter 6.

Next, the possible measurement errors are described in Chapter 7, as well as an analysis of the usefulness of the measurements performed. Finally, conclusions are presented in Chapter 8, as well as suggestions for future work.

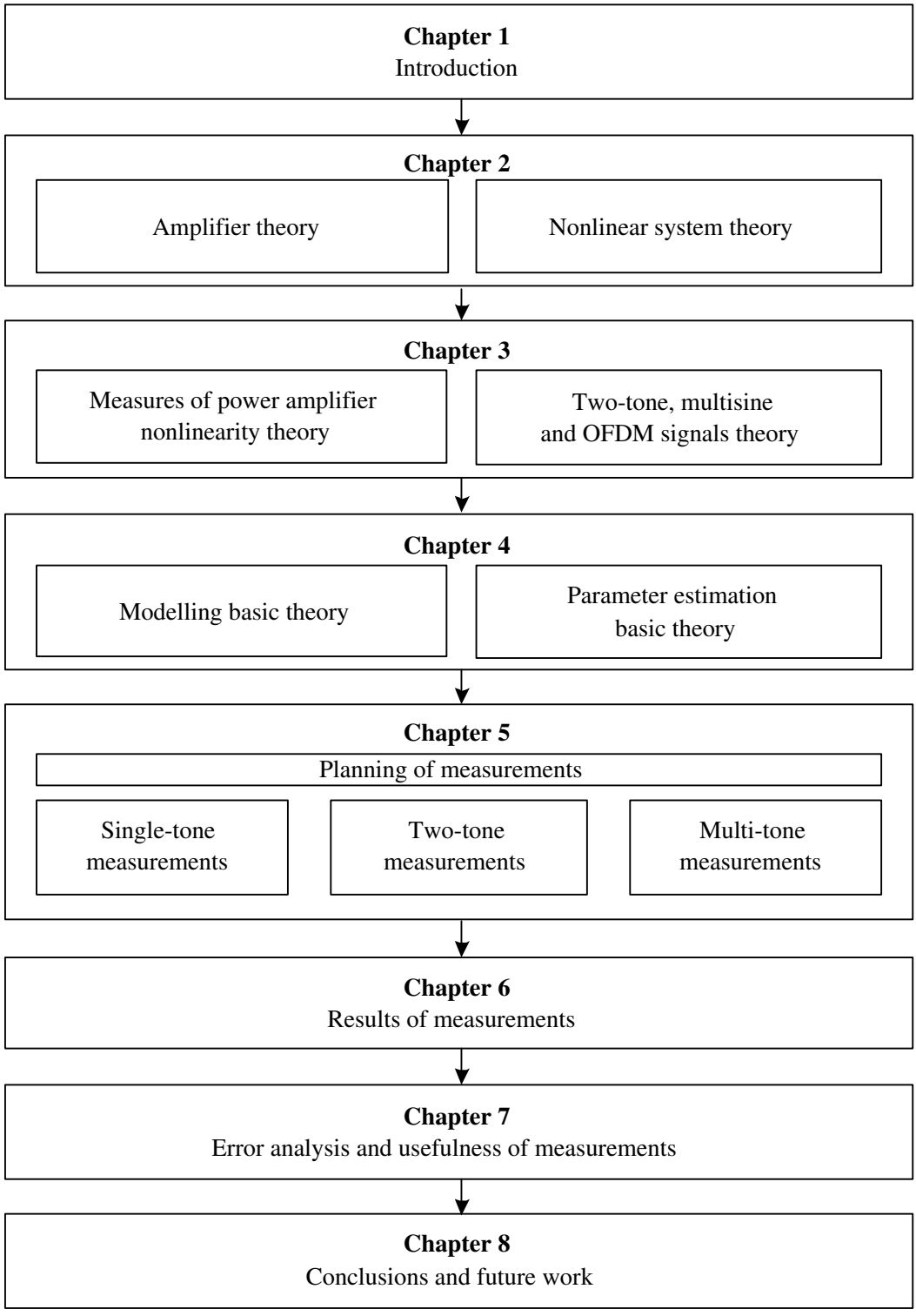

Figure 1.1: Organization of the thesis.

Chapter 2

Amplifiers

Amplifiers are very important components in modern wireless communications systems, since they give the signal to be sent the necessary power to overcome the losses that may occur during transmissions. However, they may also introduce some problems, as the need of a higher system power and so, the need of batteries that last longer, which bring along more expenses.

In general terms, an amplifier is an active component, which means that it does not follow Ohm's law [7] in a linear way and therefore, the output obtained from it may vary according to the varying input signal.

In this chapter, the main concepts related to amplifiers are described. First, the main definition of a power amplifier is given. Next, a comparison between tube based and solid state amplifiers is done. Moreover, the most commonly used classes of amplifiers are briefly described. Finally, the concepts of linearity and distortion are reviewed for systems in general, as well as for the particular case of power amplifiers.

2.1 Power amplifiers

A Power Amplifier (PA), increases the power of the input signal, so the voltage and/or the current will be increased at the output of the device. Across the years, different approaches have been taken in order to create the "perfect" power amplifier. Nowadays, the most commonly used devices are the ones based on electron beam tubes, usually Travelling Wave Tube Amplifiers (TWTA), and the Solid State Power Amplifiers (SSPA) as shown in the Table 2.1, for different microwave bandwidths.

Table 2.1: Types of amplifiers for different microwave frequency bands.

Name	Frequency Band	Solid State Type	Tube Type
X-band	10.6 – 10.7 GHz	20 W (GaN device)	3000 W (TWT)
Ka-band	22 – 36.5 GHz	6 W (0.15 μm PHEMT devices)	1000 W (Klystron)
Q-band	42.5 – 49.04 GHz	4 W	-
W-band	86 – 92 GHz	0.5 W (TRW)	1000 W (EIKA)

TWTA operation is based on the observations made by Thomas Alva Edison [8] in 1879 when he invented the incandescent electric light bulb making an electric current flow through a glass tube surrounding a vacuum. A schematic of a simple TWTA is shown in Figure 2.1.

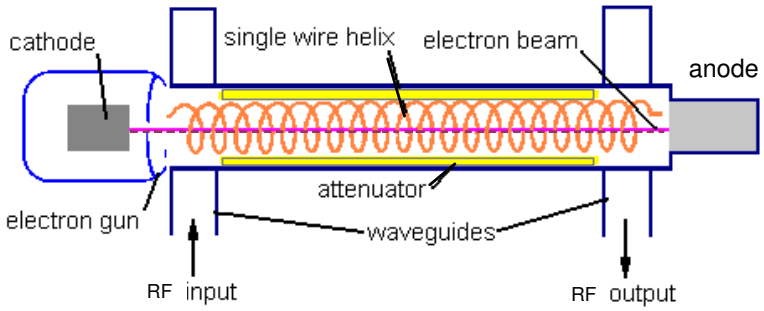

Figure 2.1: Basic TWTA [9].

At the left of Figure 2.1 there is an "electron gun", which mainly consists of a heater, a cathode and an anode. When heated, the cathode emits a stream of electrons which passes through the anode and travels as a narrow beam through the helix at the speed of light. The electron beam will transfer its energy to a signal (electromagnetic wave) travelling along the helix amplifying it. By adjusting the

length of the helix and pitch it is possible to manipulate different operating frequencies. Because of their construction, TWTAs offer large currents and therefore, high output powers can be obtained.

The term "solid state" refers to devices whose operation does not depend on wave tubes. SSPAs are made of several Gallium Arsenide (GaAs) metallic semiconductor Field Effect Transistors (FETs) that can achieve different rated output power depending on these FETs' series or parallel arrays. As an example, Figure 2.2 shows a basic solid-state amplifier circuit (Class A configuration), where Vcc is the voltage at the common collector, P_{IN} is the input power and P_{OUT} is the amplified output power.

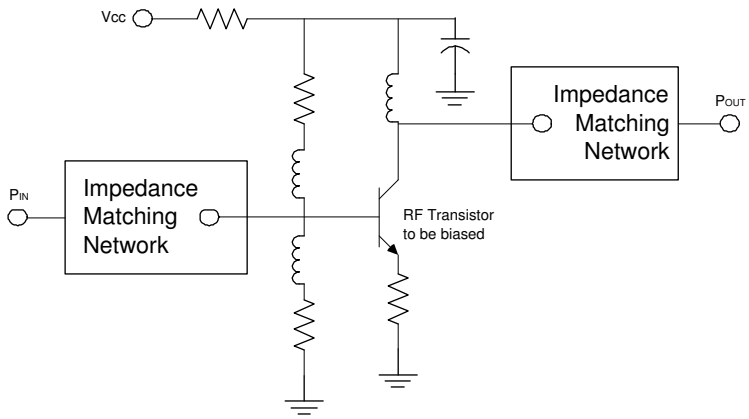

Figure 2.2: Basic SSPA (Class A configuration) [10].

When choosing an amplifier for a determined system, it is recommended to consider the advantages and disadvantages that TWTAs and SSPAs present, since each application has special needs that can be fulfilled by different amplifiers. For instance, the fact that SSPAs can work in the unlikely event of a GaAs FET failure, gives these amplifiers a marked advantage over TWTAs which will completely stop working in case any of their elements fail.

An amplifier's power efficiency (η) is the relation between its output power (P_{OUT}) and input power (P_{IN}), as defined by Equation (2.1). TWTAs have higher efficiency than SSPAs, which translates into higher linearity. At this point, the linearity of an amplifier is measured as its Third-order Intercept Point (IP3) referred to output power level (a detailed definition of IP3 is given in Section 3.1.2). This means that for a given output IP3, a tube amplifier will consume less power than a solid state one.

$$\eta = \frac{P_{OUT}}{P_{IN}} \tag{2.1}$$

It is also known that if a TWTA and a SSPA behave with the same linear characteristics (same output IP3), they will also have the same 1 dB compression point, as shown in the example of Figure 2.3. The 1 dB compression point is the point where the transfer curve of an amplifier deviates 1 dB from the ideal linear curve (see Section 3.1.4).

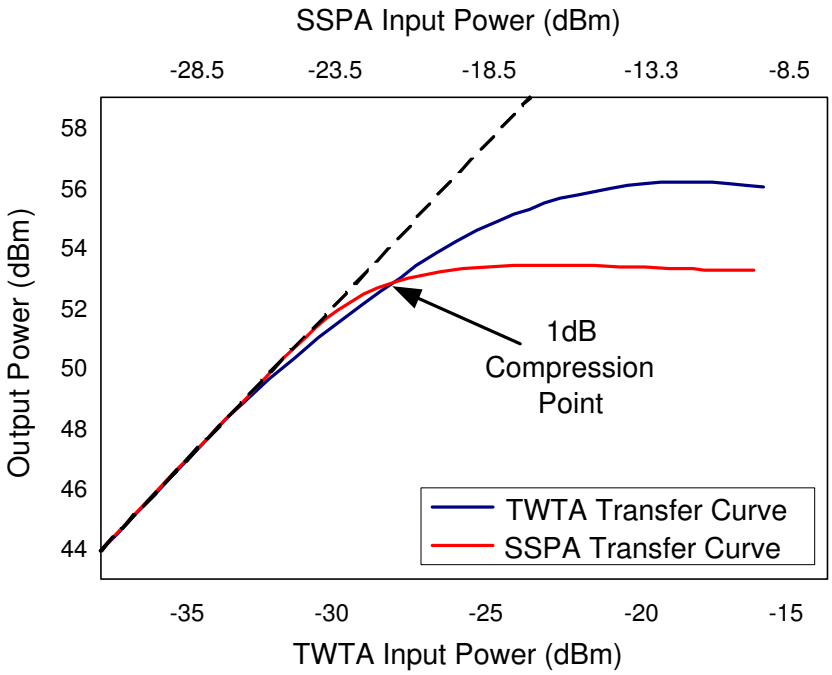

Figure 2.3: Example of TWTA and SSPA transfer curves with the same slope in their linear zone [11].

However, after the 1 dB compression point the behavior of the amplifiers is different. As shown in Figure 2.3, the TWTA transfer curve continues raising until its saturation point, while the SSPA has its saturation zone close to the 1 dB compression point.

This difference defines the naming convention for rated power of both types of amplifiers. SSPAs rated power is named after their 1 dB compression point, in the case shown in Figure 2.3 200 W (equivalent to 53 dBm). On the other hand, TWTAs are specified based on their saturation level like the TWTA in Figure 2.3 which saturation output power is 56 dBm and so it is called a 400 W amplifier.

The transfer curve of a specific amplifier type presents in itself an advantage for tube type amplifiers. Typically, SSPAs are operated in levels below its 1 dB compression point. However, TWTAs have a "power reserve" in case of high path loss as in rainy environments. This makes TWTAs more robust than SSPAs for uncertain environmental conditions.

For amplitude and phase transfer characteristics, both types of amplifiers present the same linearity pattern [11]. SSPAs behave better than TWTAs before their common 1 dB compression point and at higher input power levels, when SSPAs are already saturated, TWTAs have a better performance. This relationship may also be applied from the cost point of view in order to choose a type of amplifier to be used.

With respect to modular design of amplifiers, SSPAs give a more reliable scenario than TWTAs. SSPAs have the ability of continuing working even when a fail occurs in one of its modules, in which case it will continue operating at a lower output power. According to the "static reliability analysis" proposed in [12], TWTAs can only have 71% of the reliability of SSPAs, based on their architecture and having the same reliability for all their subsystems.

Another important aspect to consider in modular design is the power supply needed to operate the amplifiers. In this, SSPAs have a marked advantage since there exist many devices that are able to fulfill their operating voltage needs, which are typically a few volts (between +12 V and +50 V) in contrast with TWTAs, which require supplies of several thousands of volts that can be very difficult to find and complex to build.

From the cost point of view, building a modular TWTA is extremely difficult and expensive because of the complexity of the vacuum tube architecture. Moreover, there are not power supplies at the high voltage levels required by travelling tubes available in nowadays market. Consequently, for the same output power levels, it is possible to build a modular SSPA for the same cost than for an equivalent TWTA.

Even though SSPAs have several advantages on TWTAs, we should also consider that the last ones are more efficient and less expensive when used at low frequencies. Besides, tube amplifiers are widely recommended for professional audio applica-

tions (guitar amplifiers, microphone preamplifiers, equalizers, etc.) due to their specific distortion and speaker-damping characteristics, which are very difficult to imitate with SSPAs.

As mentioned before, the specific characteristics of each type of amplifiers should be taken on count when choosing one to be used in a specific system. Their advantages and disadvantages are summarized in Table 2.2.

Table 2.2: TWTAs compared to SSPAs.

	TWTA	**SSPA**
Advantages	. Amplifies a wide range of frequencies at the same time . Excellent performance in audio and satellite devices . Efficient and less expensive for high power outputs (>10 kW) and high frequencies (>50 MHz)	. Physically small . Amplifies in stages . Can continue working when partial failures occur
Disadvantages	. Difficult to repair . More expensive and complex power supply required . Shorter active life (4 to 6 years)	. High power consumption . Instabilities due to failures . Not recommended for low frequencies
Applications	. High power applications (e.g. remote sensing) . Earth stations and communication satellites . Professional audio (e.g. microphones, limiters, equalizers) . High-power UHF TV stations . FM broadcast stations Guitar amplifiers	. Low and medium power applications (e.g. space-flight) . AM and FM broadcast transmitters . TV, HF/VHF, lower power UHF, OFDM and HDTV broadcast . Telecommunications . Broadband and wireless RF . Radar . Cellular-telephone handsets . Base station transmitters

2.2 Classes of amplifiers

Power amplifiers can be classified based on their rated power as low (below 1 mW), medium (from 1 mW to 10 W) or high (above 10 W). However, it is very popular to use a "class" method to categorize them [13], based on, for example, their circuit configurations, operational topology, linearity and efficiency. Examples of the so-called linear power amplifier classes are A, B, AB and C, the most commonly used nowadays. These classes represent the amount of variation that the output signal presents in a complete operation cycle of the input signal.

Other classes of amplifiers briefly discussed are D, E, F, G, H and S, which are more recent approaches to improve Class B or C amplifiers [14]. These last classes are better known as switched mode amplifiers, because of its way of operate, or as nonlinear power amplifiers, due to their poor linearity performance. However, they can achieve higher efficiency and their linearity can be improved using linearization techniques.

An important concept used to place an amplifier into a specific class is efficiency. As mentioned in Section 2.1, an amplifier's power efficiency is defined as the relation between output power and input power. This ratio is a good measurement for amplifiers when choosing one for a specific application, since it tells how much power is spent and this can be easily related with the budget of a project.

In *Class A* amplifiers, the output signal varies through the complete cycle of the input signal. They operate at constant current, independently of the input signal level and at all times. Then, the DC current must be at least equal to the peak output current (Figure 2.4). Because of this, they are expensive when transmitting signals that have large peak-to-average signal power and also, their efficiency is limited to just 25%.

Class B amplifiers give an output signal that varies through just half of the cycle of the input signal (180°). With these devices, the output signal obtained will be much more distorted since just half of each cycle of the signal will be reproduced (Figure 2.5).

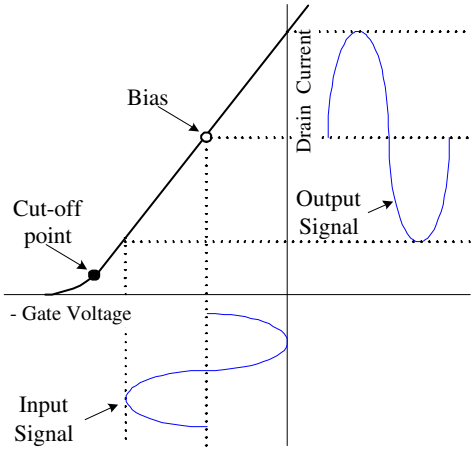

Figure 2.4: Class A amplifier's operation point.

In order to make *class B* amplifiers more useful, a "push-pull" output stage is used, which has two valves that operate for each half-cycle of the input signal (one for the positive and another for the negative). With this system, we can obtain a maximum efficiency of 78.5%, which is better than for *Class A*. However, due to the system used of two valves, some crossover distortion may be introduced, which might not be desirable in most applications.

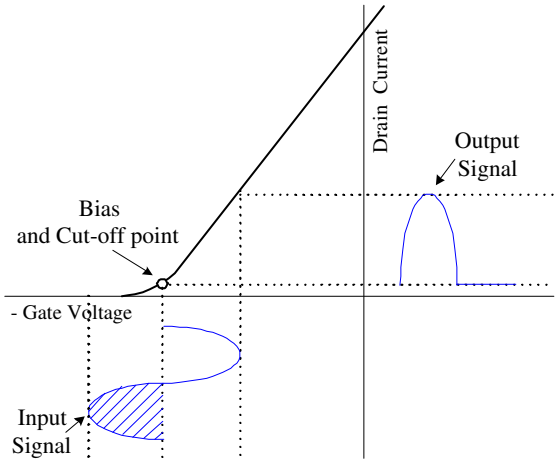

Figure 2.5: Class B amplifier's operation point.

An intermediate solution is *Class AB* amplifiers. Their bias point is set at a DC level over the zero level of *Class B* and operate at lower current in the absence of signal (Figure 2.6), which makes their power supply less expensive. It still requires a push-pull system, where the valves will overlap for a little while in their transition and may introduce some crossover effect. Anyway, this effect will be lower than for the *Class B* amplifiers but the efficiency will be improved compared to *Class A*.

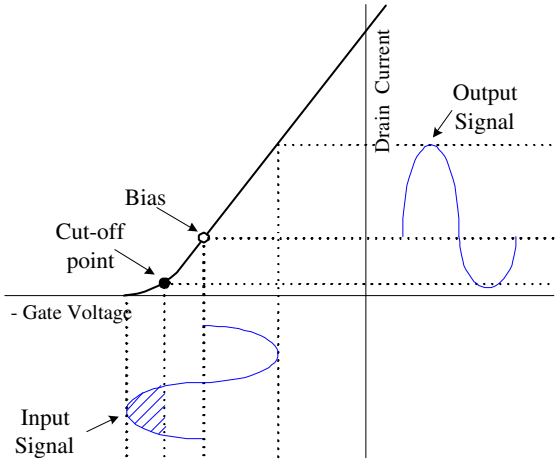

Figure 2.6: Class AB amplifier's operation point.

The output of a *Class C* amplifier is biased to operate at less than 180° of the input cycle and only with a tuned resonant circuit that gives a complete operation cycle for the tuned or resonant frequency. Because of this, these amplifiers are used in very special tuned circuit areas such as radio communications. Their theoretical efficiency is very high (even 100% can be achieved). However, it is not common to use them to produce high power levels and they tend to be very expensive to build because of the need of high-performance transistors.

In order to make comparison easier, the main characteristics of the linear amplifier classes presented are summarized in Table 2.3.

Table 2.3: Classes of linear amplifiers.

	Class A	**Class AB**	**Class B**	**Class C**
Conduction angle	Both polarities (180°)	More than one polarity (> 180°)	One polarity (180°)	Peak of one polarity (< 180°)
RF Gain	High	High / Moderate	Moderate	Low
RF Power	High	High	High	Low
Drain efficiency	Low (≤ 25%)	Moderate (25%-78.5%)	High (≤ 78.5%)	Very high (78.5%-100%)
Non-linearities	Low	Moderate	High	Very high
Operation frequency	High	Moderate	Low	Very low

Class D amplification uses digital pulses that are "on" for a short interval of time and "off" for a longer time (switched mode amplifier). The use of digital techniques allows obtaining a signal that may vary through the complete input cycle (using sampling and retention circuits) to produce an output signal based on several parts of the input signal. The main advantage of these amplifiers is that they are "on" (using power) just for short intervals and the general efficiency may be very high (usually higher than 90%).

In the operation of *Class E* amplifiers, the transistor works as an ideal switch without "on" resistance and infinite "off" resistance. This switching produces distortion, which may be translated as nonlinearities. An important characteristic of this class is that it employs an output network that shapes the waveforms of voltage and current to avoid simultaneous high voltage and high current in the transistor, which produces high efficiency [15]. Their ideal efficiency is 100% although, in practice, factors as saturation voltage and switching time reduce it.

Compared to *Class E*, *Class F* amplifiers do not require a fast switching driver signal and their implementation is easier. These amplifiers use a resonating network [14] to control their voltage and current waveforms, reducing their transistors' power dissipation and increasing their efficiency. When setting their operation point at the cutoff region for switching operation, they are able to achieve an efficiency of 100%.

Class G amplifiers are widely used in audio applications, where a narrow bandwidth is not required. These amplifiers require more than one voltage source and two or more pairs of active devices, which make the bandwidth of the whole device wide. Out of these devices, low power transistors handle the amplification most of the time and the high power ones switch only during peak signal demand. Their optimal efficiency (close to 100%) is achieved when used with signals that do not need high voltage supply (low level signals).

Class H amplifiers are based on *Class G* and, as those, they are used mainly in audio products. These amplifiers work with two different supply voltages, which are switched "on" as required, depending on the size of the signal being amplified. This allows the power supply to track the input signal and provide just enough voltage for the output signal. Their efficiency, as in *Class G* amplifiers, may be made close to 100%.

Finally, the *Class S*, also called "switching regulator", is based on *Class D* amplifiers. It uses Pulse-Width Modulation (PWM) [14], which basic operation is to create a variable duty-cycle (varying the mean levels) to form a rectangular waveform. Therefore, *Class S* amplifiers are used also as amplitude modulators. The rectangular PWM voltage waveform is applied to a low-pass filter in order to reduce distortion, increasing the efficiency compared to *Class D* amplifiers.

2.3 Linearity and distortion

In order to understand the need of linear amplifiers in modern communication systems, it is important to define what is meant by linearity. In general, a linear system is the one whose output is proportional to its input, meaning that the form of the output signal will be the same than the input, affected by a constant factor k. When $k = 1$, the output will be an exact replica of the input. Otherwise, if $k > 1$, the amplitude of the output signal will be increased (amplified) with respect to the input and if $k < 1$, it will be reduced.

Mathematically, a system is said to be linear when it accomplishes the superposition property, which combines the additivity and scalability concepts, as defined in Equation (2.2). The additivity property means that the output of a system which input is the sum of several signals will be the sum of the individual outputs of each signal when applied to the same system. On the other hand, the scalability principle simply means that, in a linear system, the response to $\alpha x_1(t)$ will be $\alpha y_1(t)$, where α is any complex constant.

$$x(t) = \alpha_1 x_1(t) + \alpha_2 x_2(t) \Rightarrow y(t) = \alpha_1 y_1(t) + \alpha_2 y_2(t) \tag{2.2}$$

When distortion occurs, the output is not an exactly scaled version of the input signal. This distortion can be caused by the nonlinear characteristics of the device, which is called nonlinear or amplitude distortion. This may happen with all classes of amplifiers presented in Section 2.2. The distortion may occur as well because the elements of a system or a device have different behavior related to the input signal at different frequencies, being referred to as frequency distortion.

Other kinds of distortion may be introduced to the transmitted signal in the form of noise inside the frequency band, which may generate additional frequency components in adjacent channels [16].

In general, distortion can be classified as memoryless distortion (instantaneous) or distortion with memory. When referring to memoryless distortion, the output depends only on the instantaneous input value. In the case of distortion with memory, the output depends not only on the instantaneous input value but also on the previous ones [17].

Nonlinear amplifiers are devices with memory, since they contain components that store energy, such as capacitors and inductors. Therefore, it results more accurate to classify systems that contain amplifiers into frequency-independent or frequency-dependent systems. Frequency-independent systems can be with or without memory, while frequency-dependent systems always contain memory components. This classification is useful when modelling the nonlinearity of power amplifiers [5].

2.4 Distortion in power amplifiers

An ideal power amplifier would have a linear transfer characteristic as shown in Figure 2.7(a), which can be represented by Equation (2.3), where K is the power gain. This means that the output power (P_{OUT}) would be a multiple of the input power (P_{IN}) and, consequently, the shape of the input and output signals is exactly the same.

Mathematically, distortion due to an amplifier occurs when adding second, third or higher terms to the ideal transfer characteristic of Equation (2.3), resulting in one of the form shown in Equation (2.4). This means that the output signal will have a different shape than the input. This is the common case since in practice 100% linear amplifiers do not exist. The transfer characteristic of a nonlinear amplifier is illustrated in Figure 2.7(b).

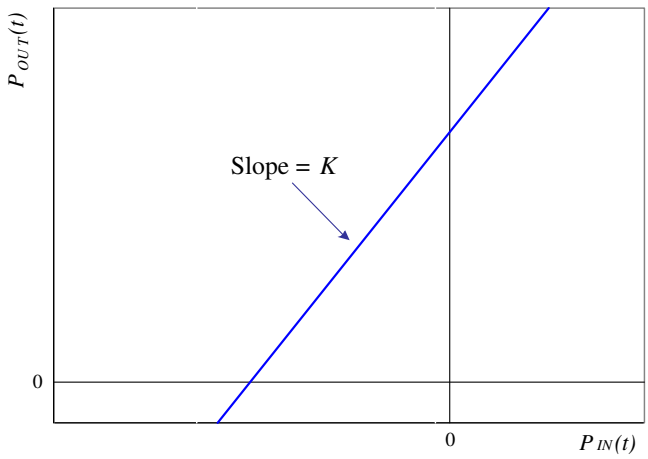

(a) Ideal amplifier

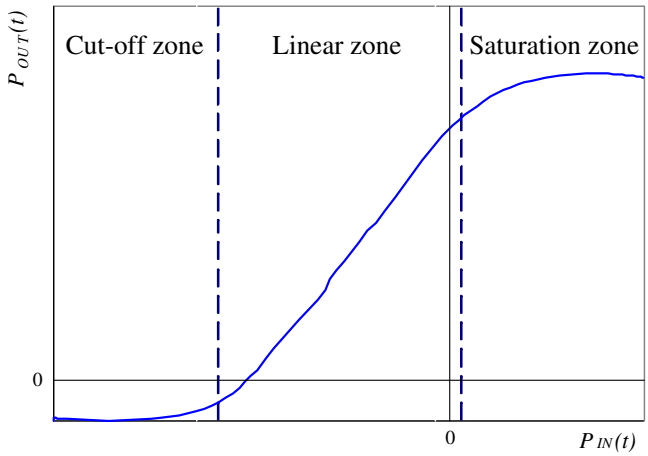

(b) Nonlinear amplifier

Figure 2.7: Transfer characteristic of an amplifier.

$$P_{OUT}(t) = K\ P_{IN}(t) \tag{2.3}$$

$$P_{OUT}(t) = K_1 P_{IN}(t) + K_2 P_{IN}^2(t) + K_3 P_{IN}^3(t) + K_4 P_{IN}^4(t) + K_5 P_{IN}^5(t) + \cdots \tag{2.4}$$

Notice that the transfer characteristic of a nonlinear amplifier has three main zones, as shown in Figure 2.7(b). In the *cut-off region* an amplifier will act as an open circuit, since the bias is not sufficient for conduction to occur. When increasing the bias, the amplifier will enter the *linear zone*, where it will act as a linear amplifier, achieving the specified maximum gain. However, if the bias is further increased, the amplifier will *saturate*, meaning that high amplitude signals will not respond to increased gain and will appear flattened (distorted).

2.5 Summary of the chapter

In this chapter basic theory about amplifiers is summarized. First, the advantages and disadvantages between the two most commonly used types of amplifiers were given. The older type, travelling wave tube amplifiers, have an excellent performance when high power outputs and high frequencies are needed. However, solid state amplifiers have become popular in the last decades due to their physical small size and their reliability in communication applications.

Next, the classes of amplifiers were described, including their topology, operation and efficiency. Classes A, B, AB and C are the most widely used, from which Class C amplifiers have the highest efficiency and linearity but they can just provide low gain amplification.

Finally, the general concepts of linearity and distortion were briefly explained and described by a graphical example. Moreover, the distortion effect introduced by amplifiers was mathematically characterized as the addition of second- or higher-order terms to their linear transfer characteristic.

Chapter 3

Power amplifier distortion measures

In order to model the nonlinearity produced by power amplifiers, it is necessary to understand different types of distortion caused by them. Moreover, the techniques to determine the level of the distortion should be considered in order to obtain the adequate parameters for modelling.

A nonlinear amplifier can distort the signal passing through the amplifier and, in addition, signals in adjacent channels or bands [14]. Amplifier distortion can be divided into two main groups: generation of harmonic components and generation of intermodulation products or Intermodulation Distortion (IMD).

The distortion based on generation of harmonic components occurs when a simple one frequency (single-tone) signal propagates through a nonlinear device. If these harmonic components are not filtered away, they will affect nearby channels or bands. On the other hand, IMD is generated when more than one frequency (multi-tone) signal is applied to the system, producing frequency components inside the signal's fundamental frequency band, which are difficult to filter out.

In this chapter, the specific distortion caused by power amplifiers when working with different signals is presented. This includes the parameters for modelling purposes that can be obtained from each type of signal (single-, two- or multi-tone), as well as the description an graphical example of each type of nonlinearity.

3.1 Distortion measures using single-tone signals

As earlier mentioned, single-tone signals passing through a nonlinear amplifier produce harmonic components, which will appear at multiple frequencies of the fundamental frequency. Usually, the frequencies where these components appear are outside the system frequency band and therefore, it is easy to eliminate them using a lowpass filter. If a filter is not used, adjacent channel interference will be present in the general system.

3.1.1 Second harmonic distortion

The simplest model of amplitude nonlinearity occurs when a term proportional to the square of the input power is added to the transfer characteristic, resulting in Equation (3.1).

$$P_{OUT}(t) = K_1\ P_{IN}(t)\ +\ K_2\ P_{IN}^2(t) \tag{3.1}$$

This type of nonlinearity is called second harmonic distortion since an additional frequency component will appear at twice the original frequency in the spectrum of the output signal. The amplitude of this component will be proportional to the coefficient of the quadratic term. Furthermore, this type of distortion will also produce a DC component in the transfer characteristic. Figure 3.1 illustrates an example of an amplifier's characteristic with a second harmonic distortion, in time and frequency domain, where f is the fundamental frequency.

It is evident that the amplitude of the second harmonic distortion increases proportionally to the square of the input signal and the constant K_2, while the amplitude of the fundamental characteristic increases only in function of the constant K_1. The point where these two amplitudes are the same is called second order Intercept Point (IP2) and is useful to calculate the distortion level at a specific input level.

The second order intercept point of a nonlinear amplifier is shown in Figure 3.2. Notice that the lines are dotted at high input levels, meaning that at very high input levels it is impossible to measure a nonlinear amplifier without destroying it and therefore, only theoretical representation can be done.

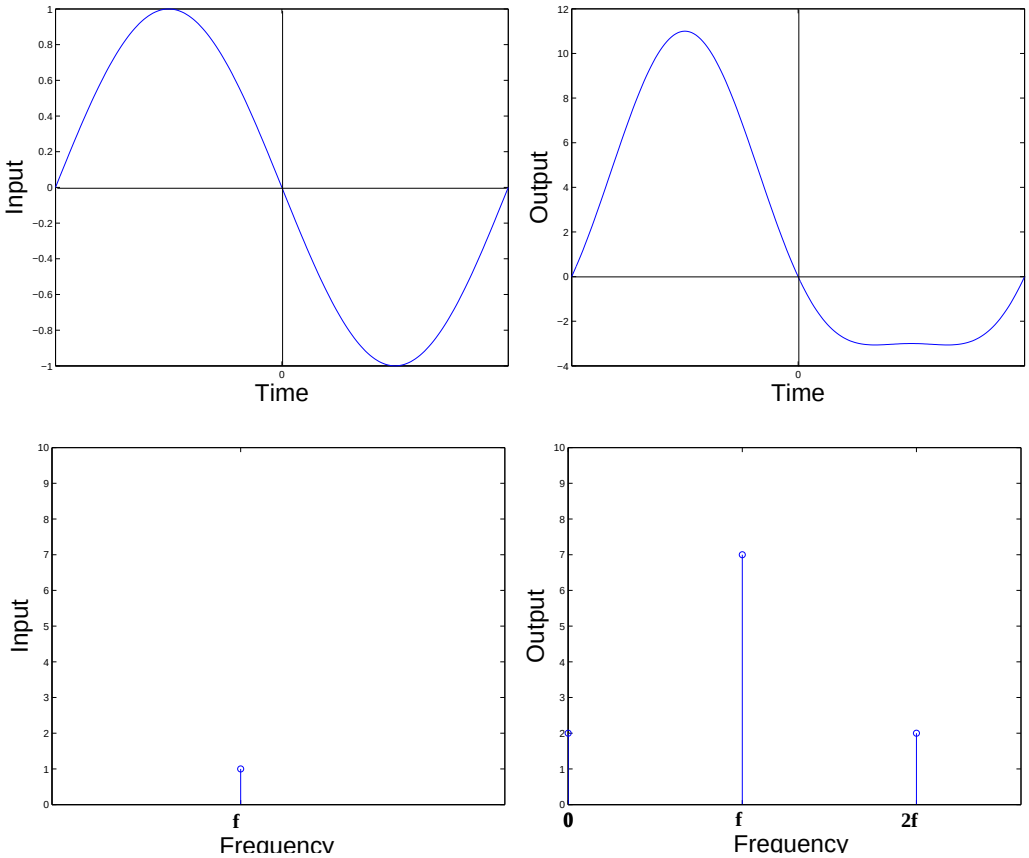

Figure 3.1: Second harmonic distortion for $P_{OUT}(t) = 7P_{IN}(t) + 4P_{IN}^2(t)$, *where* $P_{IN}(t) = \cos(2\pi ft)$, *in time and frequency domain.*

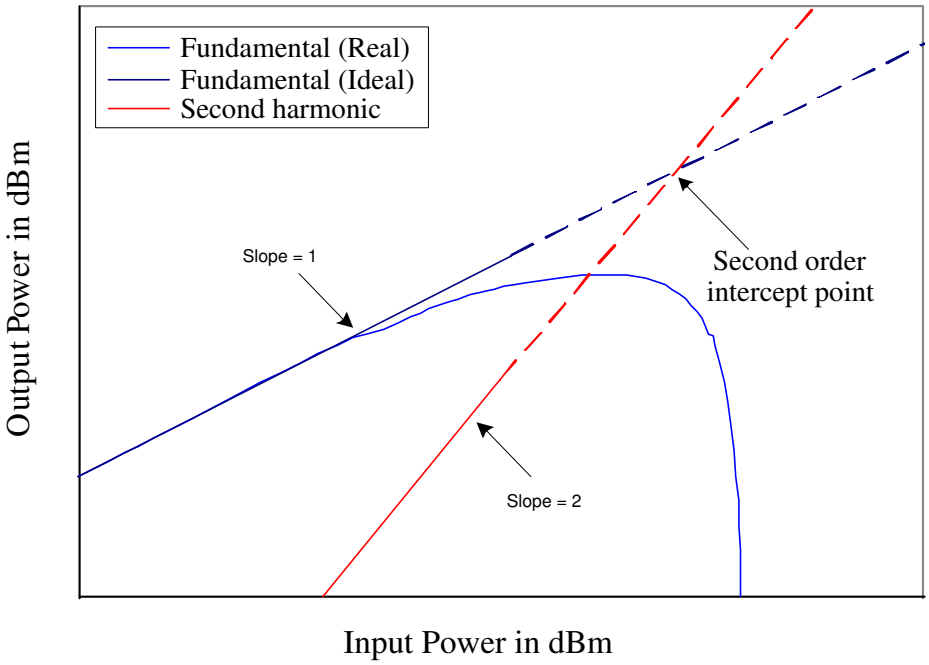

Figure 3.2: Second order intercept point of an amplifier with transfer characteristic $P_{OUT}(t) = K_1\ P_{IN}(t)\ +\ K_2\ P_{IN}^2(t)$.

3.1.2 Third harmonic distortion

When a third order term is added to the ideal transfer characteristic, as expressed in Equation (3.2), the resultant output waveform is symmetric with respect to the horizontal axis. In the frequency domain, a new component appears at the third harmonic as shown in Figure 3.3. Notice that there is no DC component.

$$P_{OUT}(t) = K_1\ P_{IN}(t)\ +\ K_3\ P_{IN}^3(t) \tag{3.2}$$

The third order Intercept Point (IP3) can be found in the same way as in the case of second harmonic distortion. Figure 3.4 illustrates the third order intercept point of a nonlinear amplifier.

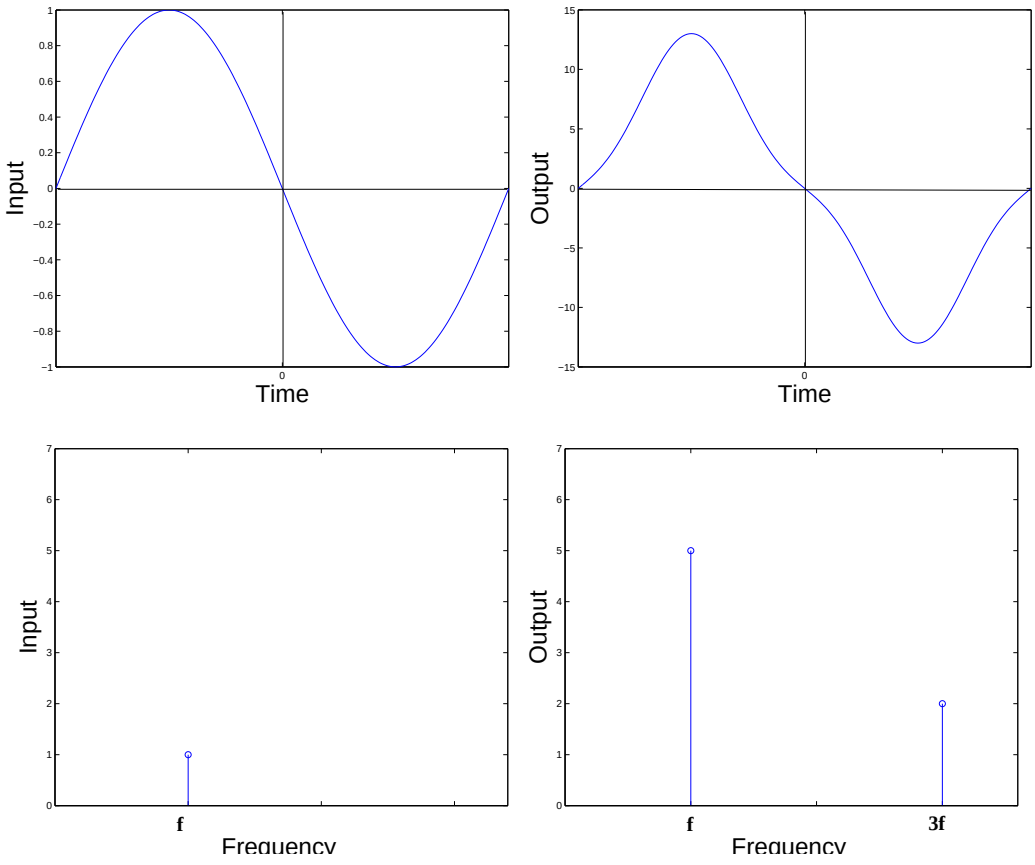

Figure 3.3: Third harmonic distortion for $P_{OUT}(t) = 5P_{IN}(t)+8P_{IN}^3(t)$*, where* $P_{IN}(t) = \cos(2\pi ft)$*, in time and frequency domain.*

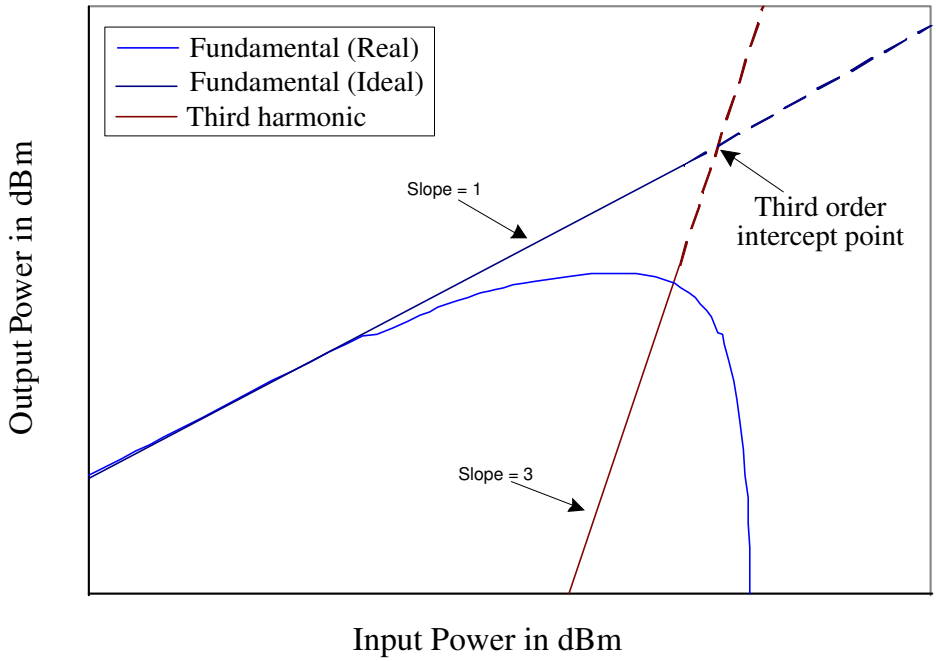

Figure 3.4: Third order intercept point of an amplifier with transfer characteristic $P_{OUT}(t) = K_1\, P_{IN}(t) \;+\; K_3\, P_{IN}^3(t)$.

Unlike an amplifier with second-order distortion, the magnitude of the fundamental tone of an amplifier with third-order distortion has a nonlinear behavior. This can be analyzed taking an amplifier with the transfer characteristic of Equation (3.2) and using as input the simple signal represented by Equation (3.3), where $\omega = 2\pi f$.

$$P_{IN}(t) \;= A\sin(\omega t) \tag{3.3}$$

Then, the output obtained when choosing a negative K_3 can be written as:

$$\begin{aligned} P_{OUT}(t) &= K_1 A\sin(\omega t) - K_3(A\sin(\omega t))^3 \\ &= K_1 A\sin(\omega t) - \frac{3K_3A^3}{4}\sin(\omega t) + \frac{K_3A^3}{4}\sin(3\omega t) \end{aligned} \tag{3.4}$$

The first term of Equation (3.4) represents the fundamental tone amplified by gain K_1. The third term shows the harmonic component proportional to gain K_3 and the cubic of the input power generated at three times the original frequency. Notice, however, that a second term is generated at the same frequency of the fundamental, meaning that the amplitude of the fundamental will be decreased

proportionally to the cubic of the input signal. This gives the characteristic form of the transfer function of an amplifier where a third order nonlinearity predominates, as the one shown in Figure 3.4.

3.1.3 Higher-order harmonic distortion

Generally, nonlinear amplifiers have transfer characteristics that include second, third and higher order harmonics, as in the general Equation (3.5), where N determines the order of the amplifier nonlinearity.

$$P_{OUT}(t) = \sum_{n=1}^{N} K_n P_{IN}^n(t) \tag{3.5}$$

Based on the concepts of second and third harmonic distortion previously presented, higher harmonic components can be divided into even-order and odd-order harmonics, whose general illustration is shown in Figures 3.5 and 3.6.

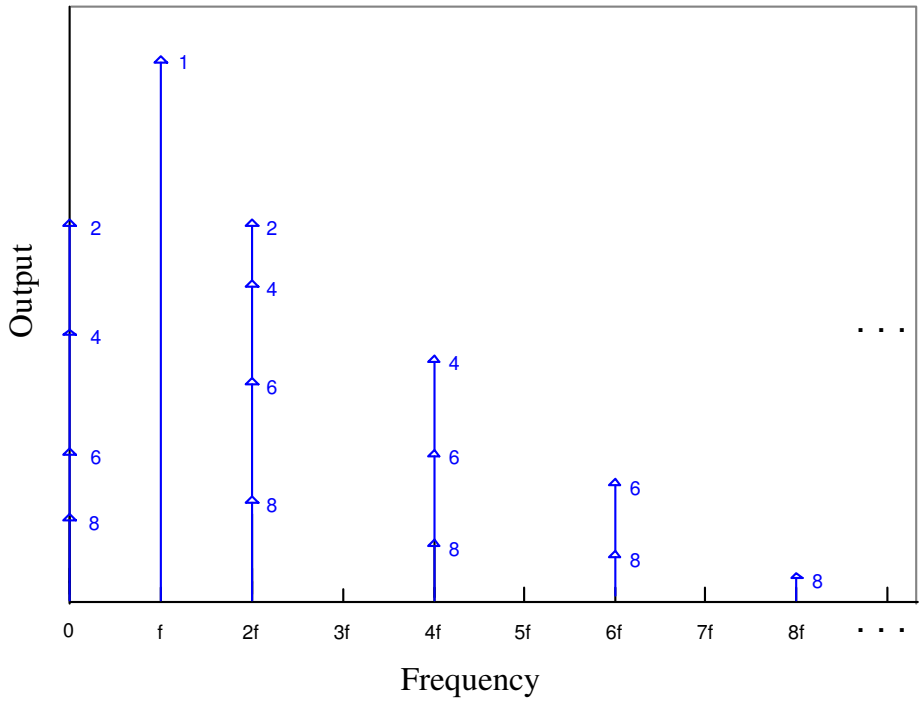

Figure 3.5: Even-order harmonic components of a nonlinear amplifier represented in frequency domain.

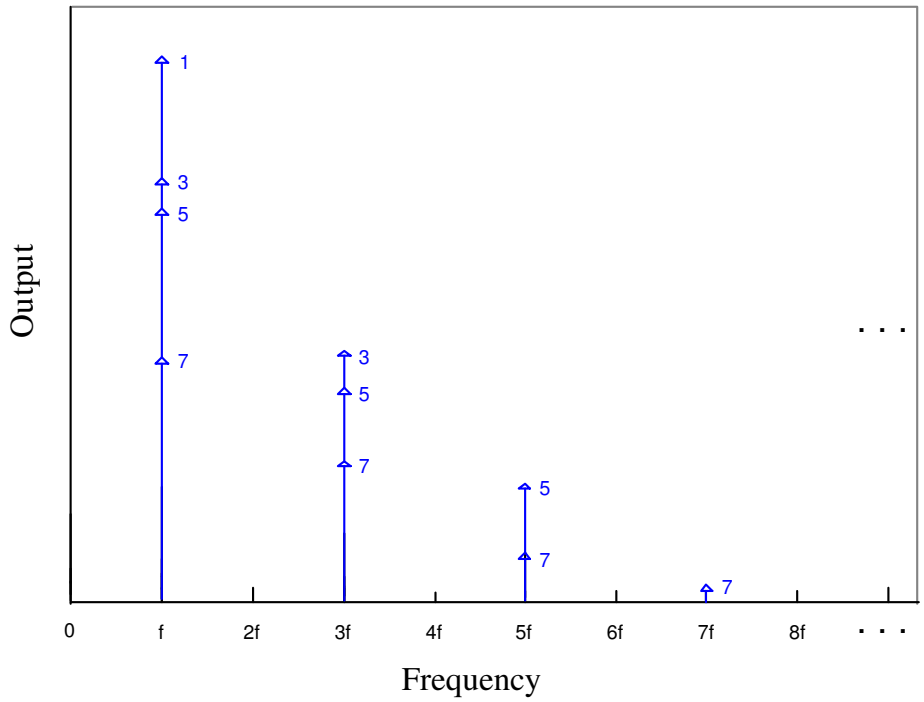

Figure 3.6: Odd-order harmonic components of a nonlinear amplifier represented in frequency domain.

In the same way, an Nth-order nonlinearity, N even or N odd, are represented by Equations (3.6) and (3.7) [5], respectively.

$$P_{OUT}(t) = K_0 + \sum_{n=1}^{N/2} \binom{2n}{n} \frac{K_{2n} P_{IN}^{2n}(\omega)}{2^{2n}} + \sum_{n=1}^{N/2} \frac{K_{2n} P_{IN}^{2n}(\omega)}{2^{2n-1}} \sum_{l=1}^{n} \binom{2n}{n-l} \cos(2l\omega t) \tag{3.6}$$

$$P_{OUT}(t) = \sum_{n=1}^{(N+1)/2} \frac{K_{2n-1} P_{IN}^{2n-1}(\omega)}{2^{2n-2}} \sum_{l=1}^{n} \binom{2n-1}{n-l} \cos[(2l-1)\omega t] \tag{3.7}$$

In the case of even-order nonlinearities, the distortion can be eliminated by filtering the harmonics and suppressing the generated DC component. However, odd-order nonlinearities will affect the amplitude of the fundamental frequency, as illustrated in Figure 3.6. Therefore, specialized linearization methods, as the ones presented in Section **??**, are necessary to minimize this distortion.

3.1.4 1 dB compression point and back-off parameter

The 1 dB Compression Point (1 dB CP) of an amplifier indicates where the characteristic of an amplifier changes from linear to saturated. In other words, the 1 dB compression point is where the gain characteristic of a nonlinear amplifier deviates 1 dB from the characteristic of an ideal amplifier, as shown in Figure 3.7.

The back-off parameter is also illustrated in Figure 3.7. This parameter indicates the difference between the reference saturation level (maximum output power or 1 dB CP) and the average signal power. The back-off parameter is commonly used by circuit designers to determine how close to the 1 dB compression point the average signal power is set.

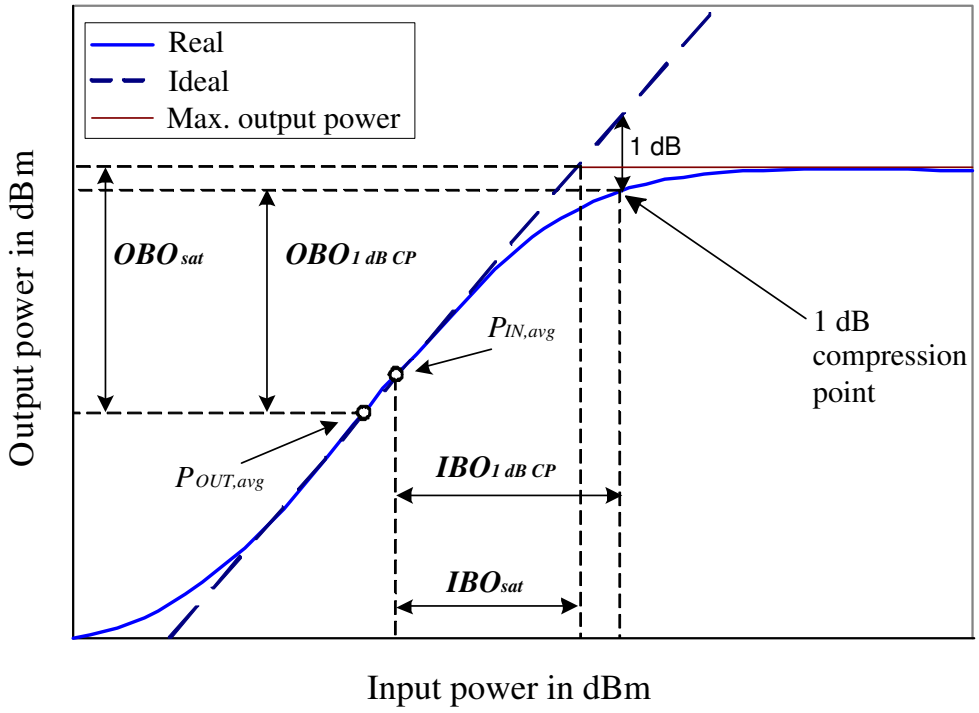

Figure 3.7: 1 dB compression point and back-off parameter.

The back-off point of an amplifier can be referred to as input (IBO) or output (OBO) levels and to saturation level (sat) or 1 dB compression point, as shown in Figure 3.7. The simplest approach is the output back-off, which is useful in system simulations, especially when referred to the saturation level (OBO_{sat}), and in circuit design, when referred to the 1 dB compression point (OBO_{1dBCP}) of the analyzed amplifier.

In general, the output back-off is easily calculated with Equation (3.8), where $P_{OUT,max}$ is the maximum output power given by the amplifier (or the 1 dB CP if referenced to it) and $P_{OUT,avg}$ is the average signal power measured from the output of the amplifier.

$$OBO = 10\log_{10}\left(\frac{P_{OUT,max}}{P_{OUT,avg}}\right) \tag{3.8}$$

The back-off parameter is calculated when a signal is introduced to an amplifier at a specific bias point. This is not the case when doing single-tone signal measurements, where input signals of different bias points are applied to the amplifier in order to perform a power-sweep or frequency-sweep measurement. Consequently, the back-off will not be calculated in this thesis but is recommended when testing specific signals, such as modulated or noisy signals.

3.1.5 AM-AM and AM-PM characteristics

The harmonic distortion concepts explained before are concentrated on amplitude nonlinearity, which is always present in nonlinear amplifiers, with or without memory. This distortion can be understood as the nonlinear relation between the input and output power of an amplifier, which is often called Amplitude Modulation to Amplitude Modulation (AM-AM) characteristic of an amplifier. The AM-AM characteristic is the conversion between the amplitude modulation present in the input signal and the amplitude modulation present in the distorted output signal. An example of the AM-AM characteristic of a nonlinear amplifier is presented in Figure 3.8(a).

Another effect, present in amplifiers is the conversion from Amplitude Modulation to Phase Modulation (AM-PM), illustrated in Figure 3.8(b). If an input carrier $P_{IN}(t)$ with a modulating signal of the form of Equation (3.9) is applied to an ideal amplifier, a zero output phase shift as in Equation (3.10), where K_ϕ is a phase shift constant, will be obtained. However, nonlinear amplifiers present memory effects and, therefore, phase distortion, in which case, the output phase is represented by Equation (3.11), where ω_C is the angular frequency of the carrier signal and ω_M is the angular frequency of the modulating signal.

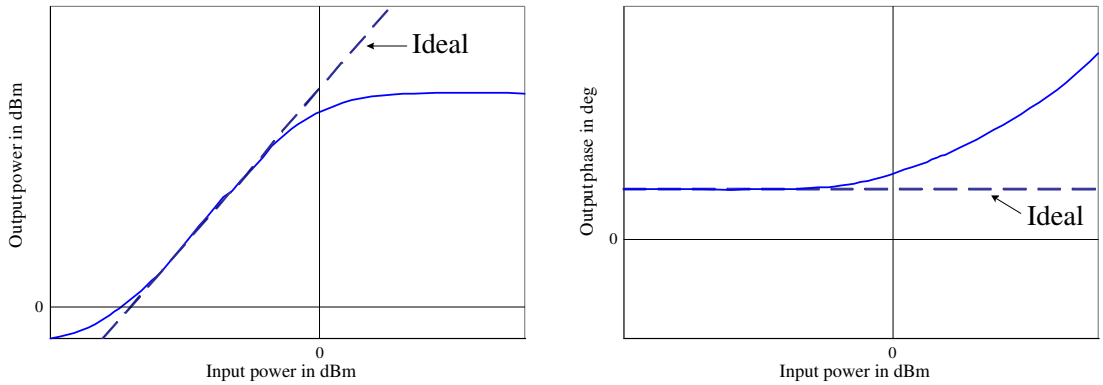

(a) AM-AM conversion (b) AM-PM conversion

Figure 3.8: Amplitude and phase distortion of a nonlinear amplifier represented respectively AM-AM and AM-PM transfer characteristics.

$$M(t) = A_M \cos(\omega_M t) \tag{3.9}$$

$$\Phi(P_{IN}(t)) = K_\phi \tag{3.10}$$

$$\Phi(P_{IN}(t)) = K_\phi \cos[\omega_C t + A_M \cos(\omega_M t)] \tag{3.11}$$

In general, if an amplifier is operated in the linear region, AM-AM and AM-PM characteristics are difficult to measure, since the harmonic components are very small compared to the strong fundamental signal. Therefore, it is easier to measure and analyze distortion tones as presented in the following sections.

3.1.6 Frequency sweep

The above measures represent instantaneous nonlinear characteristics of amplifiers. Since they do not consider memory effects (other than AM-PM conversion), the frequency-dependent behavior of the system cannot be described.

When describing narrowband devices, memory effects are often neglected since they are very small compared to the device capabilities. However, in wideband devices, memory effects can be strongly present and frequency-dependent models will produce more accurate models.

For this purpose, frequency-sweep measurements are used, where the gain and output phase of the tested amplifier are swept throughout the whole frequency band, as shown in Figures 3.9(a) and 3.9(b), where the frequency dependency of the amplifier characteristics can be noticed.

The results of this kind of measurements are useful in modelling frequency-dependent amplifiers with methods as Volterra series, Hammerstein, Wiener and Saleh models as discussed in [5].

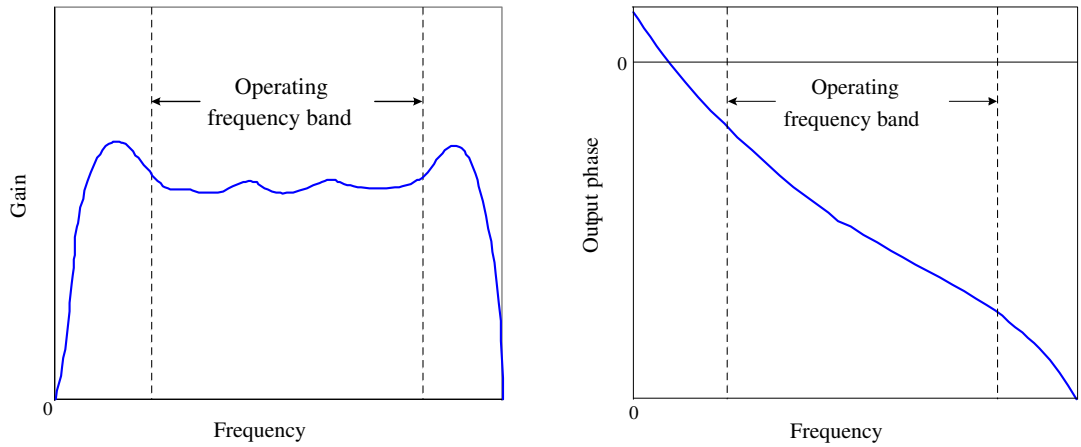

(a) Gain characteristic (b) Phase characteristic

Figure 3.9: Frequency sweep of amplifier transfer characteristic.

3.2 Distortion measures using two-tone signals

In addition to harmonic components and compression, the output of an amplifier that is fed with a multi-tone signal will contain intermodulation products or IMD, which appear inside the fundamental frequency band and are, therefore, difficult to filter away. Here, a two-tone signal is analyzed since it is the simplest possible multi-tone signal and because a very well known method to measure amplifiers, the two-tone test, is based on it.

In a two-tone test, a signal like the one defined by Equation (3.12) and depicted in Figure 3.10 is applied to the Device Under Test (DUT). The envelope of this input signal is varied throughout its complete range in order to test the whole transfer characteristic of the DUT.

$$P_{IN}(t) = A_1 cos(\omega_1 t) \; + \; A_2 cos(\omega_2 t) \tag{3.12}$$

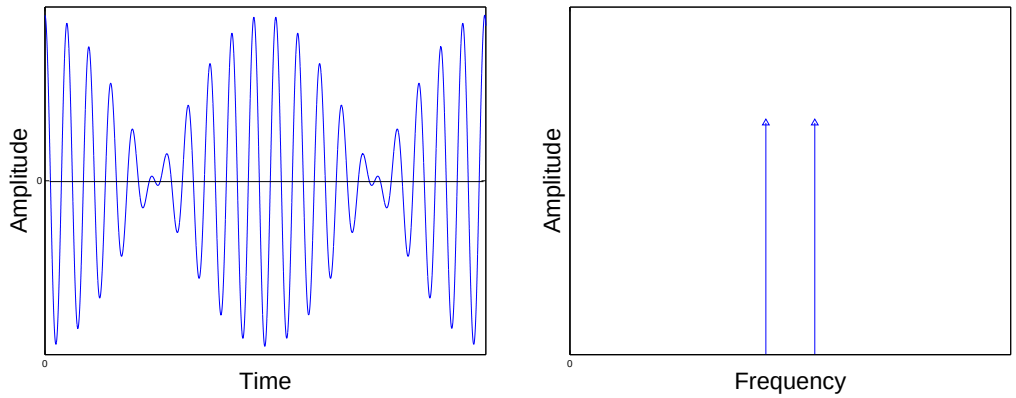

(a) Time domain (b) Frequency domain

Figure 3.10: Illustration of a two-tone signal.

3.2.1 Intermodulation products

In general, when a two-tone signal is applied to a nonlinear amplifier, harmonic zones will be generated, as explained in the previous section. Furthermore, new frequencies called Intermodulation Products (IMP) will be presented and will be of the form shown in Equation (3.13) [14], where f_1 and f_2 are the frequencies of the two input tones, m and n are positive integers (excluding zero) and $m + n$ is equal to the order of the amplifier nonlinearity.

$$f_{IMP} \; = \; m \; f_1 \; \pm \; n \; f_2 \tag{3.13}$$

According to Equation (3.13), when a two-tone signal is applied to an amplifier with second order transfer characteristic, additional frequency components will appear at $f_2 - f_1$ and $f_1 + f_2$. Additionally, each of the two input tones will have a second harmonic at $2f_1$ and $2f_2$, respectively, as explained in the Section 3.1.

Similarly and based on Equation (3.13), a two-tone signal applied to a third order nonlinear amplifier will generate the following frequency components:

$$
\begin{aligned}
f_{IMP1} &= 3f_1 \\
f_{IMP2} &= 3f_2 \\
f_{IMP3} &= 2f_1 + f_2 \\
f_{IMP4} &= f_1 + 2f_2 \\
f_{IMP5} &= 2f_1 - f_2 \\
f_{IMP6} &= 2f_2 - f_1
\end{aligned}
$$

Again, each of the input tones will have a third harmonic at three times the original frequencies. Furthermore, compression will affect the fundamental tones due to partial cancellation, as presented in the previous section.

Similarly to the second and third order nonlinearities, a two-tone signal applied to higher-order nonlinear amplifiers will affect the output signal by adding intermodulation products and harmonic components. The most commonly analyzed distortion is the one generated in the fundamental frequency band, simply called in-band distortion. In-band distortion is caused by odd-order nonlinearities, as shown in the example of Figure 3.11, where f_0 represents the center frequency of the input signal.

As presented in Figure 3.11, the Third Intermodulation Product (IMP3) is usually the strongest and closest frequency component to the fundamental output signal and, consequently, it is difficult to filter out. Therefore, for characterization and linearization purposes we are mainly interested in measuring the IMP3.

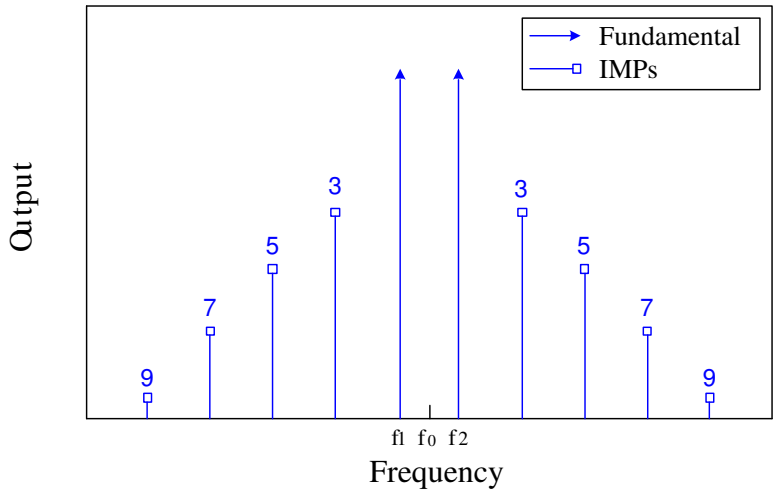

Figure 3.11: Ninth-order nonlinear amplifier in-band distortion (intermodulation products) in frequency domain when using a two-tone input signal.

Furthermore, Figure 3.12 shows the in- and out-of band harmonic components and intermodulation products generated when applying a two-tone signal to an amplifier with a seventh order nonlinearity.

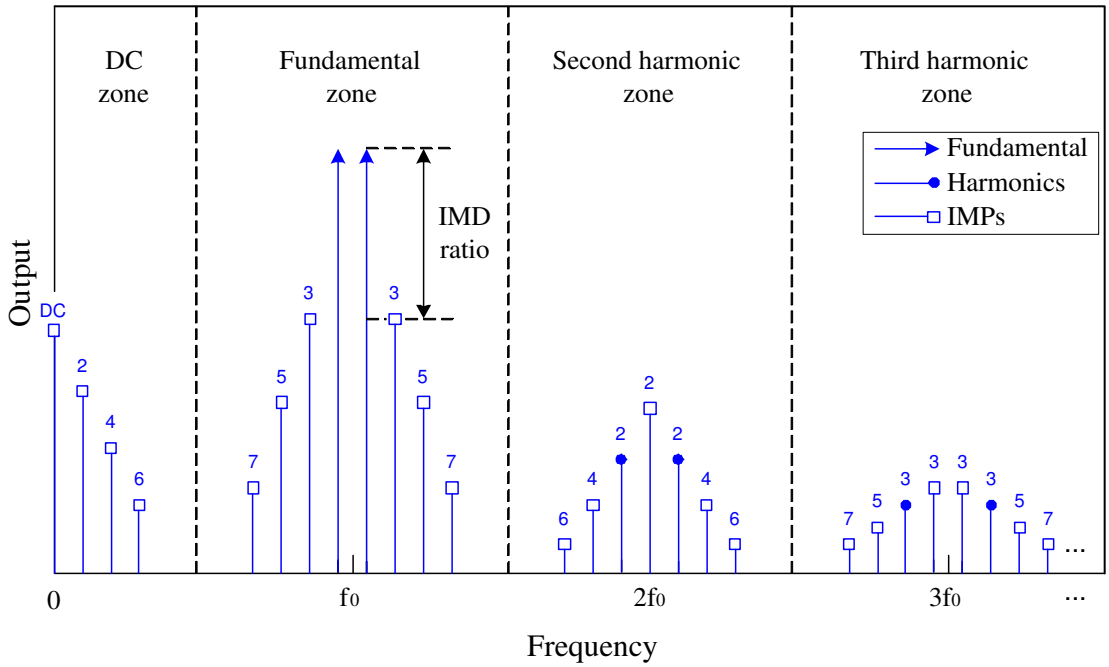

Figure 3.12: Seventh-order nonlinear amplifier response in frequency domain when using a two-tone input signal [14].

3.2.2 Intermodulation distortion ratio (P_{IMR})

The difference between the amplitude of the highest IMP and one of the two tones is called intermodulation distortion ratio (P_{IMR}) and is a common measure of IMD. In the ideal case when the input signal has equal tone levels (i.e. $A_1 = A_2$ in Equation (3.12)), the highest IMP will generally be the third-order products. IMD ratio is presented in Figure 3.12 and mathematically it is expressed as in Equation (3.14) and, when expressed in dB, by Equation (3.15), where $P_{OUT,A1}$ is the output power in one of the input tones.

$$P_{IMR} = \frac{P_{IMD}}{P_{OUT,A1}} \tag{3.14}$$

$$P_{IMR,dB} = P_{IMP3,dBm} - P_{OUT,A1,dBm} \tag{3.15}$$

3.2.3 IMD and Carrier-to-Noise Ratio (CNR)

When noise is present in a system affected by IMD, the Carrier-to-Noise Ratio (CNR) will be degraded according to Equation (3.16), where CNR_I is the CNR caused only by the system noise and C_{ID} is the difference between the Carrier-to-Interference Ratio (CIR) and the intrinsic CNR. The referred "intrinsic" noise is the noise generated by the system itself, without including any IMD, which is usually negative, implying that the system noise is higher than the one caused by the IMD.

$$CNR_{N\&IMD} = CNR_I - 10\log\left(1 + 10^{C_{ID}/10}\right) \tag{3.16}$$

For measurement purposes, noise is not included in the system (except the unavoidable intrinsic system noise). Therefore, CNR will not be calculated in this research. However, CNR is a good measure of distortion when noisy signals are applied to a system.

3.2.4 Spurious signals

Signals different than the fundamental tones, harmonic components and IMPs may appear at the output of an amplifier, which are called spurious signals. These signals may not keep any obvious relationship with the signals being amplified and may appear, disappear, move between frequencies and change level randomly.

Spurious signals consist on low-level Radio Frequency (RF) oscillations, as well as external interference caused by the high proximity of other devices in the same system. This is one of the main reasons to search for extremely stable and robust amplifiers for wireless communications.

3.3 Distortion measures using multi-tone signals

The earlier presented two-tone signal gives a good indication of the degree of distortion present in an amplifier when operating it with simple signals. However, most modern systems are based on more complex signals and therefore, other measurements are required. For example, Orthogonal Frequency Division Multiplexing (OFDM) signals are a special type of multi-tone signals, which have become very popular in modern communications due to its immunity to multipath fading channels [16].

In an OFDM transmission, the channel bandwidth is split into multiple parallel transmissions or subcarriers. In the frequency domain, the subcarriers overlap with each other, which is the main difference with the simple Frequency Division Multiplexing (FDM) method [18]. Moreover, the signals transmitted in these subcarriers are orthogonal with each other, which means that they can be clearly separated without causing any crosstalk. The spectrum of an OFDM signal with four subcarriers (fc) is illustrated in Figure 3.13, where the overlapping and the orthogonality of the signals can be easily appreciated.

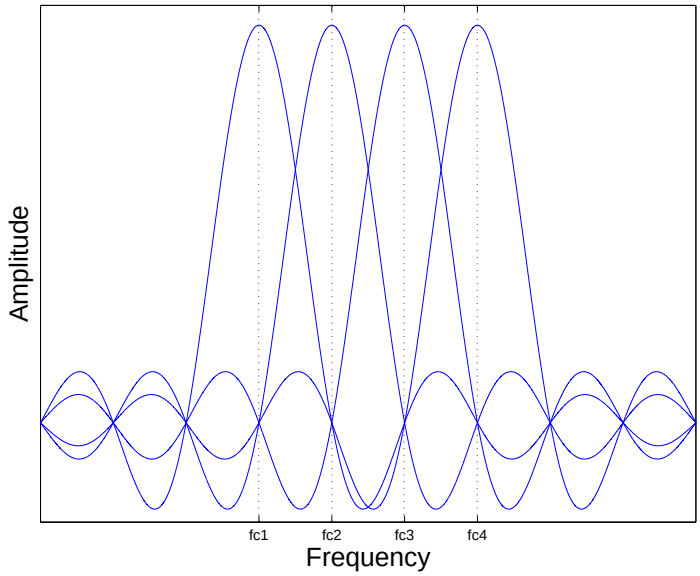

Figure 3.13: Orthogonal frequency division multiplexing signalling in frequency domain.

In this thesis, a multisine signal was chosen as test signal to perform multi-tone measurements, since it is the simplest example of a high Peak-to-Average Ratio (PAR) signal. When the bias of the amplifier is set near to the saturation zone,

the high peaks of the multisine signal are clipped at the output of the amplifier. It is possible to avoid this by setting the bias of the amplifier at a lower input level, which will result in a lower output power level. Operating the amplifier at a low bias means that it is operated at a low efficiency rate. Therefore, the problem of amplifier nonlinearity has a major effect on signals with high PAR, such as the chosen multisine signal or the more complex OFDM signal [19]. A more detailed PAR analysis in multicarrier transmission systems can be found in [20].

The chosen multisine signal ($M_s(t)$) consist of several simultaneously generated sinewaves, with constant frequency spacing, random phase (Φ) and amplitude (A) [21] and defined by Equation 3.17, where n is a positive integer and f_b is the basic frequency. Furthermore, the way of producing a practical multisine signal for measurement purposes is analyzed in Section 5.2.4.

$$M_s(t) = \sum_{k=1}^{N} A_k \cos(2\pi n_k f_b t + \Phi_k) \tag{3.17}$$

Multisine signals are a good approximation of modulated excitations and, therefore, they are widely used to test RF amplifiers. Using multisine signals instead of modulated ones for multi-tone measurements has advantages such as having good control of PAR characteristic and being easier to generate.

In general, multisine signals can be used for diverse purposes such as assessing the intermodulation distortion of RF components [22], modelling the behavior of RF circuits with short-memory effects [23] and modelling amplifiers with the Wiener-Hammerstein model [24, 25]. Moreover, special types of multisine signals can be generated for specific applications. For instance, odd-odd multisine signals, which are used as a simple test to measure the best linear approximation [26], minimum crest factor multisine signals for fast nonlinear system recognition [27] and paired multisine signals for identification of nonlinear cascade systems [28].

For any kind of multi-tone signals (e.g. multisine and OFDM signals) some standard measurements have been defined in order to determine the degree of unwanted signal energy caused by the nonlinearity of an amplifier. Next, these multi-tone nonlinearity measures are presented.

3.3.1 Adjacent Channel Power Ratio (ACPR)

The adjacent channel power ratio represents the distortion affecting adjacent channels due to the amplifier nonlinearity, as shown in Figure 3.14. It is defined as the ratio of the power in a bandwidth (P_{B2}) at certain offset (f_{off}) from the center frequency (f_0) divided by the power of the desired bandwidth (P_{B1}) situated around the center frequency.

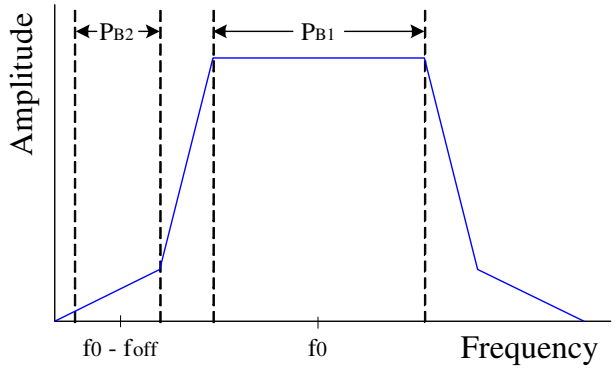

Figure 3.14: Adjacent channel power ratio.

3.3.2 Multi-tone Intermodulation Ratio (MIMR)

The distortion caused by an amplifier in a multicarrier signal is represented by the multi-tone intermodulation ratio. MIMR is defined as the ratio of the wanted tone power and the power highest IMP outside of the wanted band, as presented in Figure 3.15.

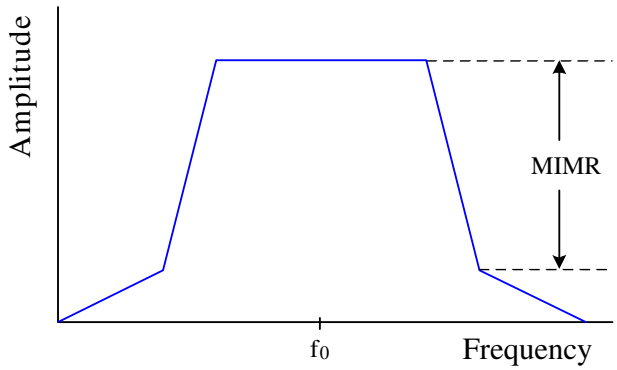

Figure 3.15: Multi-tone intermodulation ratio.

3.3.3 Noise Power Ratio (NPR)

The noise power ratio measures the in-band distortion power caused by an amplifier. It is commonly measured by extracting a portion of the input signal using a notch filter and comparing it with the extracted portion of the amplifier output, as depicted in Figure 3.16. In other words, it is the ratio of the noise power spectral density of a white noise applied to an amplifier, to the noise power spectral density without the amplifier.

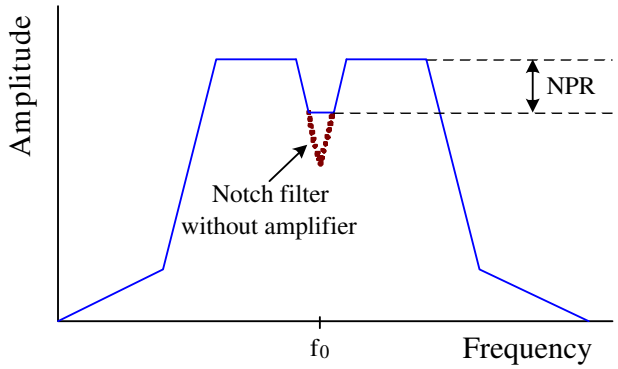

Figure 3.16: Noise power ratio.

3.3.4 Phase distortion

Phase distortion occurs when the frequency components of an input signal are delayed in different proportions by an amplifier. Consequently, any multi-tone signal (including two-tone signals) can be affected by this kind of nonlinearity. Phase distortion is usually caused by amplitude or frequency sensitive components, such as ceramic capacitors.

As an example, Figure 3.17 shows the first three frequency components of a square-wave input affected by different delays, resulting in a distorted output signal.

The relationship between time delay (τ) and phase shift (ϕ) is expressed in Equation (3.18), where f is the fundamental frequency and the phase shift is expressed in radians.

$$\tau = \frac{\phi}{2\pi f} \tag{3.18}$$

Note that if the phase shift increases proportionally to the frequency, the time delay will be the same for all frequency components. Therefore, in order to eliminate phase distortion of the output signal of an amplifier, the delay should be constant, which corresponds to linear phase.

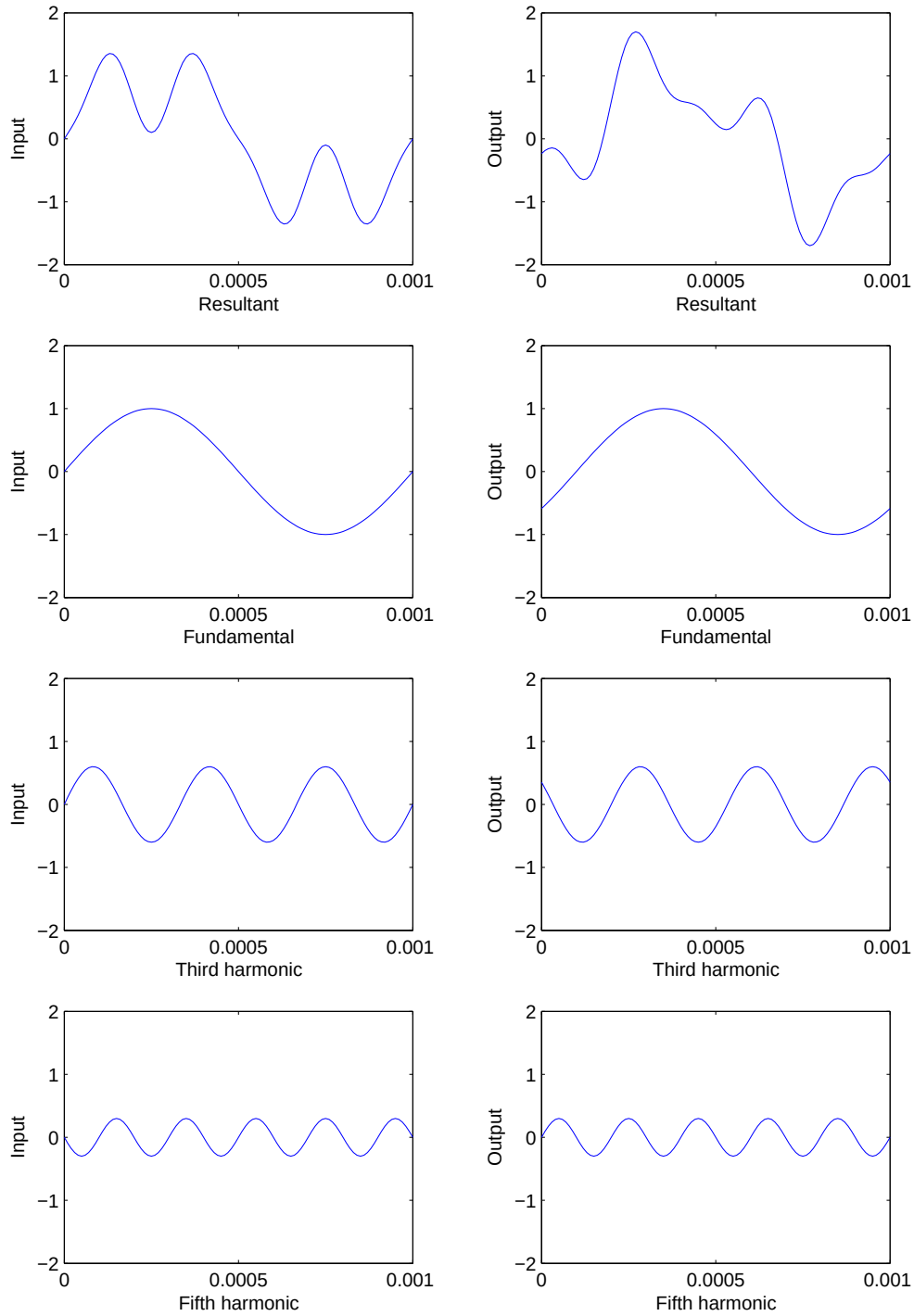

Figure 3.17: Phase distortion in time domain of a 1 kHz squarewave (Input $= \sin(2\pi ft) + 0.6\sin(2\pi(3f)t) - 0.3\sin(2\pi(5f)t)$*) applied to an amplifier with phase distortion, producing delays of 100 µs, 200 µs and 300 µs in the fundamental, third harmonic and fifth harmonic, respectively.*

3.4 Summary of the chapter

The most common distortion parameters obtained from measurements using different signals applied to power amplifiers were summarized in this chapter. Harmonic distortion appearing at frequencies multiple of the fundamental frequency is the main nonlinear effect produced by single-tone input signals. Moreover, AM-AM and AM-PM characteristic curves respectively show the output amplitude and phase behavior when varying the input signal. However, it is necessary to perform a frequency-sweep measurement, in order to represent the memory effects introduced by amplifiers. Other parameters obtained using single-tone input signals are the back-off, second- and third-order intercept points and the 1 dB compression point. The two last of these are commonly used by manufacturers as indicators of amplifiers' linearity.

When measuring the linearity of an amplifier it is convenient to use a two-tone input signal since, besides the harmonic distortion, intermodulation products will be shown in the output spectrum. The third intermodulation product present in the fundamental zone is the most important parameter obtained from a two-tone test because it is the frequency component closest to the fundamental tone and, therefore, it is difficult to filter out with simple methods.

A multisine signal was chosen in this research for measuring the effects of a nonlinear amplifier over high peak-to-average ratio signals. The characteristics of multisine signals, as well an introduction to Orthogonal Frequency Division Multiplexing (OFDM) transmission scheme, were given. Finally, the most common measures of nonlinearity obtained with multi-tone signals (adjacent channel power ratio, multi-tone intermodulation ratio and noise power ratio) were summarized.

Chapter 4

Background for planning measurements

Chapter 2 described the main characteristics of power amplifiers. Ideally, an amplifier should linearly increase the power applied to it. However, in practice, amplifiers behave in a nonlinear way, which usually causes unwanted distortion in the output of the system where the amplifier is used. Measures of amplifier distortion were presented in Chapter 3.

When the predominant distortion affecting an amplifier in a system is known, it is possible to model the nonlinearity by using an adequate estimator. This means that the data obtained from measurements of power amplifiers can be used to characterize and, later on, alleviate the nonlinearity introduced by amplifiers to a system.

This chapter provides a summary of theoretical background needed to determine the type of measurements that will better characterize amplifier distortion. First, an overview of methods for modelling nonlinear power amplifiers is given. Finally, the theory necessary to estimate the parameters required to model amplifiers is summarized.

4.1 Methods for modelling power amplifiers

Models that represent the nonlinearity of an amplifier can be accurately designed based on measurement results, such as the ones introduced in Chapter 3. In general, methods for modelling amplifiers can be classified according to the memory characteristics of the amplifier into memoryless models and models with memory [29].

Models for memoryless nonlinearities or *Zero-Memory Nonlinearity (ZMNL)* can be subdivided into two approaches. The first of these is an analytical approach, referred as memoryless baseband nonlinearity, which is based on an input signal whose power spectrum is concentrated around zero frequency. The second approach is the memoryless bandpass nonlinearity, which is mainly an empirical approach since it is characterized by measurements performed on the amplifier to be modelled.

Memoryless models are an idealization of practical systems since no physical device is truly frequency-independent, which is a requirement for a memoryless model. Therefore, *Nonlinearity with Memory (NLWM)* models are a more accurate approach for nonlinear power amplifiers.

The most commonly used ZMNL and NLWM modelling methods [29] are summarized in Figure 4.1, including references to each particular method.

An example of the application of the polynomial and Hammerstein models to characterize the ZVE-8G amplifier [5] is described in Section 7.2. This model is based on measurements performed as part of this research and is introduced in this thesis as a way or proving the usefulness of amplifier measurements.

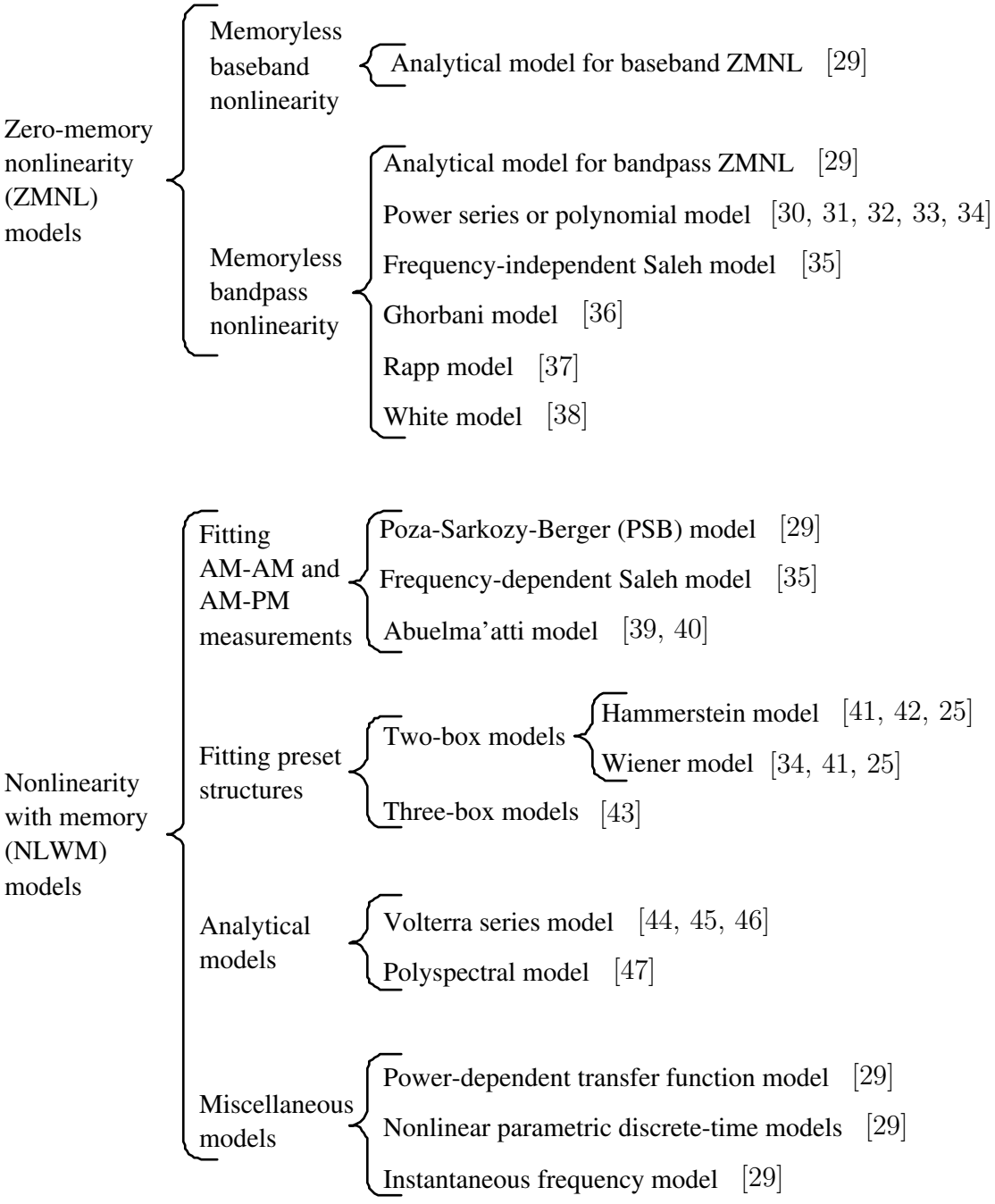

Figure 4.1: Proposed classification of commonly used modelling methods.

4.2 Parameter estimation theory

Estimation theory is applied in many modern systems, such as radar, control and communications, where the values of a set of parameters need to be estimated. In the specific case of amplifier characterization, it is necessary to estimate the parameters needed to model the nonlinear behavior of the amplifier.

In general, the problem of parameter estimation can be mathematically described as finding the unknown parameter ξ on which the R-point data set $\{d[0], d[1], ..., d[R-1]\}$ depends. Thus, Equation (4.1) defines the estimator of ξ, where g is some function [48].

$$\hat{\xi} = g(d[0], d[1], ..., d[R-1]) \tag{4.1}$$

First, it is necessary to model the data, in order to find a good estimator. Since the data is intrinsically random, the Probability Density Function (PDF), represented by $p(d[0], d[1], ..., d[R-1]; \xi)$, is used to describe it. This shows that there will be a different PDF for each different ξ, since the PDF is parameterized by ξ. Equation (4.2) presents an example of the PDF of the data when $R = 1$ and ξ is the mean.

$$p(d[0]; \xi) = \frac{1}{\sqrt{2\pi\sigma^2}} \exp\left[-\frac{1}{2\sigma^2}(d[0] - \xi)^2\right] \tag{4.2}$$

Once the PDF is specified an estimator can be determined based on Equation (4.1). However, in practice, the PDF is not given but it is necessary to choose one that is mathematically manipulable and consistent with the problem background. Therefore, the performance of an estimator critically depends on the assumptions done when choosing a PDF.

The *classical estimation* approach is the one based on PDFs similar to the one in Equation (4.2), where the parameter of interest is deterministic but unknown. When a priori knowledge exists, the unknown parameter is no longer deterministic but random and a *Bayesian estimation* approach is used instead. Then, the data is described by the joint PDF, as shown in Equation (4.3), where $p(\mathbf{D} \mid \xi)$ is a conditional PDF, summarizing the a priori knowledge of $\mathbf{D}$ conditioned on knowing ξ, and $p(\xi)$ is the prior PDF, summarizing ξ knowledge before any data is observed.

$$p(\mathbf{D}, \xi) = p(\mathbf{D} \mid \xi)p(\xi) \tag{4.3}$$

Three important points to keep in mind when choosing an estimator are:

- The performance of an estimator can only be completely described statistically or with its PDF, since an estimator is a random variable.
- Computer simulations for evaluating the performance of an estimator are never conclusive. This means that, in the best case, these simulations will give a desired accurate level of the true performance. However, if there are errors or insufficient number of experiments in the simulations, mistaken results might be obtained.
- There is a tradeoff between the performance of an estimator and the computational complexity. Consequently, optimal estimators are sometimes difficult to implement and, therefore, suboptimal estimators might be preferred.

Figure 4.2 summarizes the most commonly used optimal estimators [48], including references to each one. As mentioned in Section 4.1, the polynomial and Hammerstein models have been applied to the amplifier tested in this research. In order to obtain the parameter values of these models, the Least Squares Estimator (LSE) and Weighted Least Square Estimator (WLSE) were respectively used, as further described in Section 7.2.

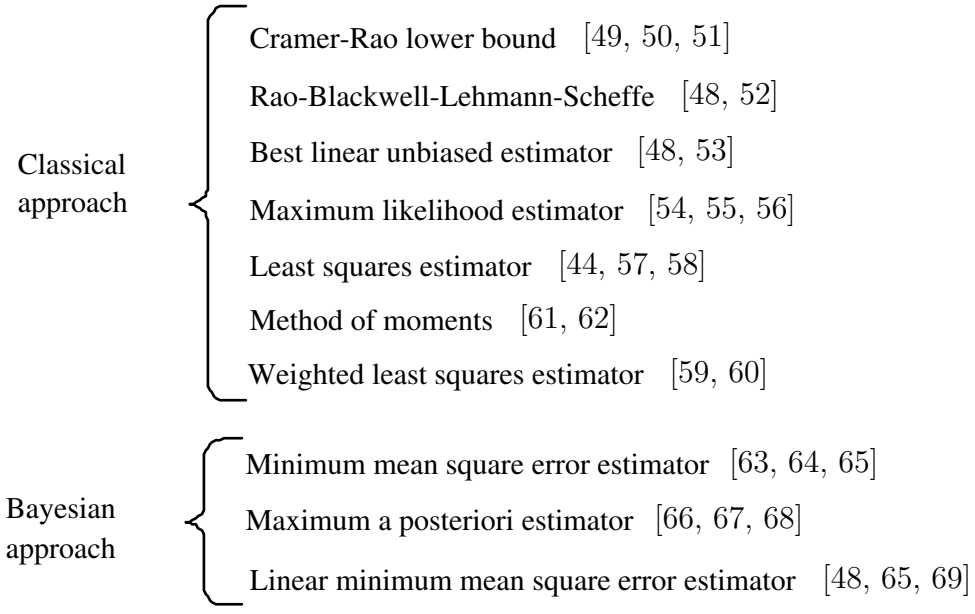

Figure 4.2: Proposed classification of commonly used estimators.

4.3 Summary of the chapter

Processing of the data obtained from the measurements performed in this thesis in order to alleviate amplifier distortion was discussed in this chapter. First, a brief overview of methods to model power amplifiers was done, including some references for more information. Moreover, the measurements performed in this research can be used in some of these methods, such as the Hammerstein model applied to the amplifier tested in this thesis [5].

Next, parameter estimation concepts useful when modelling amplifier nonlinearity were introduced. Classical and Bayesian estimation approaches were defined by the Probability Density Function (PDF) and the joint PDF, respectively. Furthermore, the most commonly used estimators were summarized and references of each were given.

The concepts covered in this chapter will not be practically applied in this thesis since the objective of the research is mainly to obtain the necessary parameters to model power amplifiers by performing different types of measurements. However, this theory gives a good background that is helpful when planning the type of amplifier measurements to be performed. Nevertheless, an example of the implementation of the results obtained in this thesis on modelling an amplifier can be found in [5] and will be briefly covered in Section 7.2.

Chapter 5

Power amplifier measurement planning

The previous chapters have covered the basic concepts about amplifier distortion. As mentioned in Chapter 3, memoryless distortion can be represented by parameters obtained from single-tone measurements, such as the AM-AM and AM-PM characteristics, which respectively show how the amplitude and phase of the output changes when varying the input power level. However, for systems with memory or when using non-constant envelope modulated input signals, it is preferable to perform a two-tone transfer characteristics measurement. Furthermore, for systems using more complex signals (e.g. OFDM signals), multi-tone measurements are recommended in order to characterize the amplifier as accurately as possible.

In this chapter, the basic knowledge required to perform amplifier measurements is summarized. First, comments on the importance of careful and good planning are given. Next, a brief description of the characteristics of the input testing signals, the equipment used, calibration procedure and noise considerations is done. Finally, the way of performing different types of amplifier tests is described, including the performance parameters, setup systems and processes for each measurement.

5.1 Before measurements

When making measurements of any kind of device, the most important is to test them "correctly". There are many factors involved in the correct testing of devices because, opposite to simulating environment, in practice there are not perfect systems.

Errors introduced for example by connector mismatches or cable losses can change the results but can be minimized by careful planning. Other areas where problems can occur are briefly described next [70]:

- Analyzing beforehand which parameters will best characterize the Device Under Test (DUT) and then, test only these will save time by avoiding doing unnecessary measurements. Moreover, the most important information of the DUT will be obtained.

- In order to have correctly done measurements, it is necessary to have the proper equipment, put it in the right order and know how to operate it. In other words, it is useful to have a setup system proper to test the wanted parameters.

- The procedure to perform measurements should be carefully planed and analyzed in order to find the possible errors, losses and power levels needed that may affect the results. Therefore, it is important to know how to perform the desired measurement.

- It is always convenient to get the parameters to be measured displayed in the screen. However, in some cases it might be needed to make some calculations in order to obtain the desired data. A proper understanding of the measuring equipment capabilities will save time and make easier to get the correct data.

The four points covered are meant to emphasize the importance of beforehand careful planning, which might save time and will give not just results but "correct" results.

5.1.1 Choice of input signal

In the specific case of amplifier measurements for modelling purposes, an extra point to those previously mentioned should be taken on count. This aspect consists of choosing the adequate excitation (i.e. input signal) that allows the output data to carry sufficient information on the parameters to be estimated.

Different input signals are used for different measures of amplifier nonlinearity. Single-tone signals are used to perform power and frequency sweeps which will give as result the input-output curves from which the 1 dB Compression Point (1 dB CP) can be extracted. Moreover, harmonic distortion can be easily obtained by using this kind of simple signals. On the other hand, two-tone signals are used to characterize the intermodulation distortion produced by amplifiers. However, the phase relationship and frequency separation of the tones composing signals with more than two tones will affect the Peak-to-Average Ratio (PAR). Consequently, multi-tone signals will enable to test the worst PAR cases. Furthermore, the more tones are used in the input signal, the best approximation of modulated signals response is obtained [71].

A one-sinusoid signal used to measure amplifier nonlinearity has the main advantage of simplicity and, consequently, the results obtained are easy to interpret [72]. The measuring dynamic and frequency ranges constitute the most important factors for single-tone input signal measurements. The dynamic range used for power-sweep measurements should cover a part of the linear zone and the nonlinear zone (i.e. from a low input level to some decibels above the 1 dB CP). On the other hand, the range for frequency-sweep measurements should be enough wide to cover the whole operating frequency range of the amplifier.

AM-AM and AM-PM characteristics obtained from single-tone measurements are static measurements, which may include thermal or DC bias effects. In the wireless communications environment this distortion occurs dynamically, since the amplitude envelope of the signals can vary according to the information rate. Therefore, amplitude and phase distortion are dynamically characterized by measuring the intermodulation distortion using a two-tone signal [43]. The separation of the input tones should be chosen according to the intermodulation product's maximum order to be analyzed. However, this depends on the maximum sampling frequency

of the generator used (i.e. AWG), as it is further explained in Section 5.2.3. Moreover, the input level used to measure the distortion introduced by the amplifier should be as close as possible to the 1 dB CP and the frequency of the two tones should fall inside the amplifier's operating frequency range.

Finally, multi-tone signals are widely used to analyze the distortion introduced by amplifiers, since they provide a good approximation to the response obtained with complex modulated signals (e.g. OFDM). For instance, it is proven that multisine input signals with constant amplitude and random phase spectrum are the most appropriate to accurately model the behavior of nonlinear power amplifiers [73]. Ideally, the input signal should cover the whole frequency band for which the model is desired. In some cases, the equipment availability might limit this range and, therefore, the maximum possible bandwidth should be used. Once more, the input level should be chosen as close to the 1 dB CP as possible, in order to obtained a good measure of the nonlinear characteristic of the amplifier.

5.1.2 Equipment

In this section, a brief description of the working of the devices used for amplifier measurements is given, including signal generators, signal detection devices, auxiliary components and DUTs. For each of these categories, specific devices were chosen in order to fully test the characteristics of the DUT and so, their main parameters are also given, in order to help in the design of test systems and in the planning and interpretation of results done in the following chapters.

Vector Signal Generator

A Signal Generator (SG) gives an AC signal of variable amplitude and variable frequency to be used when operating an amplifier or other circuit. Usually, frequency may be varied from a few hertz to some megahertz or even gigahertz. The amplitude can be adjusted from a few millivolts up to some volts and these values can be also adjusted in millidecibels form. In addition to sinusoidal signals, other commonly used waveforms, such as square or triangular, can be produced with this equipment.

Vector Signal Generators (VSG) have all these functions and, in addition, the ability of producing already modulated signals by using a "vector" or I/Q modulator, such as Phase Shift Keyed (PSK) and Quadrature Amplitude Modulation (QAM) signals.

The specific generator used in this research is the HP/Agilent 8780A Vector Signal Generator [74]. Its main characteristics can be found in Appendix A.1.

Arbitrary Waveform Generator

An Arbitrary Waveform Generator's (AWG) basic functioning is similar to that of a signal generator. The difference consists on its ability to create and modify signals with arbitrary shape, amplitude and/or frequency (including multi-tone signals) in a continued and live mode, meaning that any change on the signal parameters can be instantaneously observable in the device output.

AWGs have the possibility to import and export waveforms generated by other programs (e.g. use as input signal an own generated MATLAB signal saved in a 3 1/2 in. floppy disk), which makes this device very versatile and useful when testing active components that may behave differently for different types of waveforms.

During the measurements done, a LeCroy LW420 Arbitrary Waveform Generator was used [75]. Its most important parameters are summarized in Appendix A.2.

Network Analyzer

A Network Analyzer (NWA) has the capability of testing a device without any other measuring equipment. This is possible since it has its own generator integrated as well as a monitor where graphical results are displayed. Several representations of the waveform used as input can be displayed, as gain and phase for a range of different frequencies and even Schmidt diagrams.

NWAs are very useful when testing a specific component since all "Scattering Parameters" (S-parameters) can be easily analyzed. In a two-port device (e.g. NWA), there are four main S-parameters, named with the following convention:

$S_{\text{OUT IN}}$ $\quad$ OUT = port where signal output is measured
IN = port where signal is applied

Figure 5.1 shows how parameters S_{11} and S_{22} represent port reflections that are used when measuring return loss, Standing Wave Ratio (SWR) [76], reflection coefficients and impedance of the DUT. S_{12} and S_{21} represent, respectively, "forward" and "reversed" directions used for measurements of insertion loss, transmission coefficient, group delay, electrical delay, gain and deviation from linear phase. These last two are basic data to describe amplifiers' nonlinear characteristics. A mathematical analysis of S-parameters can be found in [77].

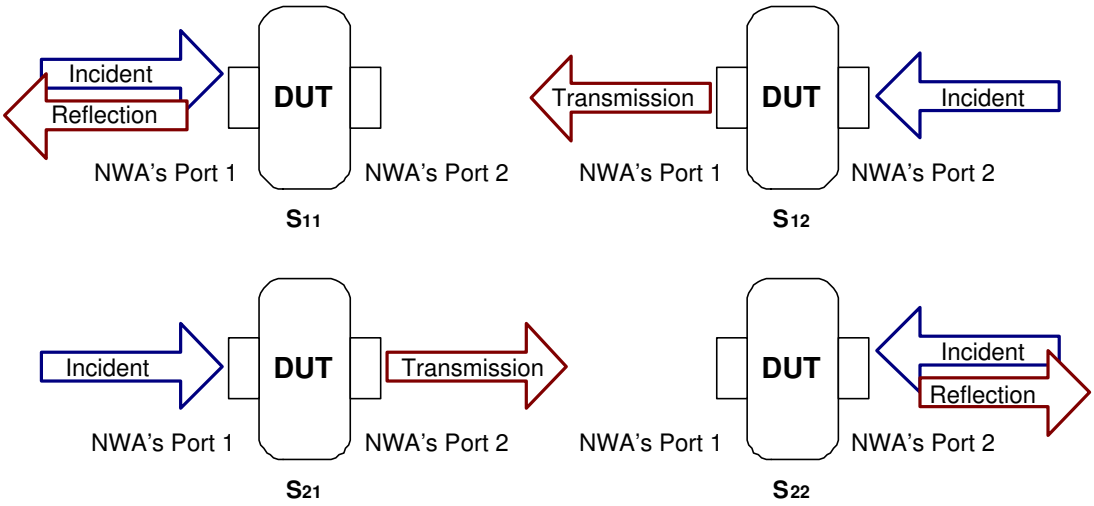

Figure 5.1: S-parameters.

An Agilent Technologies PNA Series Microwave Network Analyzer model E8363A is used in this research. Basically, this device works as a computer, which can be even connected to the internet or to a network printer. Its main characteristics can be seen in Appendix A.3. Note that the specifications shown in Table A.3 are just the ones used for the specific amplifier tested, which range is 2 to 8 GHz. For information on different ranges see [78].

Spectrum Analyzer

A Spectrum Analyzer (SA) is a superheterodyne receiver. This means that it has a local oscillator (variable frequency oscillator) that keeps a difference between itself and the received frequency, resulting in a constant "Intermediate Frequency" (IF).

Its main purpose is to receive a range of signals and display their frequency components in a graphic form. The procedure to do this is based on the relationship between time and frequency domains that can be mathematically analyzed via Fourier transforms.

In a SA, the convolution of a very narrow band-pass filter (ideally an impulse) and the received signal is done, resulting in the frequency domain characteristics (spectrum) of the signal. The filter mentioned is a critical part in this kind of sweeping devices. It is called "resolution filter" and is, in fact, the bandwidth of the intermediate frequency.

In the specific case of amplifier measurements it is very important to analyze the spectrum of its output since different types of distortions may appear on it, as explained on Chapter 3. Other parameters that can be obtained with this device are power, frequency, noise, sensitivity and modulation.

The spectrum analyzer used in this specific measurements is an Agilent Technologies 8564EC. Its more important specifications for the range of the amplifier used are shown in Appendix A.4. The complete data sheet can be found in [79].

Active Components

Components to be measured can be classified as passive and active. The first ones are the devices that do not affect their resistance, impedance or reactance when alternating currents are applied to them. This means that they will consume energy (change energy into other forms than electrical, as heat or light) or store it (as in electromagnetic fields). Examples of these devices are resistors, inductors and capacitors [80]. Passive elements will not be explained in more detail since they are linear devices.

An active component is "1. a component which adds energy to the signal it passes; 2. a device that requires an external source of power to operate upon its input signal(s); 3. any device that switches or amplifies by the application of low-level signals" [81]. In other words and for the purpose of this thesis, active components are the ones that when an AC signal is applied to them their impedance or resistance will change, and so, they will amplify, rectify, modify or distort these

signals. Common active devices are vacuum tubes, diodes and transistors. All these devices may be measured in the same way as the amplifier in this research, since amplifiers are also active components, which are nonlinear elements.

The amplifier used in this thesis is a wide frequency band Mini-Circuits ZVE-8G power amplifier [82]. Its main specifications are summarized in Appendix A.5 and, since it is the most important element in this thesis, it is shown in Figure 5.2.

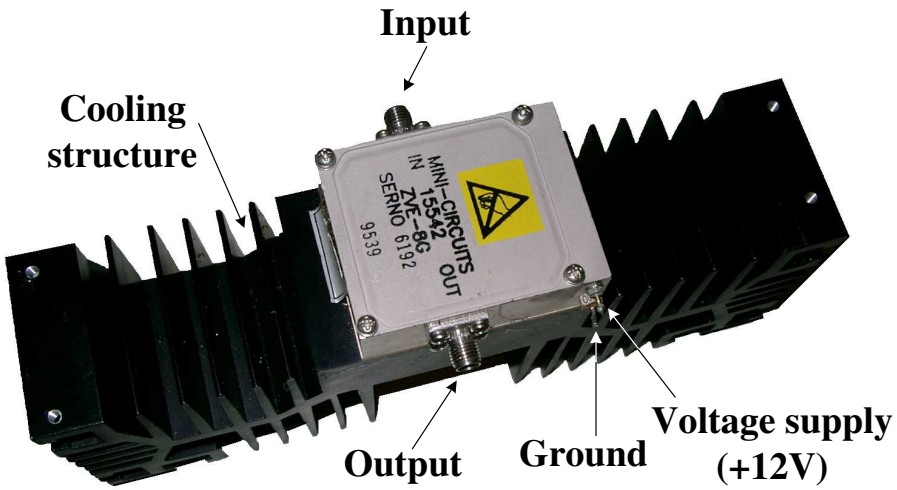

Figure 5.2: Mini-Circuits power amplifier model ZVE-8G, device under test in this thesis, with nominal gain of 30 dB and operating frequency range of 2 to 8 GHz.

Devices needed to perform correct measurements

These devices are the ones that are used to correct the measurements and to make them more accurate. For the purposes of these particular measurements, the only devices of this type used are attenuators, which main task is to avoid errors due to the saturation point of the reading devices (network analyzer and spectrum analyzer).

According to the specifications of Tables A.3 and A.4 the saturation point of the NWA is 0.6 dB with the maximum input level of +5 dBm and the minimum saturation point for the SA occurs with a -5 dBm input level. So, with the purpose of using the same attenuator(s) during the whole set of measurements, the maximum input level to be applied to the reading devices is -5 dBm.

Based on this and for the amplifier used we have the system shown in Figure 5.3 from which we derive the minimum needed attenuation (Att) equal to 38 dB (with a maximum input power level of +3 dBm to the amplifier). The attenuation used for the measurements in this thesis is 40 dB, due to the availability of equipment at the measuring laboratory. This attenuation is obtained with 10 dB and 30 dB Midwest Microwave attenuators, which main characteristics are shown in Appendix A.6.

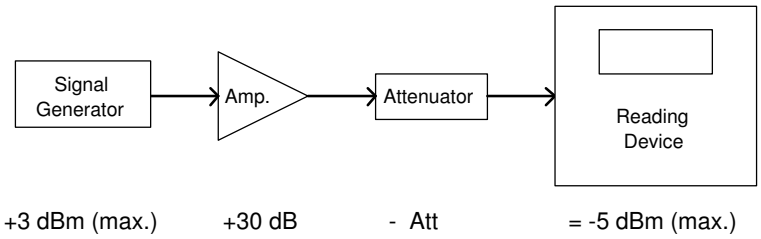

Figure 5.3: System for calculation of attenuation needed for correct measurements.

The maximum input level to the amplifier was calculated based on the attenuators' power specification, which is 2 W. This means that the maximum power applied to them, and so the maximum output power from the amplifier, should be +33 dBm. Then, the maximum input level applied to the input of the amplifier should not be greater than +3 dBm.

With this input level defined, we make sure that the saturation zone of the amplifier will be tested. According to Table A.5, 1 dB compression point of the amplifier, referenced to the output power, is +30 dBm. Therefore, the saturation zone of the amplifier begins at +1 dBm of input level, making the maximum input level (+3 dBm) enough to measure the whole characteristics of the amplifier.

5.1.3 Calibration

There are two types of calibration: instrument calibration and measurement calibration [83]. Every instrument was built to function in a specific way and so, it was set up (calibrated) to accomplish its tasks in a proper way. However, aging, temperature, usage and other factors can vary the equipments' original values and some adjustments might be necessary for their optimum operation. This is the called *instrument calibration* and it is usually done by a technician of the instrument manufacturer company, who ensures that the device is working within the specifications.

On the other hand, *measurement calibration* corrects systematic errors using an equation called error model. The systematic errors are the ones caused by imperfections in the equipment (e.g. adapter interface or interconnecting cables) and test setup. They are predictable, can be calculated and can be mathematically reduced but never totally removed due to limitations in the calibration process. The amplitude at the DUT input and the frequency response accuracy are some of the most important parameters that may be affected with an uncalibrated device.

Measurement calibration is recommended when:

- the best possible accuracy is desired
- adapting to a different connector type
- connecting cables in the system
- measuring through a wide frequency span
- connecting auxiliary devices in the input or output of the DUT

Each measuring device has its own calibration method(s) that should be performed to assure that the obtained results are less affected by external factors to the DUT. In the particular case of amplifier measurements, the calibration process of the NWA and the SA will be discussed in more detail in Section 5.2.1.

5.1.4 Noise

In radio frequency and microwave measurements, the ultimate sensitivity of the detector system is determined by the noise presented to the system and the noise introduced by the system itself. This means that the weakest signal that a system can detect depends on the amount of noise affecting it. This is why good knowledge of the test equipment's noise helps to make the results of measurements more accurate.

Sources of noise can be external to the measurement system or within the system itself. Electrical motors, dirty switch contacts and thunderstorms are examples of external sources. Although these affect all systems, in radio or microwave frequencies the internal sources are predominant and so, these are briefly explained next.

Thermal noise, also called Johnson or Nyquist noise [84, 85], is the most important internal type of noise because it is produced by any kind of component, active or passive, and trends to be dominant in most systems. It refers to the electrical noise that is produced with the random motion of electrons in a conductor due to heat (without average current flowing through the conductor). The current between two points, produced by the movement of electrons, generates a voltage. For RF and microwave frequencies, this voltage has a uniform spectral distribution, which makes this type of noise often called "white noise". Since thermal noise affects active and passive devices, any component in a system will affect the overall system noise by generating "noise power", which is defined as:

$$P_n = ZTB,$$

where P_n is the noise power in watts, T is the absolute temperature of the source, B is the bandwidth of the system and Z is the Boltzmann constant ($\approx 1.38 \times 10^{-23}$ J/°K).

In addition to thermal noise, active devices produce other types of noise. A current in a conductor, produced by random emanation of electrons, generates random fluctuations called shot noise. In vacuum tubes, induced grid noise is produced as a result of fluctuations in the electron stream passing adjacent to a grid. Partition noise occurs in multi-electrode active devices, such as transistors and valves. When the charge carriers in a current have the possibility of dividing between two or more paths, the noise is generated in the resulting components of the current by the statistical process of partition. Finally, Flicker noise, also called contact noise or excess noise, is generated by the imperfect contact between two conducting materials, which causes the conductivity to fluctuate in the presence of a DC current.

Furthermore, the characteristic noise of an amplifier determines how well it performs. The main noise parameters used to specify an amplifier performance [85] are summarized next.

Noise temperature ($\mathbf{T_n}$) Temperature in degrees Kelvin at which thermal noise power is equal to the amount of available noise power (P_n) from the output of the device.

$$T_n = \frac{P_n}{Z} = 7.25 \times 10^{22} P_n$$

Noise ratio ($\mathbf{r_n}$) Ratio of the noise temperature to the actual temperature (T_a). (The noise ratio minus unity is often called excess noise ratio)

$$r_n = \frac{T_n}{T_a} = \frac{P_n}{ZT_a}$$

Noise factor (F) Ratio of the total available output noise power per unit bandwidth to the portion caused by an input with a noise temperature of 290°K.

$$F = \frac{T_n}{290 + 1}$$

Noise figure ($\mathbf{N_f}$) Equivalent of the noise factor in dB, which can be also defined as the ratio of the input Signal-to-Noise Ratio (SNR) to the output SNR.

$$N_f = 10 \log F = 10 \log \left(\frac{SNR_{input}}{SNR_{output}} \right)$$

Effective input noise temperature (T_e) Temperature of the input at which the available noise output power is twice that which would be available if the input were at absolute zero. It determines an input temperature at which the input thermal noise and the internal thermal noise from the device contribute equally to the output noise.

$$T_e = 290(F - 1)$$

Operating noise figure or noise sensitivity (τ_s) Ratio of available noise power from the output when the input is at its normal operating temperature (T_o) to the contribution which the input would make to the available output noise power if it were at the standard temperature (290°K).

$$\tau_s = F - 1 + \frac{T_a}{290}$$

Noise measurements of the previous parameters are used mainly to compare the performance of amplifiers. For the purpose of amplifier nonlinearity measurements, the noise parameters proper to each specific amplifier do not give relevant information. Therefore, noise measurements are not needed in this research and so, they were not performed and analyzed. However, more information about noise measurements can be found in [70] and [77].

5.2 Performing measurements

In this section, the performance parameters, setup systems (based on the equipment introduced in Section 5.1.2) and the process to make different kind of amplifier measurements are described. First, basic measurements of cables and loss due to passive devices are explained. Next, single- and two-tone signal measurement procedures are given. Finally, multi-tone signal testing using a multisine signal is described.

5.2.1 Passive device measurements

When measuring amplifiers, passive devices are included in the setup system. In this thesis, these devices are divided into *devices needed to interconnect measuring systems*, such as cables and adapters, and *devices needed to perform correct measurements*, which in this research consist only of attenuators, as explained in Section 5.1.2.

Devices needed to interconnect measuring systems

Measurements of cables and adapters are done in order to obtain the loss introduced by them. However, it is possible to avoid the effect of this loss in the measurement results by calibrating the measuring equipment including all the cables and adapters used during a particular test.

A THRU response calibration is the simplest that can be performed to NWAs and to SAs including cables and adapters. The THRU response calibration is done by measuring the system without connecting the DUT. In other words, the internal generator of the measuring device is connected to the RF input of the same device.

Next, a THRU response calibration (or transmission calibration) function should be chosen from the calibration menu in the measuring device. In this type of calibration, a frequency sweep will be performed using an internal testing signal. The curve obtained from this sweep is recorded and used as reference to obtain the differences to the normalized values. After the calibration, the measuring device

should show a flat trace of 0 dB gain for the whole frequency range of the measuring device.

The THRU response calibration method was chosen since it is useful when performing transmission measurements in any one direction (e.g. S12 or S21 in a NWA). With this method, frequency response transmission tracking errors are corrected , such as frequency response of connecting cables [83].

Appendix B.1 shows the setup systems used to calibrate the NWA and the SA in this research. In general, they consist of connecting the output of the measuring device's internal generator to the RF input of the same device.

These are simple setups to calibrate the equipment. However, it is important to include all the cables and adapters that are needed to, later on, include the DUT in the system. If it is necessary, it is better to include an extra adapter than leaving out a needed one. The way of connecting the cables and adapters in the setup system is also presented in Appendix B.1.

In this thesis, the devices used to measure amplifiers are a network analyzer and a spectrum analyzer. Although the calibration of these is similar, there are specific commands to be used in each one. The processes to calibrate the specific network analyzer and spectrum analyzer used in this thesis are presented in detail in Appendix C.1.

Notice that in order to ensure the adequate calibration of the NWA and SA frequency- and/or power-sweep measurements should be performed. Therefore, the way to perform these kind of measurements with a NWA and a SA in Appendix C.

Furthermore, the specific settings used to calibrate the network analyzer and the spectrum analyzer, as well as the calibration results of each device can be found in Section 6.1.1.

Devices needed to perform correct measurements

Attenuation measurement is done in order to obtain the attenuation level for different frequencies and input power levels. Ideally, the attenuation level should always be the same, for all the frequencies and for all the input power levels inside the specified operation range. However, in practice, some variations in the attenuation level may occur, which should be taken into account in order to obtain more accurate results.

The setup system used to measure attenuators is shown in Appendix B.2. In these measurements, the attenuators used have the same maximum input power (Table A.6) and therefore, the order in which they are connected does not affect the measurements.

However, special attention should be paid when connecting the attenuators if they have different maximum input power ratings. In this case, the output of the network analyzer should be connected to the input of the attenuator with the highest maximum input power rating. This is done in order to dissipate as much power as possible in the first attenuation stage and, in this way, avoid damaging the other attenuators. Finally, the output of the last stage attenuator should be connected to the RF input of the NWA.

In order to perform accurate attenuation measurements it is necessary to first correctly calibrate the NWA. Next, simple steps are followed to set the device for obtaining the desired parameters. This procedure is presented in Appendix C.3. Furthermore, the results of the attenuation measurements are presented in Section 6.1.2.

5.2.2 Single-tone signal measurements

The data obtained from measurements using a single-, two- and multi-tone input signal give the necessary parameters for modelling the nonlinearity of the measured amplifier. For single-tone signal measurements, these modelling parameters are based on the distortion measures presented in Section 3.1.

Next, a summary of the measures to be made using a single-tone input signal is presented, followed by the used setup systems and the general procedure to perform the measurements.

Modelling parameters from single-tone signal measurements

In this thesis, the measurements based on single-tone signals are divided according to the main measuring device used to perform them. Therefore, the single-tone signal measurements made are presented next divided into those obtained by using a Network Analyzer (NWA) and the ones realized with a Spectrum Analyzer (SA).

Input power level sweep and frequency sweep are the measurements done in this thesis using a NWA. AM-AM and AM-PM curves are obtained by varying the input power level and taking the output power level corresponding to each one of these. This is done for one specific frequency at a time. Therefore, the process should be repeated for every desired frequency.

As its name indicates and as it is explained in Section 3.1.6, for a frequency sweep, a fixed input power level is used while varying the frequency along the whole frequency range of the amplifier. The gain or phase obtained from each frequency depicts the behavior of the amplifier for its whole operating frequency range.

On the other hand, the SA allows the easy analysis of the whole operating frequency range of the amplifier by automatically performing a frequency sweep of the range specified for a fixed input power level. Therefore, it is easy to measure the fundamental, second and third harmonics at a determined input power level.

It is possible to perform an input power level sweep for a specific frequency by varying the input power level to obtain an output power level for each of these

input power levels. If these measurements are done in order to model an amplifier used in a specific application, this procedure is usually done just for the specific frequency at which the amplifier is used. If the intention is simply to model an amplifier regardless the application in which it will be used, the frequency can be freely chosen within the operating frequency range of the amplifier to be measured.

The modelling parameters that are obtained and calculated from these measurements are summarized in Table 5.1.

Table 5.1: Modelling parameters using single-tone input signals.

Measuring device	**Type of measurement**	**Modelling parameters**
Network analyzer (NWA)	Frequency sweep	▪ Gain curve for full frequency operating range ▪ Phase curve for full frequency operating range
	Input power level sweep	▪ AM-AM characteristic curve ▪ AM-PM characteristic curve
	Calculated	▪ 1 dB compression point
Spectrum analyzer (SA)	Frequency sweep	▪ Harmonic distortion (harmonics)
	Input power level sweep	▪ Fundamental frequency curve ▪ Second harmonic curve ▪ Third harmonic curve
	Calculated	▪ Second order intercept point (IP2) ▪ Third order intercept point (IP3)

Setup system and process to perform single-tone signal measurements

Figure B.4(a) in Appendix B.3.1, represents in a simple way how the NWA is used to measure an amplifier with a single-tone input signal, which is generated by the same NWA's internal generator. On the other hand, Figure B.4(b) shows the actual setup system used in this thesis for this kind of measurements. Respectively, Figures B.5(a) and B.5(b) in Appendix B.3.2, present the schematic and practical setup system for single-tone signal measurements using a spectrum analyzer.

The detailed processes to perform single-tone signal measurements, using the previous systems, are presented in Appendix C.4. Moreover, the results obtained from the measurements using a single-tone signal, including the calculated parameters, are presented in Section 6.2.

5.2.3 Two-tone signal measurements

The first step to perform a two-tone test is to generate the two-tone signal itself. There are different approaches to achieve this, such as the ones presented in [86] and [87]. The election of the method is purely subjective and mostly depends on the equipment available and personal preferences.

The method used in this research to generate a two-tone signal is presented next, followed by the complete setup system to generate it and to perform two-tone tests. Moreover, the parameters to be obtained from this type of measurement are presented, as well as the procedure to perform the test.

Generation of a two-tone signal

A two-tone signal is simply a combination of two sinusoidal signals each of different frequency. In this thesis, the method used to generate a two-tone signal consists of producing a baseband signal with an specific frequency and upconverting it. This is done using an Arbitrary Waveform Generator (AWG) to obtain one tone and a Vector Signal Generator (VSG) to upconvert it and obtain the second tone, as shown in Figure 5.4.

The frequency of the baseband signal (fm) should be chosen as half of the desired separation of the two tones, giving the full separation after the upconversion (Figure 5.4).

Furthermore, the maximum separation of the two tones ($2Tone_{max.sep.}$) depends directly on the generator's (AWG) sampling rate (SR), according to Equation 5.1, where $MaxIMP$ is the maximum intermodulation product that can be captured by the SA.

$$2Tone_{max.sep.} = \frac{SR}{2\ MaxIMP} \tag{5.1}$$

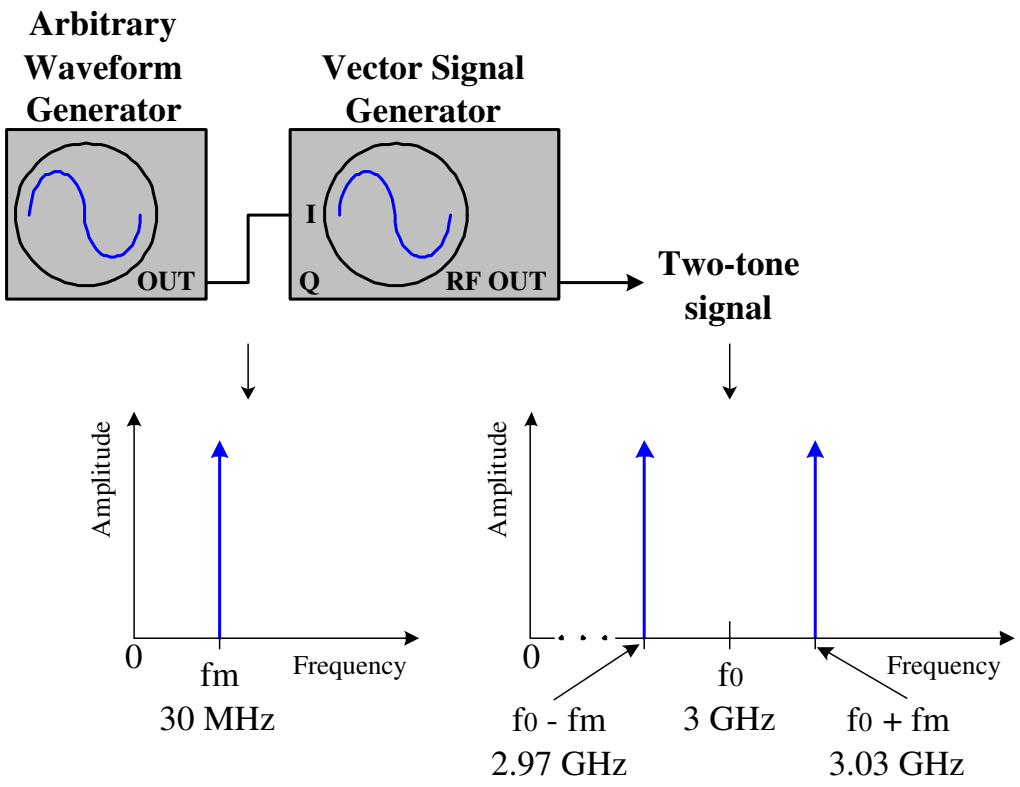

Figure 5.4: Schematic system for generation of two-tone signal.

Notice that the factor two in the denominator is required by the Shannon sampling theorem [88], i.e. the sampling frequency should be at least two times the highest frequency present in the signal, in order to be able to reconstruct correctly the whole frequency spectrum.

In the case of this thesis, we are mainly interested in measuring the Third Intermodulation Product (IMP3). Since the sampling rate of the AWG is 400 MS/sec (from Table A.2), the maximum tone separation is approximately 66.67 MHz. Therefore, a 60 MHz separation was chosen, assuring that the IMP3 can be seen in the SA.

Moreover, the frequency used for the upconversion will define the center frequency (f_0) of the two tones. For this research, 3 GHz is chosen, which is the maximum frequency achievable with the VSG used. This procedure generates the resultant two-tone signal of Figure 5.4.

As previously mentioned, an arbitrary waveform generator is used to obtain a

single tone. Next, the output of the AWG is connected to the RF input of the VSG. Finally, it is possible to feed the resultant two-tone signal into a spectrum analyzer, in order to obtain a graphical representation of the spectrum of the signal.

The setup system used to generate the two-tone signal in this thesis consists of the AWG and the VSG shown in Figure B.6 (Appendix B.4), which presents the whole setup system used to perform a two-tone signal measurement.

The main characteristics of the specific equipment used can be found in Tables A.2 and A.1, as introduced in Section 5.1.2. Furthermore, the detailed steps to generate a two-tone signal are presented in Appendix C.5 and the generated two-tone signal is shown in Section 6.3.1.

Modelling parameters from two-tone signal measurements

For two-tone signal measurements the only measuring device used in this thesis is the spectrum analyzer, which gives enough data to characterize an amplifier. As mentioned in the previous section, a SA automatically sweeps the specified frequency range for a fixed input power level.

In order to characterize the nonlinearity of the amplifier the input power level should be chosen within the saturation zone of the amplifier, where the nonlinearity is stronger. The 1 dB compression point is a good indicator of the input power level where the amplifier is not anymore linear. This parameter was obtained from the single-tone measurements performed and, subsequently, it is the one used as the input power level for the two-tone test. Moreover, the same measurements are made at a low input power level in order to compare the linear and nonlinear zones of the amplifier.

By just connecting the generated two-tone signal to the SA it is possible to measure the two input tones. Furthermore, after connecting the amplifier, it is possible to analyze the harmonics and the IMPs present in the output of the amplifier. As explained in Section 3.2.1 the most interesting zone of the spectrum to be analyzed is the fundamental zone, since the distortion inside this region (i.e. in-band distortion) is difficult to filter out.

Subsequently, the modelling parameters obtained and calculated from this two-tone test are summarized in Table 5.2.

Table 5.2: Modelling parameters using two-tone input signals.

Type of measurement	**Modelling parameters**
Frequency sweep (at low input power level)	▪ Intermodulation products present in DC, fundamental, second and third harmonic zones
Frequency sweep (at 1 dB CP)	▪ Plain two tones and spurious signals at DC fundamental, second and third harmonic zones ▪ Intermodulation products present in DC, fundamental, second and third harmonic zones ▪ Third Intermodulation Product (IMP3) in the fundamental zone
Calculated	▪ Intermodulation Distortion Ratio (P_{IMR})

Setup system and process to perform two-tone signal measurements

The setup system shown in Appendix B.4 consists of the setup system used to generate a two-tone signal (i.e. AWG and VSG) and the testing system. The two-tone signal is fed to the input of the amplifier, followed by the attenuators and the measuring device. In this thesis, the measuring device is a spectrum analyzer, which main specifications are summarized in Table A.4.

The process used in this research to measure the response of two-tone signals passing through an amplifier is presented in Appendix C.6. Furthermore, the modelling parameters obtained from the two-tone test are summarized in Section 6.3.2.

5.2.4 Multi-tone signal measurements

In this section, the way of performing multi-tone signal measurements is presented. First, an multisine signal is obtained using MATLAB software. Next, the modelling parameters to be obtained from this type of measurements are summarized. Finally, the setup system and specific process to perform the measurements are explained.

Generation of a multisine signal

Although it is possible to generate a RF passband multisine signal with MATLAB software, it was not possible to use it in this thesis due to the equipment availability at the laboratories used for this research. Therefore, a baseband multisine signal was generated using the MATLAB script designed by M.Sc. Mei Yen Cheong.

The MATLAB code consists firstly on generating two random arrays, each of 150 elements corresponding to the 150 sinusoids that will form the baseband multisine signal. One of these arrays contains the amplitude of each sinusoid, which was chosen as the simplest possible (i.e. 1 V each). The other array contains a random phase for each sinusoid, with the constraint that each value should be a multiple of 2π.

Next, a time array is created whose length depends on the chosen frequency resolution for displaying the spectrum (i.e. 195.3125 kHz) and the sampling frequency (i.e. 400 MS/sec.). Furthermore, a complex sinusoid is composed for each amplitude array element and its corresponding phase array element. Finally, the 150 sinusoids are added together to form the final baseband multisine signal.

Figure 5.5 shows the resultant baseband multisine signal in time and frequency domain, which consists of 150 sinusoids, covering approximately 30 MHz bandwidth. Notice that the signal generated with this script is a partial multisine signal, which will only contain a number of tones equal to half of the final signal. The complete multisine signal is obtained after the upconversion, which will double the number of tones.

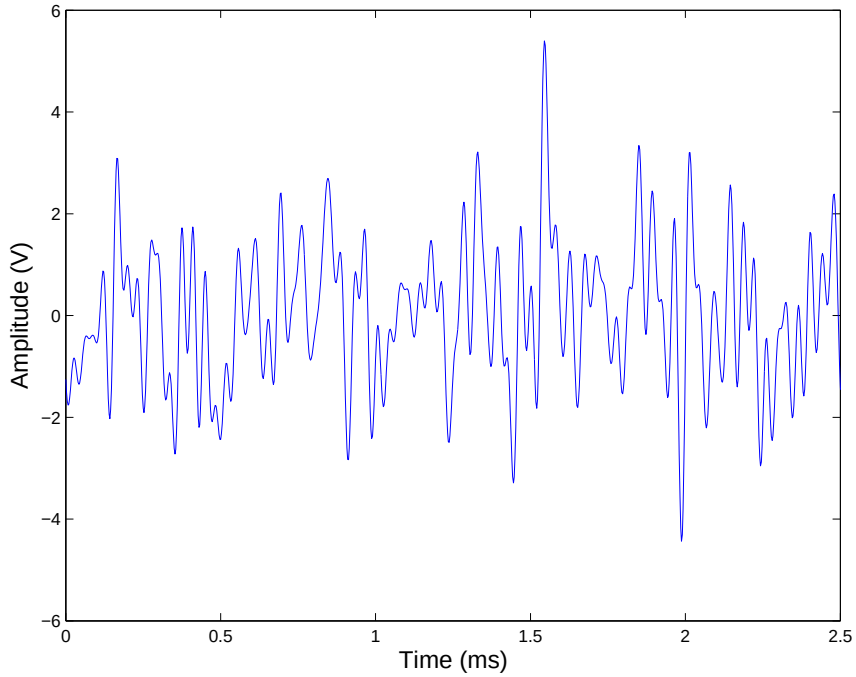

(a) Time domain

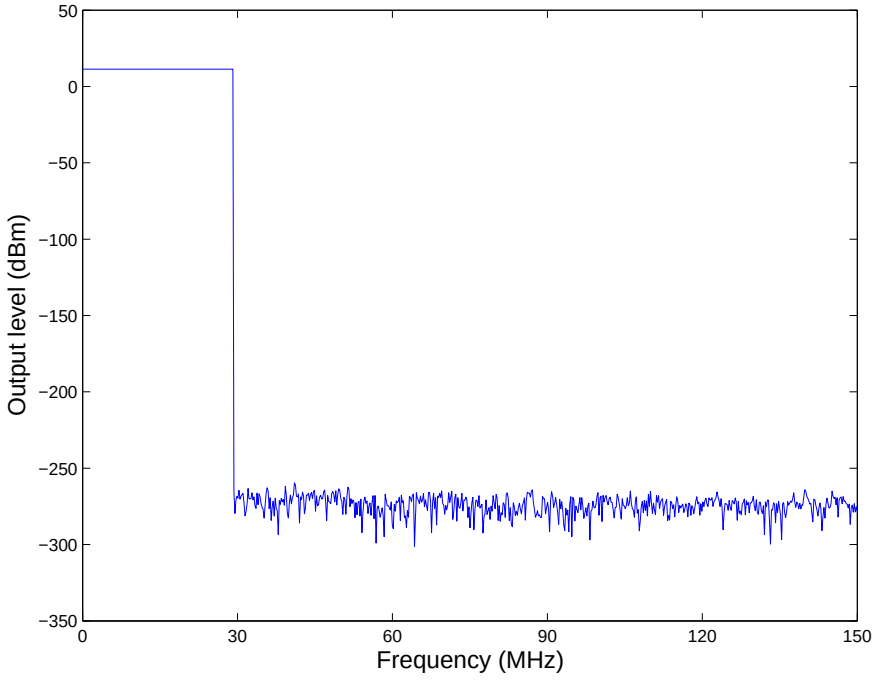

(b) Frequency domain

Figure 5.5: Baseband analog multisine signal obtained with MATLAB *software.*

The multisine signal complex values obtained from the MATLAB script, as well as their corresponding time values, were saved in a floppy disk of 3 1/2 inches and fed into the AWG. Next, the obtained signal was upconverted using a VSG in order to generate an RF passband multisine signal. The setup system used to obtain the final multisine signal to be used in this research is shown in Appendix B.5. Notice that a spectrum analyzer is included in this setup system, in order to obtain a graphical representation of the final signal. Moreover, the detailed steps to generate a multisine signal are presented in Appendix C.7 and the generated signal is shown in Section 6.4.1.

Modelling parameters from multi-tone signal measurements

The modelling parameters obtained and calculated in this research using a multi-tone signal are summarized in Table 5.3.

Table 5.3: Modelling parameters using multi-tone input signals.

Type of measurement	Modelling parameters
Frequency sweep (at low input power level)	▪ Harmonic distortion present in fundamental, second and third harmonic zones
Frequency sweep (at 1 dB CP)	▪ Plain multisine signal frequency spectrum at fundamental, second and third harmonic zones ▪ Harmonic distortion present in fundamental, second and third harmonic zones ▪ Average power of the desired bandwidth (P_{B1}) ▪ Average power at certain offset from the center frequency (P_{B2}) ▪ Power at center frequency ▪ Highest power level outside the wanted bandwidth
Calculated	▪ Adjacent Channel Power Ratio (ACPR) ▪ Multi-tone Intermodulation Ratio (MIMR)

Notice that in this research the Noise Power Ratio (NPR) is not included in the parameters to be obtained from multi-tone measurements. However, its concept was introduced in Section 3.3.3, since it is recommended to perform this test in order to include in the modelling the in-band distortion caused by the amplifier. More information on NPR measurement can be found in [89].

Setup system and process to perform multi-tone signal measurements

Two-tone signals are a special case of multi-tone signals. Consequently, the setup system to perform multi-tone measurements is the same than the one presented in Appendix B.4 for two-tone signals. The only difference consists in the insertion of the floppy disk containing the multisine signal generated with the MATLAB script in to the diskette drive of the arbitrary waveform generator, as shown in Appendix B.5.

Similarly, the process to perform any kind of multi-tone signal measurement is the same followed for two-tone signal measurements, which is presented in Appendix C.6. Finally, the measured and calculated multi-tone parameters can be found in Section 6.4.2.

5.3 Summary of the chapter

This chapter described the necessary aspects to perform measurements of amplifier nonlinearity. First, factors to take on count before measurements were introduced, such as the needed characteristics of the input testing signal and a brief description of the equipment to be used. The most important equipment specifications are summarized in Appendix A. Furthermore, measuring devices calibration and noise considerations were explained, which are planning matters important for the good development of the measurements.

Finally, the procedure and setup systems to perform passive devices, single-, two- and multi-tone signal measurements, as well as the way of generating two-tone and multisine signals, were presented. Emphasis was made on the modelling parameters to be obtained from single-, two- and multi-tone signal measurements, which are summarized in Tables 5.1, 5.2 and 5.3, respectively.

Chapter 6

Power amplifier measurement results

The measurements in this thesis have been performed as a practical approach of the theory summarized in Chapters 2 to 5. Basic distortion measures of a nonlinear amplifier using single-, two- and multi-tone input signals were obtained. Mathematical analysis of these measures makes it possible to obtain more detailed parameters, which can be used for modelling and linearization purposes.

In this chapter, the most important results obtained from each type of measurement are presented. Due to its length, the complete set of data and plots can be found in Appendix D. In some cases, it is not possible to obtain modelling parameters directly from the measuring device. Therefore, the calculations and parameters obtained from them are presented whenever necessary. Moreover, the specific values used to setup the measuring devices in order to obtain the desired parameters are presented. Finally, comments on the setup systems and the obtained results are given.

6.1 Passive device measurements

In this thesis, extra devices have been divided into passive and auxiliary devices. As introduced in Section 5.2.1, passive devices loss can be corrected in a high degree by calibrating the measuring devices including all passive devices in the process. On the other hand, attenuators are the only auxiliary devices used in these measurements. Next, the results from the calibration of the network analyzer and spectrum analyzer are presented, as well as the measured attenuation.

6.1.1 Devices needed to interconnect measuring systems

The processes presented in Appendix C.1 were followed in order to calibrate the measuring devices. Next, the specific parameters and adapters used for calibrating each device are presented. Moreover, the results after each calibration are shown and explained.

Calibration of network analyzer

To perform measurements with the Network Analyzer (NWA) used in this thesis (Table A.3), and according to the equipment availability, it was necessary to use four adapters to connect the NWA's end cable connectors to the attenuators and amplifier. In addition to these, an extra adapter was necessary to perform the calibration of the device. All the adapters used are shown in Figure 6.1. A more detailed description of each type can be found in [90].

The process followed to calibrate the NWA is presented in Appendix C.1.1 and the setup system used is shown in Appendix B.1.1. The values of the parameters used for calibration are presented in Table 6.1.

It is important that the interpolation function is set to "ON" before calibration. This function allows to make power-sweep measurements for different frequencies, since it generates different sets of corrected data based on the set obtained from the calibration process. In other words, the calibration system interpolates the error terms whenever the stimulus parameters are changed.

APC 2.4 mm female jack to APC 3.5 mm male plug

SMA female jack to SMA male plug

SMA female jack to SMA female jack (extra for calibration)

SMA male plug to SMA female jack

APC 3.5 mm male plug to APC 2.4 mm female jack

Figure 6.1: Adapters used with a network analyzer for measurements and calibration of the device itself.

Table 6.1: Calibration parameters used for the network analyzer.

Parameter	Value
Start frequency	1 GHz
Stop frequency	9 GHz
Power level	0 dBm
Power	ON
Start power	-27 dBm
Stop power	3 dBm
Center frequency	5 GHz
Number of points	1401
Calibration	ON
Interpolation	ON

After the calibration was performed, the screen shown in Figure 6.2 was obtained in the NWA when checking its calibration settings.

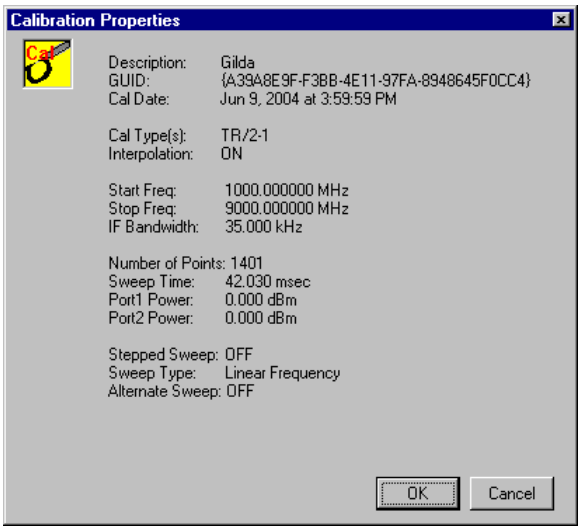

Figure 6.2: Network analyzer calibration settings.

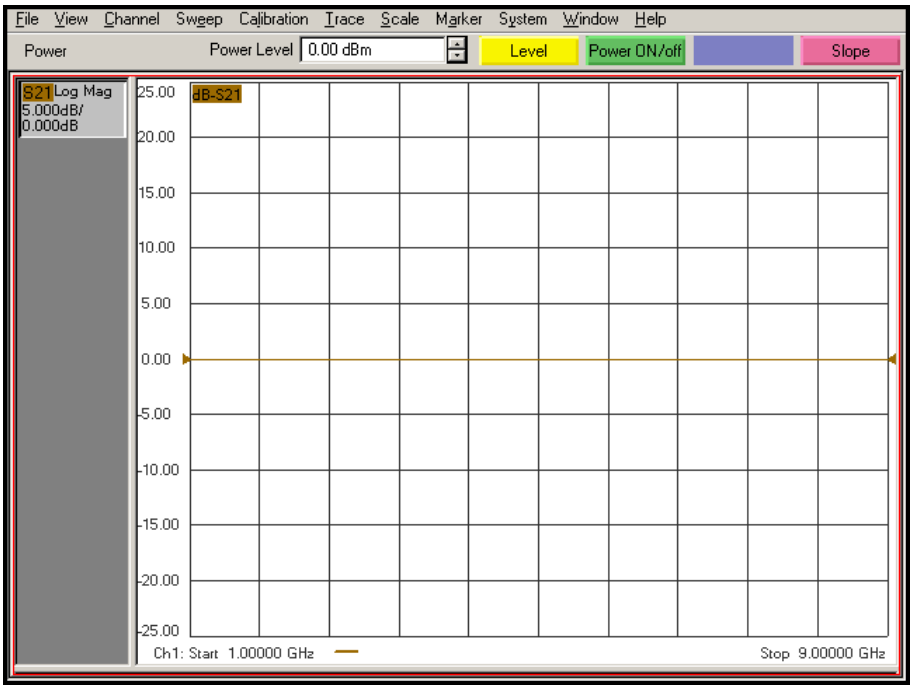

(a) Frequency sweep from 1 GHz to 9 GHz at 0 dBm

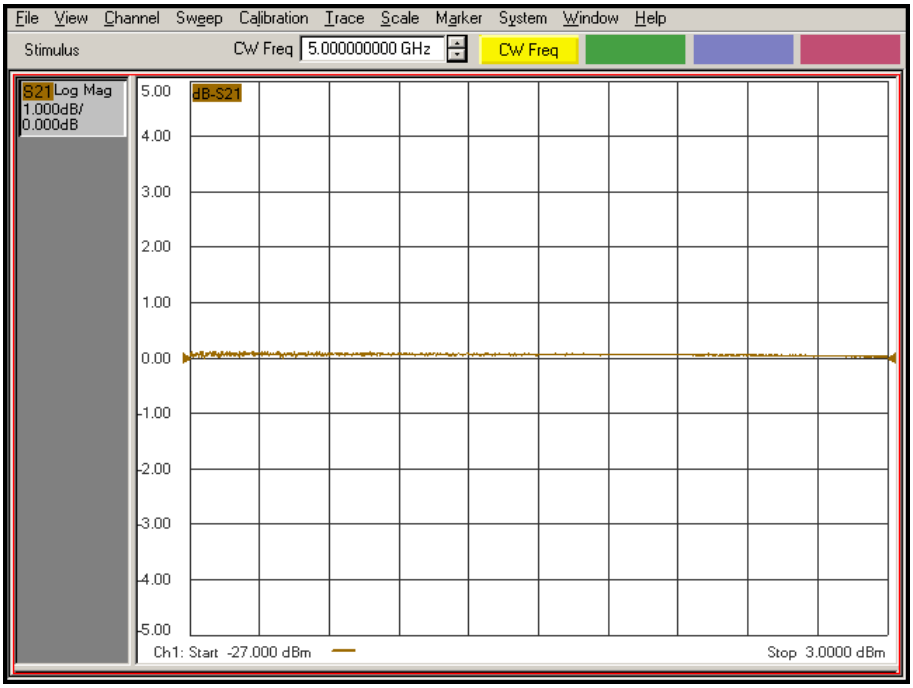

(b) Power sweep from -27 dBm to +3 dBm at 5 GHz

Figure 6.3: Results after calibration of network analyzer for a) frequency sweep and b) power sweep.

Next, frequency and power-sweep measurements were taken in order to check the calibration results. As explained in Section 5.2.1, the ideal result after a calibration is a flat trace of 0 dB gain for the frequency range calibrated. Figure 6.3(a) shows that the maximum error after calibration is less than 0.05 dBm, which is very small for the purposes of this thesis and when compared to the expected amplifier gain of 30 dB.

In the same way, Figure 6.3(b) shows that, for a power sweep, the maximum deviation from the ideal output expected after calibration is less than 0.15 dBm. This error is considered small in this thesis since this maximum occurs at very low input power levels, which might be confused with the inherent noise of the NWA. However, when the input power level is increased the error becomes smaller, as can be seen in Figure 6.3(b).

Calibration of spectrum analyzer

The calibration of the spectrum analyzer is only necessary when the ambient temperature changes more than 10°C [91], which is not the situation in the development of this research since the laboratory where the equipment is placed has a regulated temperature. However, the process to calibrate the SA can be found in Appendix C.1.2 and can be performed as a way to test the correct functioning of the device.

Since the SA does not have an error correction feature (like the one in the NWA), a reference level measurement was performed in order to determine the attenuation of the cables used for the measurements.

The setup system shown in Appendix B.1.2 was connected using the SA's −10 dBm/300 MHz calibration signal, the cables to be used and the same extra adapter used for the NWA's calibration (Figure 6.1). The measurement of the cables attenuation was performed following the process in Appendix C.2.

Figure 6.4 shows the results obtained. The signal amplitude measured is −10.33 dBm. As previously mentioned, the amplitude of the input signal (i.e. calibrating signal in SA) is −10 dBm. Consequently, the attenuation introduced by the cables to the measuring system is 0.33 dBm. This attenuation has a small

effect on the measurements if compared with the 30 dB gain of the DUT. Therefore, cable attenuation will not be included in further calculations. Nevertheless, this attenuation should be considered when high accurate measurements are required.

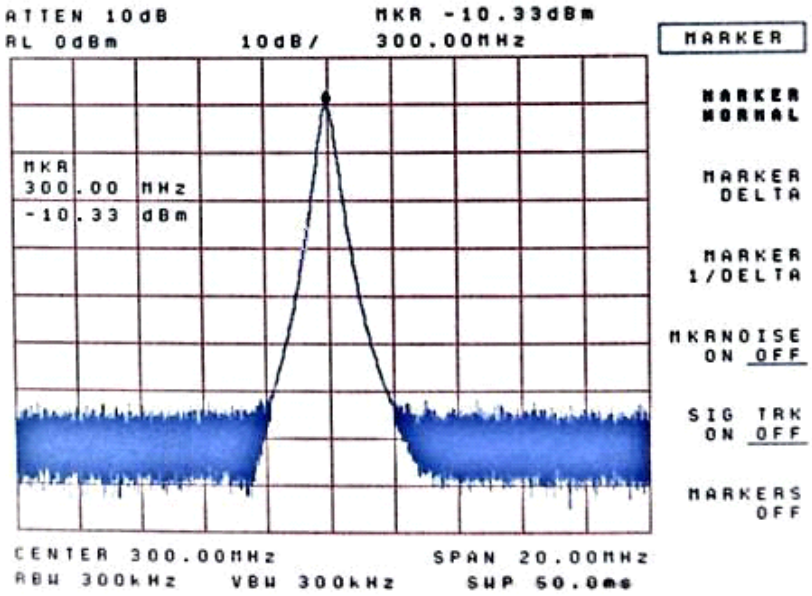

Figure 6.4: Cable attenuation measurement performed with a spectrum analyzer.

6.1.2 Devices needed to perform correct measurements

The setup system shown in Appendix B.2 and the process presented in Appendix C.3 were followed in order to measure the attenuators used in this research.

As an example of attenuation measurements, the result of a frequency sweep with input power level of 0 dBm is presented in Figure 6.5(a). In the same way, a power sweep with an input signal of 5 GHz gave the curve shown in Figure 6.5(b). More examples of measurements of the attenuators with different input signals are shown in Appendix D.1.

The attenuation obtained was in average -40.45 dB, which follows the expected -40 dB. The maximum deviation was less than the specified total attenuation accuracy range of ± 1.3 dB (Table A.6). This means that the attenuators were correctly measured and properly working for the rest of the measurements.

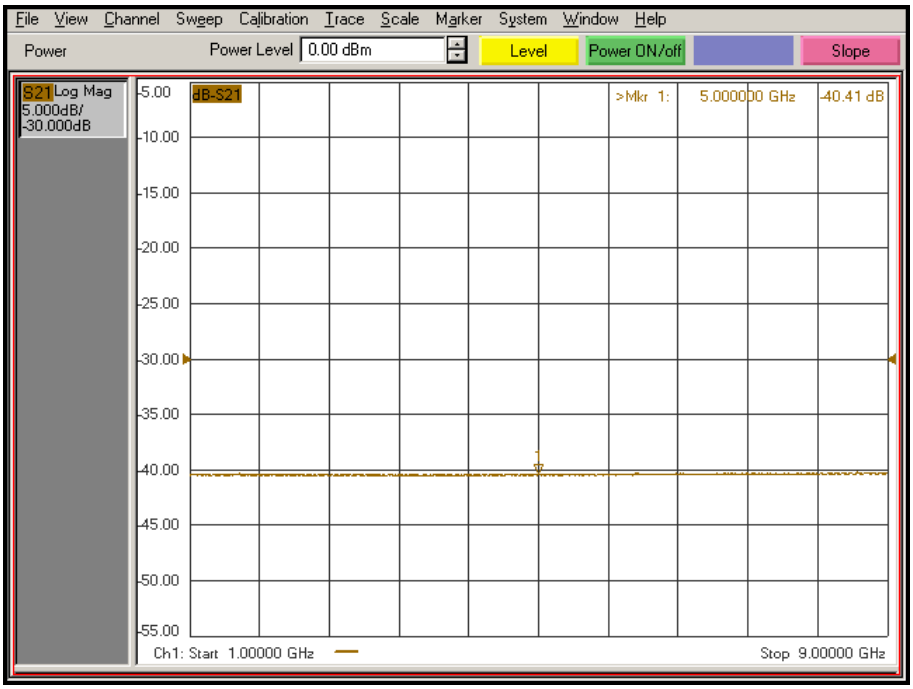

(a) Frequency sweep from 1 GHz to 9 GHz at 0 dBm

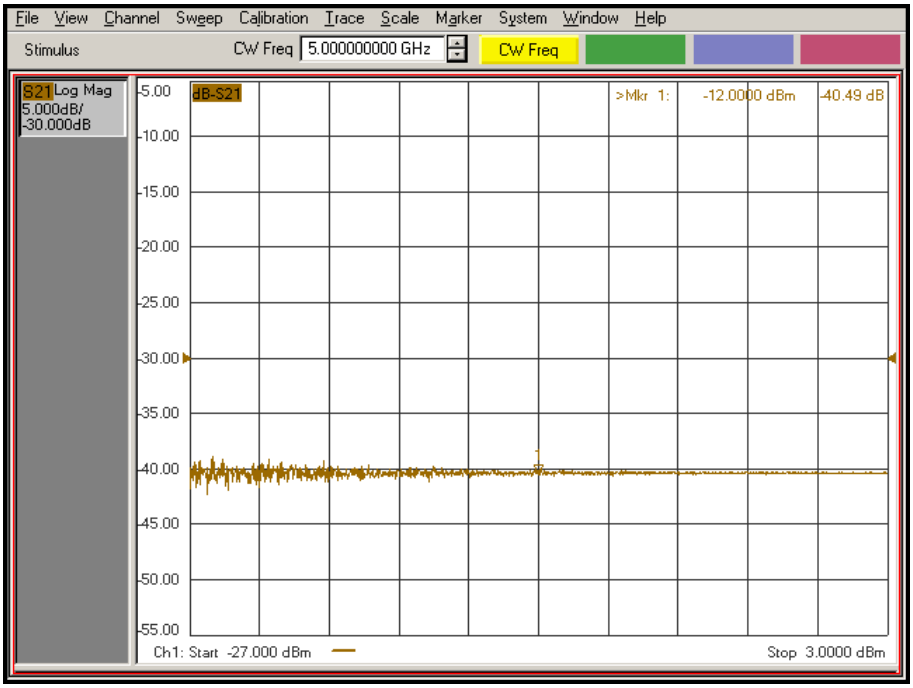

(b) Power sweep from -27 dBm to +3 dBm at 5 GHz

Figure 6.5: Example of attenuation measurement results for a) frequency sweep and b) power sweep.

6.2 Single-tone signal measurements

As explained in Section 5.2.2, different measures can be taken from an amplifier by using either a network analyzer or a spectrum analyzer. In this section, the results obtained using both devices are presented.

6.2.1 Results obtained using a network analyzer

Power- and frequency-sweep measurements were performed by using the setup system shown in Appendix B.3.1, following the process presented in Appendix C.4.1 and with the settings summarized in Table 6.2.

Table 6.2: Settings for ZVE-8G amplifier single-tone signal measurements using a network analyzer.

Type of sweep	Parameter	Value
Frequency sweep	**Frequency range**	1 to 9 GHz
	Input level	-25, -20, -15, -10, -5, 0 and +3 dBm
	Number of points	1401
Input level sweep	**Frequency**	1, 2, 3, 4, 5, 6, 7, 8 and 9 GHz
	Input level range	-27 to +3 dBm
	Number of points	601

Figures 6.6(a) and 6.6(b) are an example of the results obtained when performing measurements of the amplifier tested using a single-tone input signal. The first of these represents a frequency sweep of the amplifier output for a very low input power level, -20 dBm. The second figure is the result of a power sweep performed to the DUT using an input signal with 5 GHz frequency, which is the center frequency of the amplifier's operational range.

Figure 6.6(a) shows that the amplifier works properly for the specified range (Table A.5). The average gain inside the amplifier's operational frequency band (2 to 8 GHz) read from the NWA is approximately -7 dB. Notice that this includes the attenuation used, the nominal value of which is 40 dB. Therefore, the average gain of the amplifier is approximately 33 dB, which is 3 dB more than the minimum specified by the manufacturer.

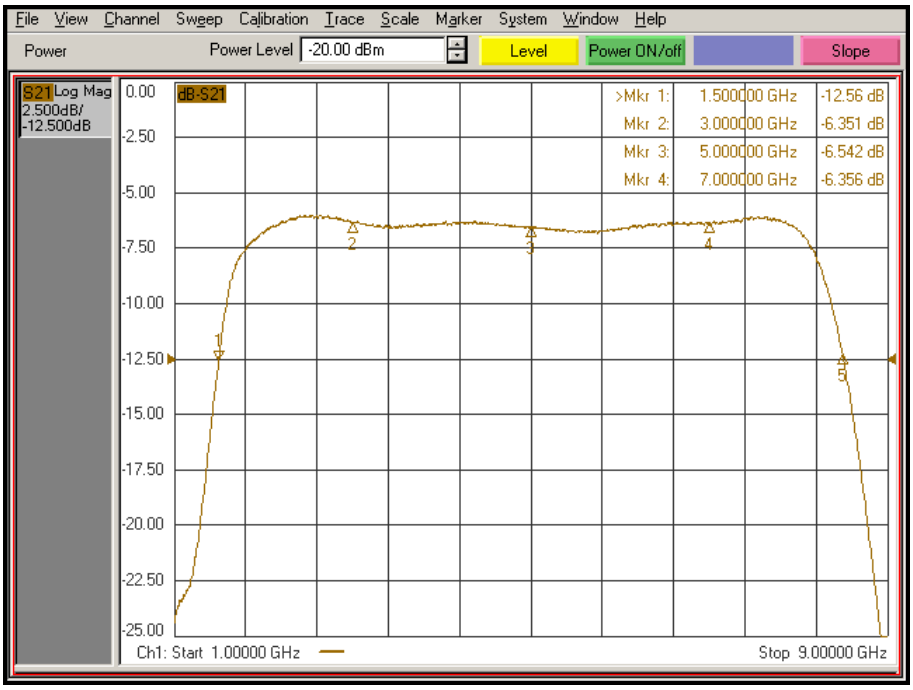

(a) Frequency sweep from 1 GHz to 9 GHz at -20 dBm

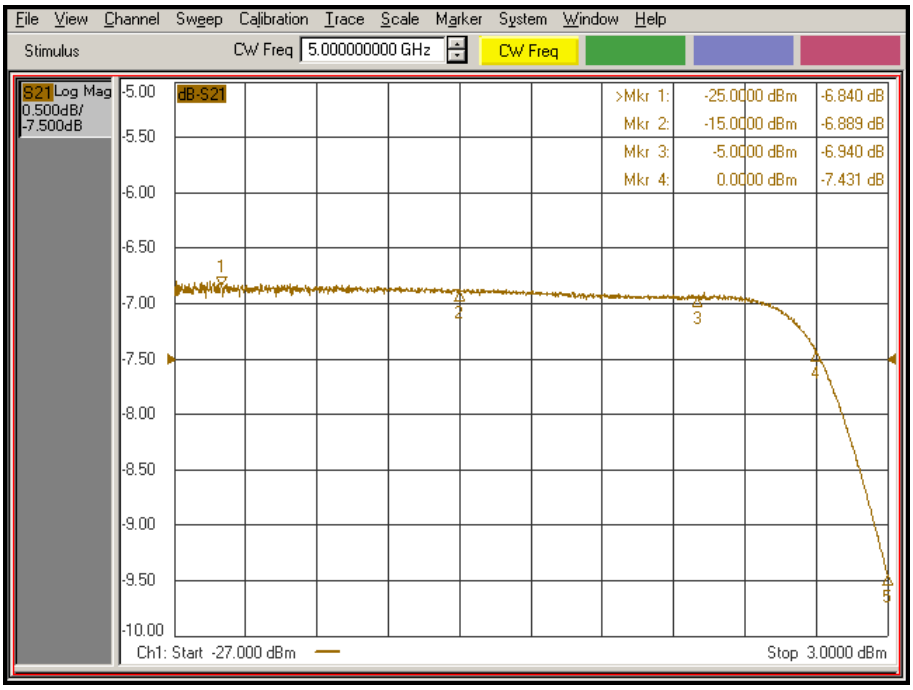

(b) Power sweep from -27 dBm to +3 dBm at 5 GHz

Figure 6.6: Example of NWA screen for a single-tone signal measurement of a Mini-circuits ZVE-8G amplifier. a) Frequency sweep. b) Power sweep.

On the other hand, the compression suffered by the amplifier at high input power levels can be seen in Figure 6.6(b). Moreover, the linearity of the amplifier is noticeable before the saturation zone. Screenshots of the NWA whilst performing single-tone measurements with input signals outside the amplifier's operational range can be found in Appendix D.2.1.

A useful feature of the network analyzer used is that it can produce data files which contain the measured points in a numeric format. As an example, Figure 6.7 shows the file obtained when performing a frequency sweep with the NWA.

The most important information in these files are the first, fourth and fifth columns. The first column register the measured stimulus, in this case the frequency in hertz of the input signal applied to the amplifier. The fourth and fifth columns represent, respectively, the real and imaginary components of the NWA's S_{21} corrected parameter, in this case the cascaded attenuators and amplifier output.

Ampm20dB.s2p - Notepad

File Edit Format View Help

```
!Agilent E8363A: A.02.62
!S2P File: Measurements: S11, S21, S12, S22:
# Hz  S  RI   R 50
1.000000e+009  0.000000e+000  0.000000e+000 -5.830690e-002 2.079878e-003 0.000000e+000
1.005714e+009  0.000000e+000  0.000000e+000 -5.816808e-002 9.613486e-003 0.000000e+000
1.011429e+009  0.000000e+000  0.000000e+000 -5.766180e-002 1.695510e-002 0.000000e+000
1.017143e+009  0.000000e+000  0.000000e+000 -5.632817e-002 2.355411e-002 0.000000e+000
1.022857e+009  0.000000e+000  0.000000e+000 -5.417658e-002 3.132280e-002 0.000000e+000
1.028571e+009  0.000000e+000  0.000000e+000 -5.107474e-002 3.719212e-002 0.000000e+000
1.034286e+009  0.000000e+000  0.000000e+000 -4.737339e-002 4.224302e-002 0.000000e+000
1.040000e+009  0.000000e+000  0.000000e+000 -4.269075e-002 4.773194e-002 0.000000e+000
1.045714e+009  0.000000e+000  0.000000e+000 -3.720873e-002 5.291135e-002 0.000000e+000
1.051429e+009  0.000000e+000  0.000000e+000 -3.207259e-002 5.585045e-002 0.000000e+000
1.057143e+009  0.000000e+000  0.000000e+000 -2.693017e-002 6.020957e-002 0.000000e+000
1.062857e+009  0.000000e+000  0.000000e+000 -2.002332e-002 6.181337e-002 0.000000e+000
1.068571e+009  0.000000e+000  0.000000e+000 -1.462897e-002 6.438315e-002 0.000000e+000
1.074286e+009  0.000000e+000  0.000000e+000 -8.128902e-003 6.538455e-002 0.000000e+000
1.080000e+009  0.000000e+000  0.000000e+000 -2.466732e-003 6.631552e-002 0.000000e+000
```

Figure 6.7: Example of a data file obtained from the network analyzer. The first column refers to frequency in Hz and the third and fourth columns present, respectively, the real and imaginary parts of the corrected and measured S_{21} parameter.

The analysis of the measurements is easier with the data recorded from the NWA. Figures 6.8(a) and Figure 6.8(b) show respectively the gain and phase curves obtained from frequency-sweep measurements of different input power levels applied to the tested amplifier. It is easily noticed that input power levels inside the linear zone behave in similar way and with approximately the same gain and phase. However, as the input power level is increased, the amplifier approaches the satu-

ration zone and, therefore, the gain approaches zero. Moreover, the gain flatness (i.e. variation of gain over the full operating frequency range) is approximately 0.96 dB, which falls inside the manufacturer specification (i.e. ±2 dB).

The process to generate these curves simply consists on calculating the gain and the phase of each measured output point (S_{21} parameter in the NWA). In the case of the gain, it is also necessary to add to each resultant the nominal attenuation value (i.e. 40 dB) in order to obtained the real input-output relation for each measured frequency. This whole process was easily done by using simple MATLAB commands.

By manipulating the data obtained from the measurements performed with the NWA it is possible to obtain the AM-AM and AM-PM characteristics of the tested amplifier. The process is the same than the one used to produce the previous frequency-sweep plots but using the power-sweep files.

Figure 6.9(a) shows a set of curves that represent the AM-AM characteristic of the DUT for different input frequencies. The results show that for the frequencies inside the operational range of the amplifier (i.e. 2 to 8 GHz) the curves behave in similar manner. On the other hand, the curves outside this frequency range have an unpredictable behavior and low gain (e.g. 1 GHz and 9 GHz curves in Figure 6.9(a)). Moreover, it is easy to notice the linear and saturation zones of the amplifier, which may slightly vary depending on the operating frequency.

The AM-PM characteristic of the amplifier tested for different input frequencies is presented in Figure 6.9(b). Similarly to the AM-AM characteristic and according to the expected results, the curves representing frequencies inside the amplifier's operational range behave linearly before the saturation zone, where it deviates from the ideal flat line showing higher phase distortion. Moreover, it can be seen that the frequencies outside the operational range have an undetermined behavior with respect to their phase distortion.

The complete set of plots obtained from frequency and power-sweep measurements can be found in Appendix D.2.2 and Appendix D.2.3, respectively.

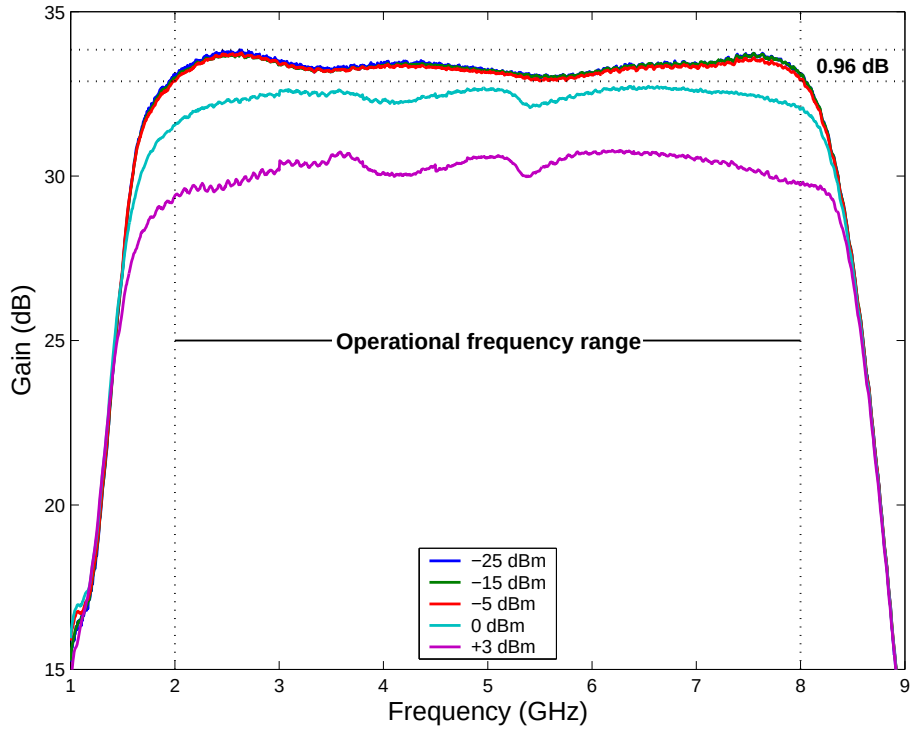

(a) Gain curve obtained from a frequency sweep from 1 GHz to 9 GHz

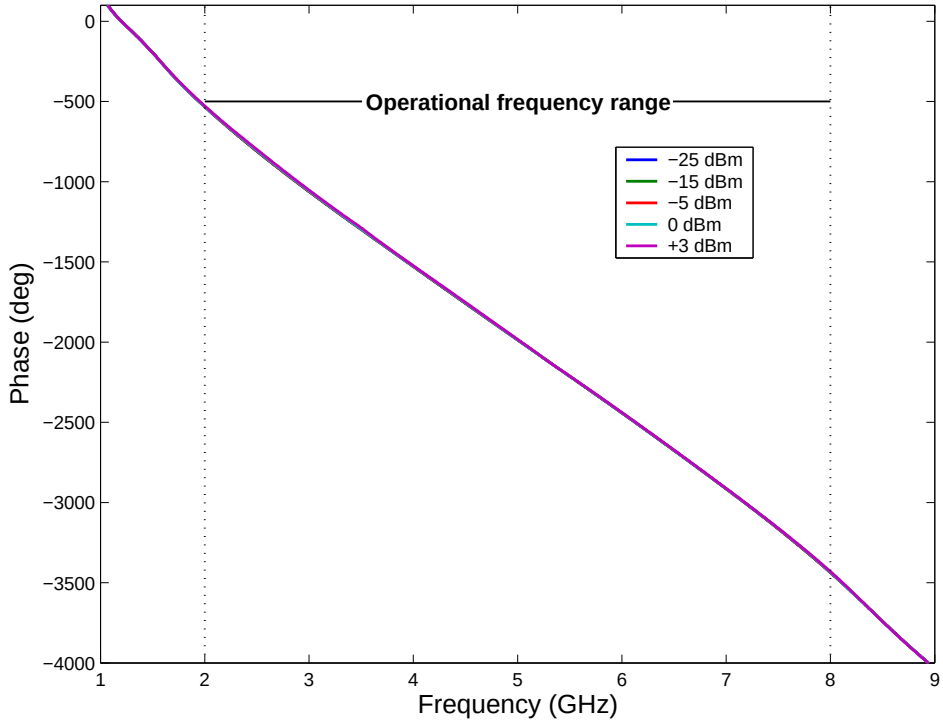

(b) Phase curve obtained from a frequency sweep from 1 GHz to 9 GHz

Figure 6.8: Frequency-sweep curves, result of single-tone tests performed to the ZVE-8G amplifier using the network analyzer and applying different input power levels. a) Gain. b) Phase.

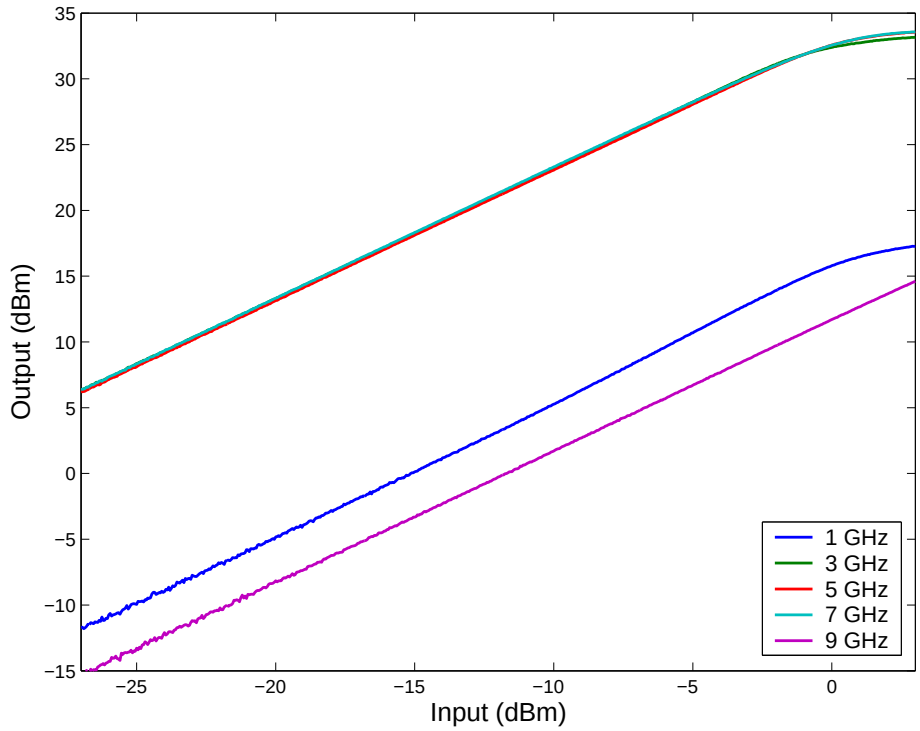

(a) AM-AM characteristic curves of ZVE-8G amplifier

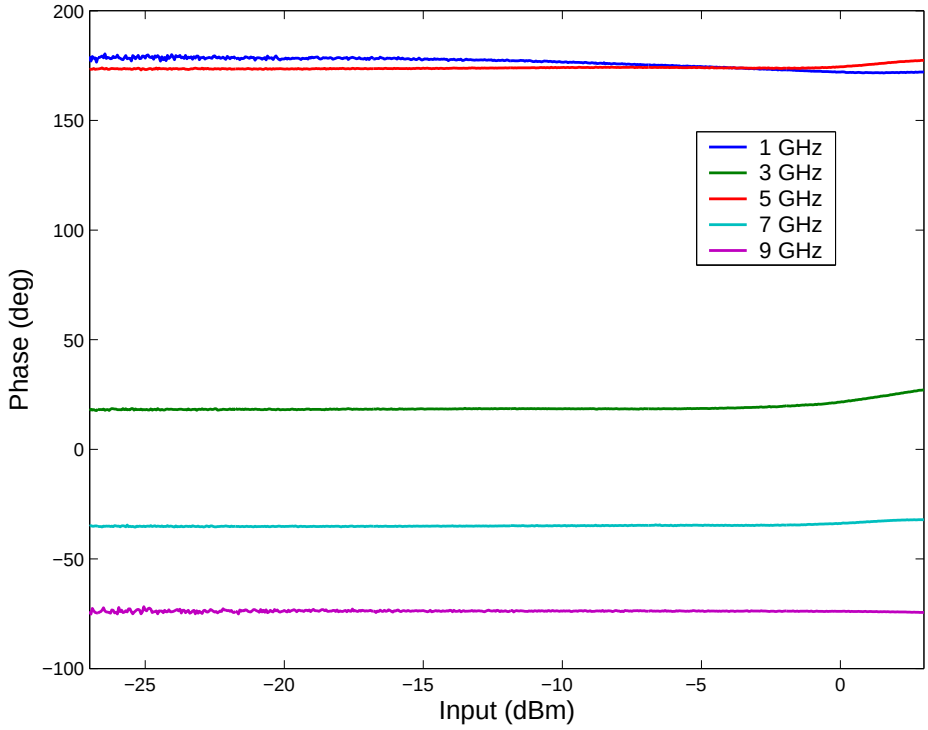

(b) AM-PM characteristic curves of ZVE-8G amplifier

Figure 6.9: Amplitude and phase response obtained from single-tone tests performed to the ZVE-8G amplifier using the network analyzer and applying different input frequencies. a) AM-AM. b) AM-PM.

The 1 dB compression point was calculated for each measured frequency based on the AM-AM characteristic obtained from the performed power-sweep measurements. As an example, Figure 6.10 shows the calculated 1 dB CP for the amplifier tested at 3 GHz frequency.

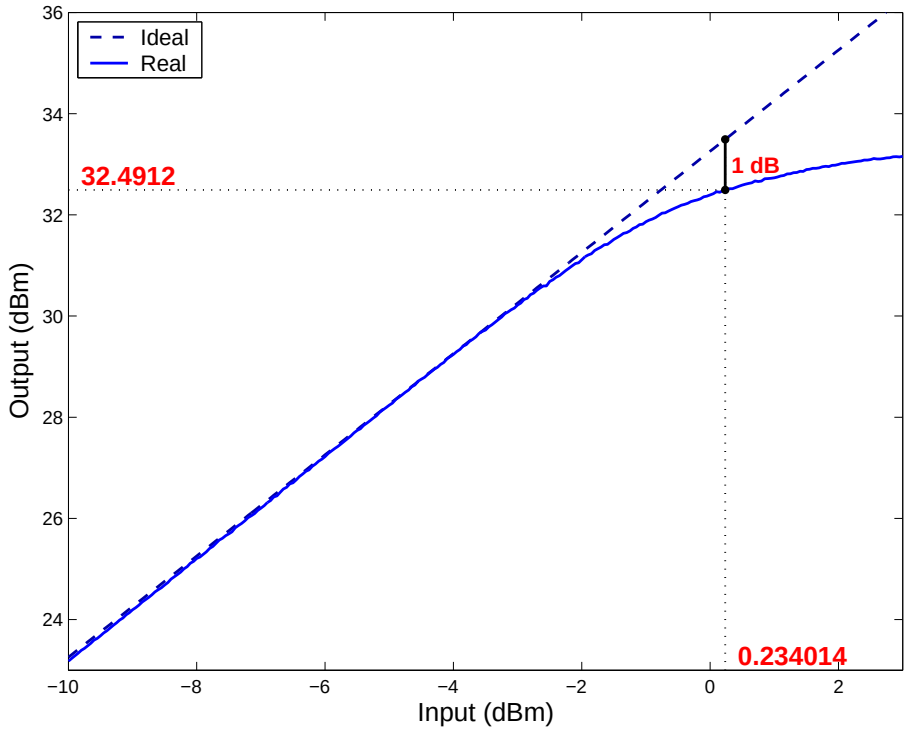

Figure 6.10: 1 dB compression point for ZVE-8G amplifier operated at 3 GHz, calculated based on its AM-AM characteristic obtained from the corresponding power-sweep measurement performed with the network analyzer.

The plots representing the 1 dB CP of all the frequencies measured inside the amplifier's operational band can be found in Appendix D.2.4 and a summary of the results is shown in Table 6.3.

The results of these calculations were the expected. According to the manufacturer's specifications summarized in Table A.5, the 1 dB compression point referred to output power is +30 dBm, when the gain is 30 dB. However, the measurements performed showed that the average gain of the amplifier is approximately 33 dB, as discussed at the beginning of this section. Consequently, it was expected that the 1 dB CP would be approximately +33 dBm (referred to output power), which fits to the results presented in Table 6.3.

Table 6.3: Summary of 1 dB compression point results for ZVE-8G amplifier.

Input frequency (GHz)	**1 dB CP (dBm)** (referred to input power level)	**1 dB CP (dBm)** (referred to output power level)
2	-1.16	+30.81
3	+0.23	+32.49
4	-0.19	+32.15
5	+0.86	+33.01
6	+0.99	+32.99
7	+0.43	+32.80
8	-0.01	+32.00

6.2.2 Results obtained using a spectrum analyzer

Single-tone signal measurements using a spectrum analyzer were performed based on the setup system shown in Appendix B.3.2 and following the process described in Appendix C.4.2. Moreover, Table 6.4 presents the settings used for the frequency- and level-sweep measurements performed with the SA.

Table 6.4: Settings for ZVE-8G amplifier single-tone signal measurements using a spectrum analyzer.

Type of sweep	**Parameter**	**Value**
Frequency sweep	**Input frequency**	3 GHz
	Input level	
	Measurements at 1 dB CP	0 dBm
	Measurements at low input level	-20 dBm
	Frequency range	
	Full span	0 Hz to 10 GHz
	DC	0 Hz to 0.05 GHz
	Fundamental	2.95 GHz to 3.05 GHz
	Second harmonic	5.95 GHz to 6.05 GHz
	Third harmonic	8.95 GHz to 9.05 GHz
Input level sweep	**Input frequency**	3 GHz
	Input level sweep range	
	Fundamental	-14 to +3 dBm
	Second harmonic	-12 to +3 dBm
	Third harmonic	-10 to +3 dBm
	Input level sweep step	0.5 dBm
	Frequency	
	Fundamental	3 GHz
	Second harmonic	6 GHz
	Third harmonic	9 GHz

Figure 6.11 shows the second and third harmonics obtained when performing a frequency-sweep measurement to the ZVE-8G amplifier with a SA. As expected, input levels within the linear zone of the amplifier do not produce harmonic distortion, as depicted in Figure 6.11(a), where an input level of -20 dBm is applied to the DUT. However, harmonic distortion occurs when levels equal or above the 1 dB compression point of the amplifier are applied to it (Figure 6.11(b)). Notice that, since the amplifier is operated at 3 GHz, the second and third harmonics are found in 6 GHz and 9 GHz, respectively.

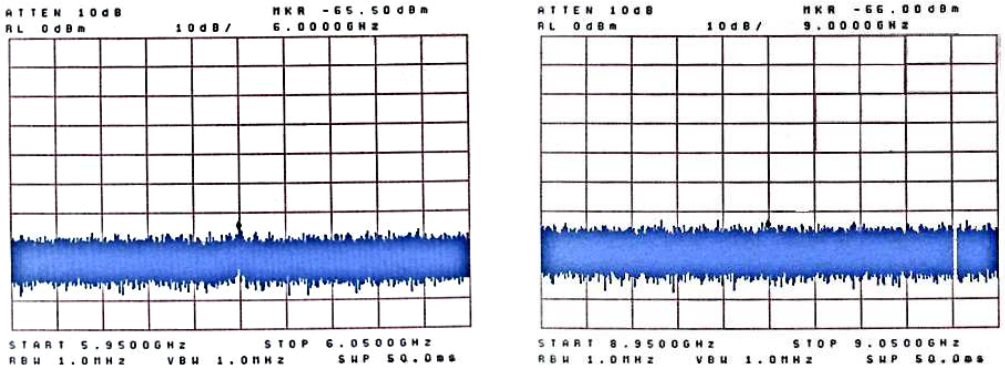

(a) Input level = -20 dBm

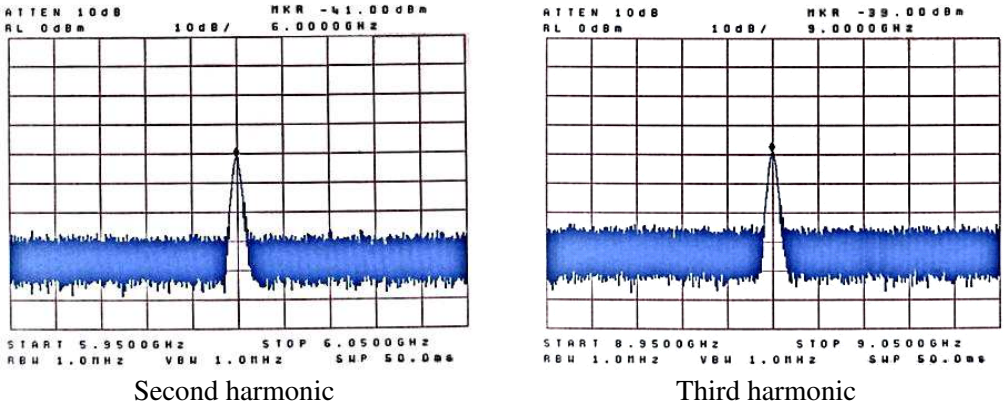

(b) Input level = 0 dBm (1 dB CP)

Figure 6.11: Second and third harmonics of ZVE-8G amplifier operated at 3 GHz obtained from single-tone measurements performed with a spectrum analyzer at a)low input power level and b) 1 dB compression point input level.

Next, an input level-sweep measurement was performed to each harmonic, as well as to the original tone (fundamental), in order to find their characteristic curves.

The data obtained from these measurements can be found in Appendix D.2.6 and a plot representing the characteristic curves of the fundamental, second and third harmonics is presented in Appendix D.2.7.

After processing the data obtained, the second-order intercept point (IP2) and third-order intercept point (IP3) were calculated by extending the ideal characteristic of each harmonic until they intersect the fundamental ideal curve. Figure 6.12 shows the resultant practical and ideal curves, as well as the IP2 and IP3 found.

According to the manufacturer, the ZVE-8G's IP3 referred to output level should be +40 dBm when the 1 dB CP referred to output level is +30 dBm (Table A.5). However, the measured and calculated 1 dB CP when operating the DUT at 3 GHz is +32.49 dBm, as presented in Figure 6.10. Therefore, an approximately +42.49 dBm IP3 referred to output level is expected. Thus, the IP3 referred to output level obtained is +42.12 dBm, which fits the expected value.

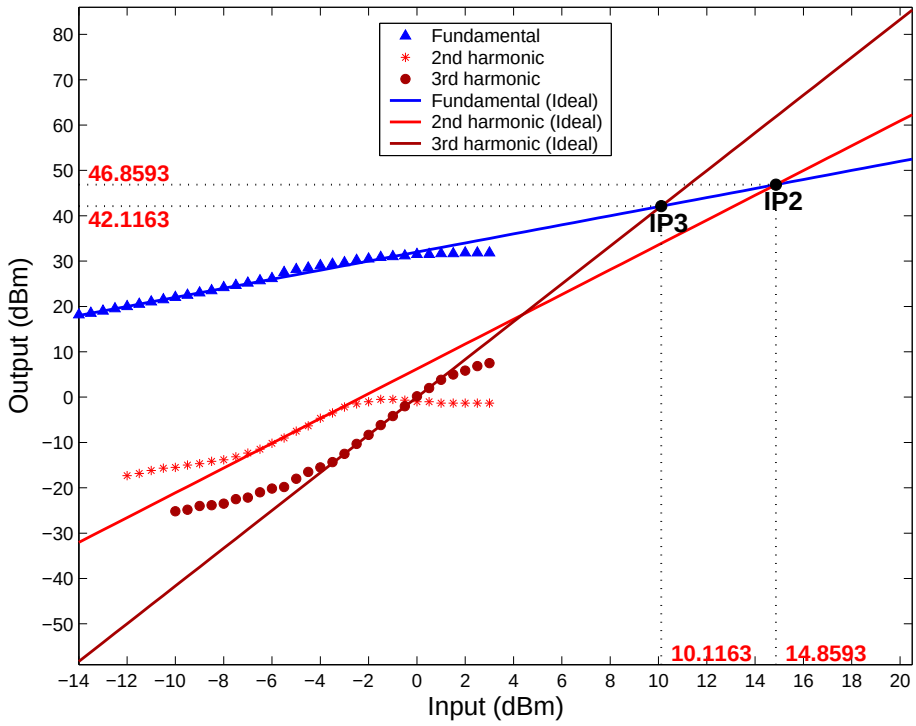

Figure 6.12: Second-order intercept point (IP2) and third-order intercept point (IP3) for ZVE-8G amplifier operated at 3 GHz, calculated based on its fundamental, second harmonic and third harmonic curves obtained from the corresponding input level sweep measurement performed with the spectrum analyzer.

6.3 Two-tone signal measurements

Two-tone signal measurements were performed following the process in Appendix C.6 and with the settings present in Table 6.5. Moreover, a spectrum analyzer was used as measuring device as shown in the setup system depicted in Appendix B.4. Next, the results obtained from measuring the plain two-tone signal and the actual two-tone signal test performed with the ZVE-8G amplifier are presented.

Table 6.5: Settings for ZVE-8G amplifier two-tone signal measurements using a spectrum analyzer.

Parameter	Value
Center frequency	3 GHz
Two tone separation	60 MHz
Input level	
Measurements of plain two-tone signal	0 dBm
Measurements at 1 dB CP	0 dBm
Measurements at low input level	-20 dBm
Frequency range	
Full span	0 Hz to 10 GHz
DC	0 Hz to 0.1 GHz
Fundamental	2.9 GHz to 3.1 GHz
Second harmonic	5.9 GHz to 6.1 GHz
Third harmonic	8.9 GHz to 9.1 GHz

6.3.1 Generated two-tone signal

The screen presented in Figure 6.13 shows the spectrum of the fundamental zone obtained when measuring the generated two-tone signal at a high input level. The set of screens showing the full span, DC, second harmonic and third harmonic zones is included in Figure D.13 (Appendix D.3.1).

The results of measuring the plain two-tone signal show that there are not harmonics or intermodulation products for the whole operating range of the amplifier. Therefore, any component (besides the original two tones) present in the spectrum when including the amplifier in the setup system is the result of the distortion introduced by the amplifier.

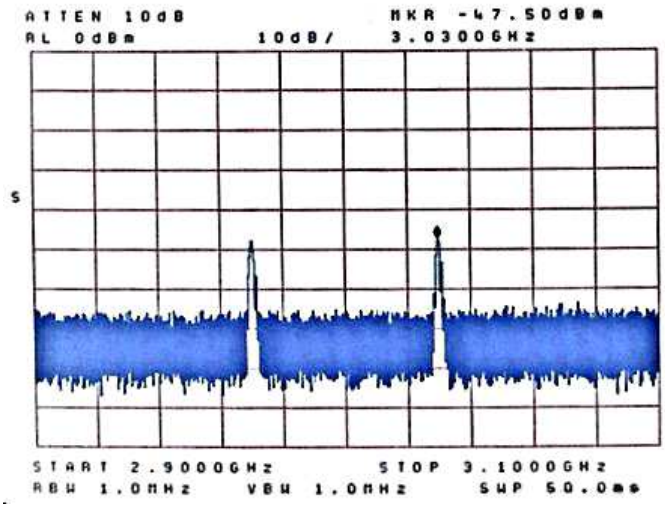

Figure 6.13: Frequency spectrum of the fundamental zone of the generated two-tone signal obtained with a spectrum analyzer. The two-tone signal has a center frequency of 3 GHz, tone separation of 60 MHz and it is tested at a high input power level equal to the 1 dB CP of the DUT (0 dBm).

6.3.2 Two-tone signal applied to amplifier

The two-tone signal of Figure 6.13 was applied as input signal to the ZVE-8G amplifier. When the level of the input signal is low, no harmonic or intermodulation distortion affects the operation of the amplifier, as presented in Figure 6.14, which shows the frequency spectrum of the measured full span of the DUT operated at 3 GHz and -20 dBm input level.

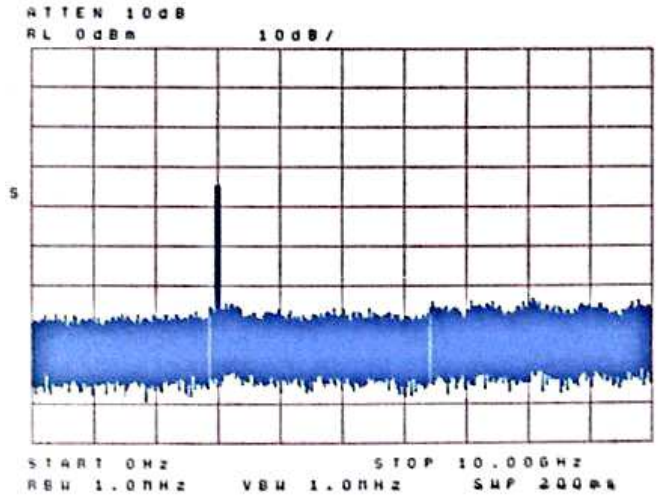

Figure 6.14: Frequency spectrum of the measured full span of ZVE-8G amplifier obtained from a two-tone signal measurement. The input signal has a low input power level equal to -20 dBm.

On the other hand, Figure 6.15 shows the distortion caused by the amplifier for high input levels ($\geq$1 dB CP). The data obtained from two-tone signal measurements, as well as the full set of screens, can be found in Appendix D.3.

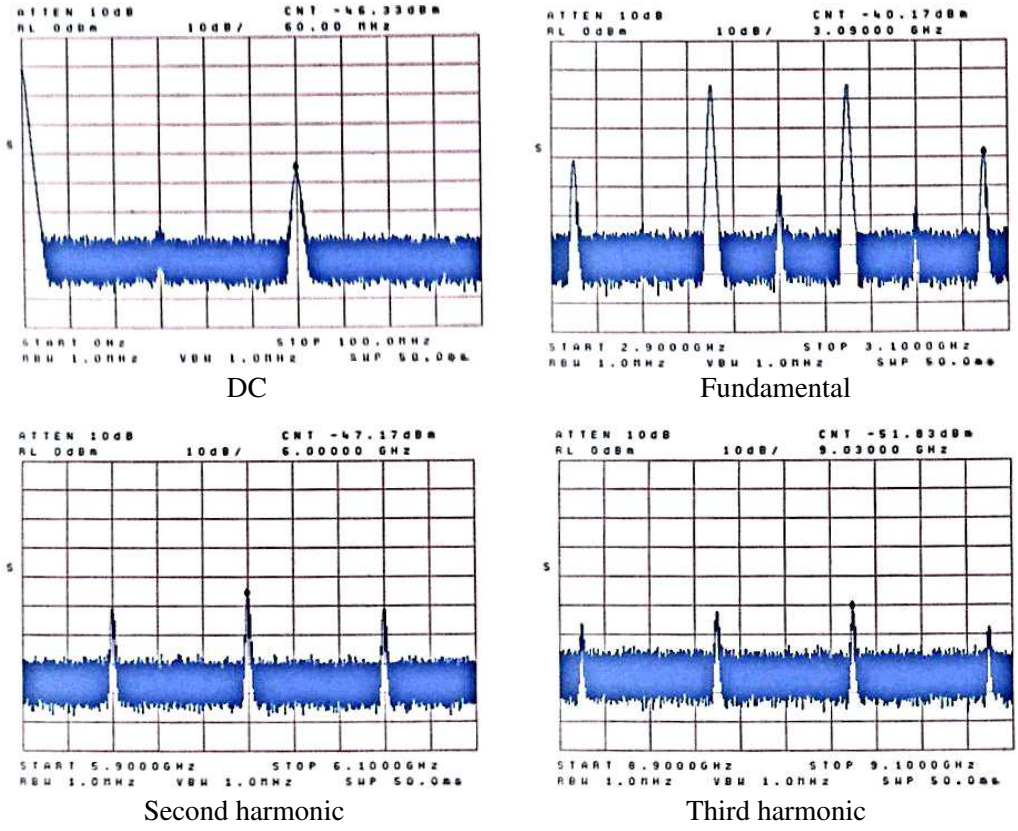

Figure 6.15: Intermodulation products present at DC, fundamental, second harmonic and third harmonic zones of ZVE-8G amplifier obtained from two-tone signal measurements performed with a spectrum analyzer. The two-tone input signal has a center frequency of 3 GHz, tone separation of 60 MHz and input power level equal to the DUT's 1 dB compression point input level (0 dBm).

Table 6.6 summarizes the frequency components measured in the fundamental, second and third harmonic zones of the ZVE-8G amplifier when operating it at a high input level equal to its 1 dB CP. A plot of the reconstruction of the spectrum based on this data is included in Appendix D.3.3.

An important parameter obtained from Table 6.6 is the third intermodulation product (IMP3) in the fundamental zone. The IMP3 is the frequency component closest to the original tones and, therefore, it is difficult to filter out.

Table 6.6: Frequency components obtained from two-tone signal measurements of ZVE-8G amplifier when operated at 0 dBm.

Cause of frequency component	**Frequency (GHz)**		**Output level (dBm)**
Input tone	f_1	3.03	+24.83
	f_2	2.97	+24.83
Second-order nonlinearity	$2f_1$	6.06	-11.50
	$2f_2$	5.94	-11.50
	f_1+f_2	6.00	-7.17
	f_1-f_2	0.06	-6.33
Third-order nonlinearity	$3f_1$	9.09	-17.50
	$3f_2$	8.91	-17.50
	$2f_1+f_2$	9.03	-11.83
	$2f_2+f_1$	8.97	-11.83
	$2f_1-f_2$	3.09	-0.17
	$2f_2-f_1$	2.91	-0.17

The input signal used has a center frequency of 3 GHz, a 60 MHz tone separation and a input level of 0 dBm. When applying this signal to the ZVE-8G amplifier (two-tone signal measurement), the IMP3 is obtained at 3.09 GHz and has an amplitude of -0.17 dBm.

Finally, it is easy to calculate the intermodulation distortion ratio (P_{IMR}) of the ZVE-8G amplifier from the data summarized in Table 6.6. This is done based on the definition introduced in Equation 3.15, which express that the P_{IMR} is the difference between one of the fundamental two tones (i.e. +24.83 dBm) and the highest IMP (i.e. IMP3 = -0.17 dBm), which gives a P_{IMR} equal to 25 dB or -25 dBc .

6.4 Multi-tone signal measurements

The settings summarized in Table 6.7 and the process in Appendix C.6 were used in order to perform multi-tone signal measurements. As explained in Section 5.2.4, the setup system for these type of measurements is the same used for two-tone signal measurements (Figure B.6, Appendix B.4). Moreover, a simple multisine signal was chosen in this research to be used as input to the DUT for multi-tone signal measurements, as indicated in Section 3.3. In the next sections, the results obtained from measuring the plain multisine signal and the nonlinear effect when applying this signal to the ZVE-8G amplifier are presented.

Table 6.7: Settings for ZVE-8G amplifier multi-tone signal measurements using a spectrum analyzer.

Parameter	Value
Center frequency	3 GHz
Signal bandwidth	60 MHz
Offset frequency	60 MHz
Average factor (with averaging function)	100
Input level	
Measurements of plain multisine signal	0 dBm
Measurements at 1 dB CP	0 dBm
Measurements at low input level	-20 dBm
Frequency range	
Full span	2.9 Hz to 9.1 GHz
Fundamental	2.9 GHz to 3.1 GHz
Fundamental (Zoom)	2.970 GHz to 2.972 GHz
Second harmonic	5.9 GHz to 6.1 GHz
Third harmonic	8.9 GHz to 9.1 GHz

6.4.1 Generated multisine signal

The setup system in Appendix B.5 was used to generate a bandpass multisine signal, using the baseband multisine signal generated with MATLAB software and described in Section 5.2.4.

The complex data representing the baseband multisine signal in time-domain generated with MATLAB software was saved in a floppy disk. This was introduced into the Arbitrary Waveform Generator and the screen obtained after loading the MATLAB file is shown in Figure 6.16.

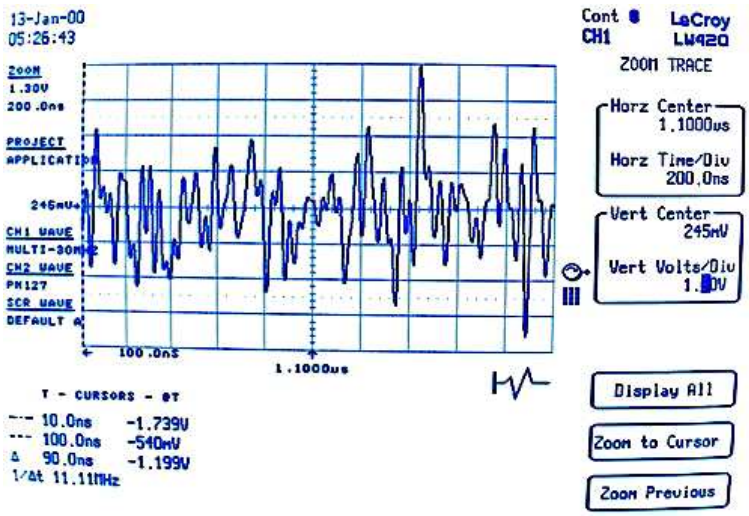

Figure 6.16: Arbitrary Waveform Generator's screen showing the part of the baseband multisine signal in time domain used for multi-tone measurements of ZVE-8G amplifier.

Figure 6.17 shows the results obtained from measuring the fundamental zone of the generated multisine signal at a high input level (=0 dBm). Other zones similarly measured are included in Figure D.17 (Appendix D.4.1).

The results of this measurement show that there is a small spurious signal present in the second harmonic zone at 6 GHz. Besides this, there are no other components in the spectrum. Therefore, any other component when feeding the DUT with this signal will be considered distortion introduced by the amplifier.

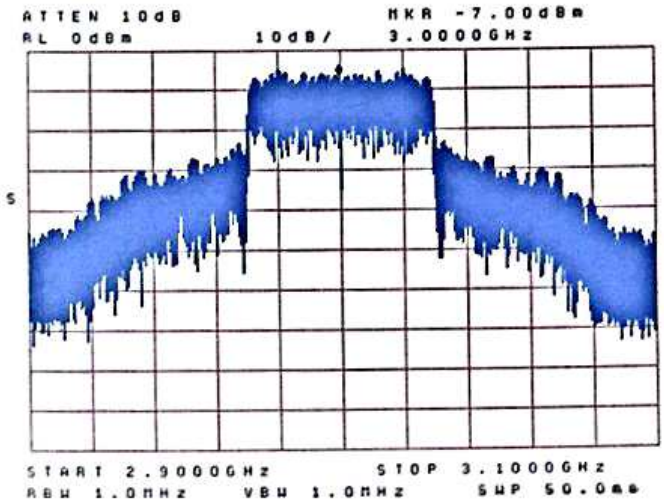

Figure 6.17: Frequency spectrum of the fundamental zone of the generated multisine signal obtained with a spectrum analyzer. The multisine signal has 300 tones, a center frequency of 3 GHz, bandwidth of 60 MHz and it is tested at a high input power level equal to the 1 dB CP of the DUT (0 dBm).

6.4.2 Multisine signal applied to amplifier

Multi-tone measurements were performed by applying the multisine signal of Figure 6.17 as input signal to the ZVE-8G amplifier. Next, the results of these measurements are presented using examples whenever possible. The data obtained from multi-tone signal measurements, as well as the full set of screens, can be found in Appendix D.4.

As an example of the results obtained for low input power levels, Figure 6.18 shows the frequency spectrum for the measured full span of the DUT operated -20 dBm input level. This input level falls into the linear zone of the amplifier. Therefore, no harmonic distortion affects the operation of the amplifier, which means that there are not frequency components, others than the original and the spurious at 6 GHz, in the resultant frequency spectrum.

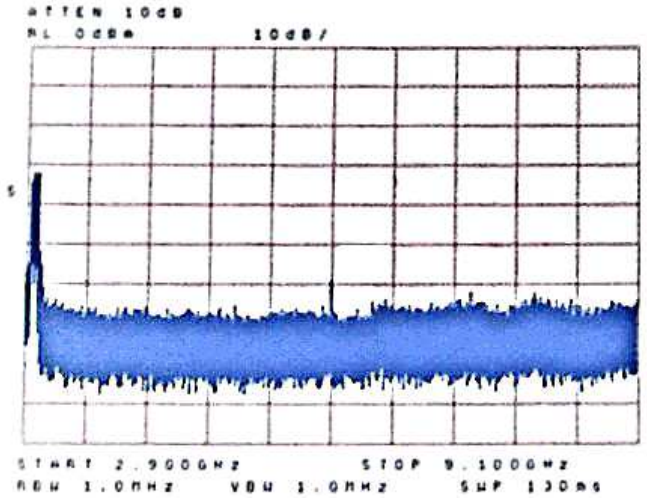

Figure 6.18: Frequency spectrum of the measured full span of ZVE-8G amplifier obtained from a multi-tone signal measurement. The input signal has a low input power level equal to -20 dBm.

As previously explained, for low input levels there is not distortion components introduced by the amplifier. However, when the DUT is operated at high input levels ($\geq$1 dB CP), harmonic distortion is present in the resultant spectrum, as shown in the example of Figure 6.19.

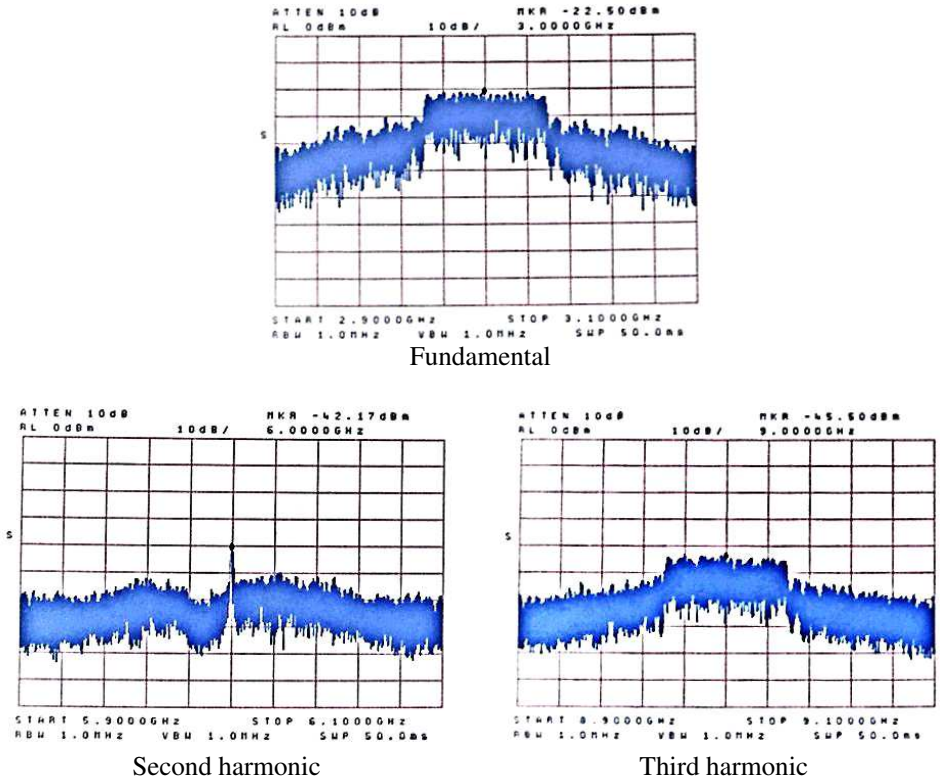

Figure 6.19: Frequency spectrum of the fundamental, second harmonic and third harmonic zones of ZVE-8G amplifier obtained from multi-tone signal measurements performed with a spectrum analyzer. The multisine input signal has a center frequency of 3 GHz, bandwidth of 60 MHz and input power level equal to the DUT's 1 dB compression point input level (0 dBm).

In order to calculate the Adjacent Channel Power Ratio (ACPR) of an amplifier it is necessary to measure the average power of the desired bandwidth (P_{B1}) and the average power at certain offset from the center frequency (P_{B2}) when performing a multi-tone signal measurement. Figure 6.20 presents an example of these measurements. The average power was obtained by using the SA's averaging function with an average factor of 100. P_{B1} was measured at the center frequency of the input multisine signal, 3 GHz.

On the other hand, the offset to be used for measuring P_{B2} should be equal to the channel spacing specified for a transmission scheme. Generally, when the purpose of the measurements is to model the behavior of an amplifier, a transmission scheme is not specified and, consequently, there is not a specific channel spacing. Therefore, and in order to model the worst case scenario, the channel spacing should be chosen as equal to the bandwidth of the multi-tone signal. Thus, the offset was chosen as 60 MHz and, subsequently, the average power P_{B2} was measured at 2.94 GHz.

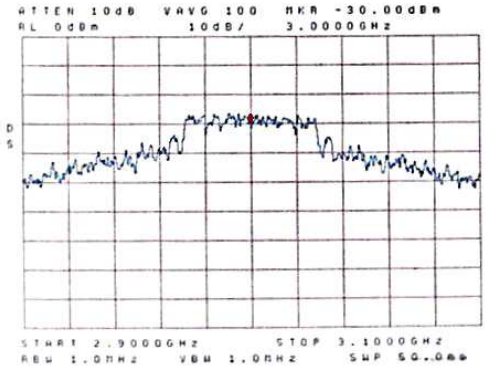

(a) Measurement at center frequency (i.e. 3.00 GHz)

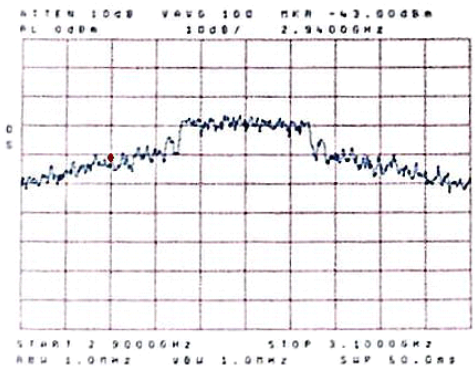

(b) Measurement at offset frequency (i.e. 2.94 GHz)

Figure 6.20: Example of ACPR measurement performed to the ZVE-8G amplifier using a spectrum analyzer. The multisine input signal has a center frequency of 3 GHz, bandwidth of 60 MHz and input power level equal to the DUT's 1 dB compression point input level (0 dBm).

The measurements to calculate the Multi-tone Intermodulation Ratio (MIMR) are performed similarly to the ones needed for ACPR calculation. The main difference is that there is not averaging function used. As an example, Figure 6.21 shows the measurement of the power at the center frequency (i.e. 3 GHz) and the highest power level outside the wanted band, which was found at 2.97 GHz.

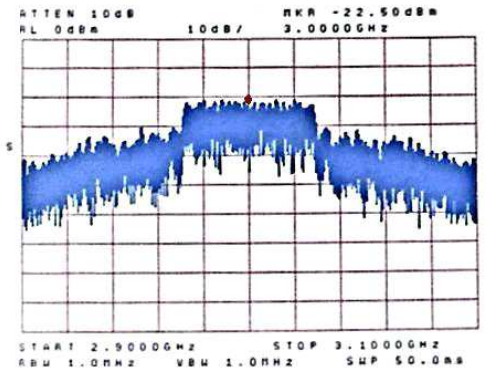

(a) Measurement at center frequency (i.e. 3.00 GHz)

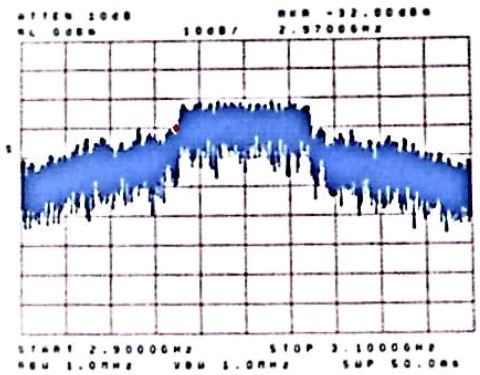

(b) Measurement at the highest power outside the wanted band (i.e. 2.97 GHz)

Figure 6.21: Example of MIMR measurement performed to the ZVE-8G amplifier using a spectrum analyzer. The multisine input signal has a center frequency of 3 GHz, bandwidth of 60 MHz and input power level equal to the DUT's 1 dB compression point input level (0 dBm).

ACPR and MIMR parameters' calculation was based on their corresponding definition, described in Section 3.3. The results of these calculations for the input signals tested are summarized in Table 6.8. The data obtained from the multi-

tone measurements performed, used to calculate ACPR and MIMR can be found in Appendix D.4.2.

The results presented in Table 6.8, show the expected behavior. ACPR and MIMR get higher (referenced to the carrier power) as the nonlinearity of the amplifier is increased (i.e. input level is increased inside the saturation zone), which means that the distortion outside the desired band gets stronger.

Table 6.8: Results of Adjacent Channel Power Ratio (ACPR) and Multi-tone Intermodulation Ratio (MIMR) calculations. The data was obtained using a spectrum analyzer and a multisine input signal.

Signal measured	**ACPR (dBc)**	**MIMR (dBc)**
Plain multisine input signal (at 1 dB CP = 0 dBm)	-28.33	-17.33
Input signal applied to DUT (at low input level = -20 dBm)	-25.50	-16.00
Input signal applied to DUT (at 1 dB CP = 0 dBm)	-13.00	-9.50

6.5 Summary of the chapter

This chapter presents the results of practical measurements based on the theory and procedures described in Chapters 2 to 5. The setup systems and processes used for all the measurements are compiled in Appendix B and C, respectively. Moreover, the figures, data and plots (others than the presented in this chapter) obtained from the tests can be found in Appendix D.

The results of passive devices were good. After the calibration of the Network Analyzer (NWA) the maximum deviation from the ideal flat frequency-sweep trace was 0.05 dB, which is considered small when compared to the amplifier's specified gain (i.e. 30 dB). The calibration of the Spectrum Analyzer (SA) was performed in order to check the correct functioning of the device. Cable attenuation was measured with the spectrum analyzer, giving a 0.33 dB result. Furthermore, the measured attenuators nominal value was 40.45 dB, which is correct according to the specified by the manufacturer (i.e. 40±1.3 dB).

Different parameters were obtained using single-tone input signals with a NWA and a SA. The results were good and inside the amplifier manufacturer's specifications. The average gain obtained inside the amplifier's operational range (i.e. 2 to 8 GHz) was 33 dB (3 dB more than the minimum specified). From the NWA, frequency-sweep, AM-AM and AM-PM curves were depicted and the 1 dB compression point (1 dB CP) was calculated for each of the frequencies measured (results summarized in Table 6.3). As an example of the reliability of the results obtained from these measurements, the output 1 dB compression point for a 3 GHz input signal was +32.49 dBm. The value of this parameter found in the specifications is +30 dB when the gain of the amplifier is 30 dB. Therefore, the 1 dB CP obtained is approximately the expected, based on the measured gain (i.e. 33 dB).

With the SA and an input signal of 3 GHz and 0 dBm, the second- and third-harmonic curves of the ZVE-8G amplifier were obtained and the corresponding second-order intercept point (IP2) and third-order intercept point(IP3) were calculated. From these, the obtained output IP3 (i.e. +42.12 dBm) was compared with the expected value (+42.49 dBm), giving a positive result.

The generated signal to be used as input for the two-tone signal measurement was measured, giving as result components in the two expected frequencies. No other components were detected for low or high input levels. Therefore, when using this signal as input to the amplifier tested, any component shown in the output spectrum will be distortion introduced by the amplifier. Next, the two-tone signal measurement was performed. The harmonics and intermodulation products were summarized in Table 6.6 and the intermodulation distortion ratio was calculated, giving a result of 25 dB.

In order to perform multi-tone signal measurements, a multisine signal was used, which was measured as well, giving as result the expected spectrum in the fundamental zone and a spurious signal in the second harmonic zone. The resultant spectrum when applying the multisine signal to the amplifier showed no harmonic distortion for low input power levels and strong distortion for high input levels ($\geq$1 dB CP), as theoretically predicted. Finally, calculations of the adjacent power channel ratio and the multi-tone intermodulation ratio showed the expected behavior, giving higher levels (referenced to the carrier power) for high input levels, consequently causing higher nonlinear distortion.

Chapter 7

Measurement errors and use of results

The theory summarized in this thesis was taken to practice in Chapter 6, where measurements of amplifier nonlinearity were performed. Single-, two- and multi-tone signals were used in order to obtain different measures and parameters that are useful for modelling and, furthermore, alleviating the distortion caused by amplifiers.

In this chapter, two main factors to consider after the performed measurements in this research are covered. First, an analysis of the possible errors that may have occurred during the planning and measurement process is done. This analysis is based on experiences and knowledge acquired during the whole measurement process. The second aspect to be considered in this chapter is the usefulness of the measurements, which is supported by an actual example of the application of the results in modelling the measured amplifier. Finally, examples of the general use of amplifier measurements are commented and references for these are given.

7.1 Discussion of measurement errors

Making accurate measurements is a difficult task since it requires precision during the whole process of planning, selecting the adequate devices, connecting systems and reading results. Therefore, the error analysis is a complex process, which involves a big amount of factors, from connection mismatches to implicit errors in the measuring devices. This is why, in this section, the intention is not to quantify the error obtained while performing the measurements but to analyze the possible causes of these errors and to give recommendations for future measurements which might require a higher accuracy.

On the statistical point of view, it has been calculated that higher-order Intermodulation Products (IMPs) have higher variance. Therefore, low-order IMPs can be measured accurately while higher-order ones give more problems. Fortunately, the lower-order IMPs (usually IMP3) are the main focus of the measurements, as pointed out in Section 3.2.1. Moreover, it is possible to adjust the variance of the IMP3 by proper biasing of the amplifier and to fine-tune the phase-shift in order to obtain more accurate measurement results [92].

Next, the most common error factors occurring during the practical measurements are commented. The first obvious aspect influencing the accuracy of the measurements is the accuracy of the measuring devices (i.e. network analyzer and spectrum analyzer). For low input levels the accuracy of the results is limited by the device's floor noise and magnitude and phase uncertainty. For high input levels, compression limits the accuracy. Moreover, generators (i.e. arbitrary waveform generator and vector signal generator) can affect the results by introducing subharmonics and spurious signals.

Before calibrating or measuring, check that all cables and adapters are correctly tightened in order to avoid errors due to mismatches. If the effect of mismatches cannot be neglected, it should be kept as constant as possible. This should be taken into account during the calibration and the measurement itself.

Using an extra adapter when calibrating the measuring devices can produce errors in measurements. However, in my personal experience, loss due to connectors when calibrating is higher if an adapter is taken out of the calibration system

instead of adding one. In general, the loss caused by adapters is usually very low ($\approx<$ 0.15 dBm). This loss can be minimized by using as few parts as possible. Moreover, calibration should be done without attenuators, in order to avoid errors caused by very low power signals confused with the measuring device's intrinsic noise.

In the specific case of amplifier measurements, it is highly recommended to make sure that the amplifier is connected to the system before feeding it with the power supply. Likewise, it is important not to forget to turn off the power supply of the amplifier, when finishing working with it. This simple precautions will avoid damaging the device and, subsequently, erroneous results.

Attention should be paid when setting the measuring devices to obtain a specific parameter. First, calibration of the measuring device should be correctly done. In the case of measurements with a network analyzer, the interpolation and correction features should be turned on before performing any power- or frequency-sweep. On the other hand, when working with the spectrum analyzer, the "RF output" of the vector signal generator should be active and for two- and multi-tone measurements the "Vector" function should be turned on as well.

Other errors in measurements are generated due to the use of input signals that do not have the properties mentioned in Section 5.1.1, which yield to incorrect results. For example, when performing an input power level sweep, the input level should be varied from a low input power level to a level few decibels above the saturation point of the amplifier indicated on its specifications. This should be done in order to assure the measurement of the amplifier nonlinearity. Moreover, measurements should be done only up to a few decibels (1 or 2 dB) above the 1 dB CP. This will avoid possible oscillations on the output gain for high input power levels, which occurs as a result of the clipping effect produced by the amplifier at too high input power levels. Furthermore, the selection of the tone separation (two-tone signal) and the bandwidth (multi-tone signal) should be done carefully, in order to capture all the desired intermodulation products.

In general, and in order to perform more accurate measurements, it is necessary to work with good quality equipment, which can be chosen by analyzing the accuracy parameters found in any device's specifications. This should be also taken into account for other devices, such as adapters, cables and their connectors.

7.2 Using the measurement results

As presented in Chapter 6, the results of the measurements performed in this research are reliable. Therefore, they can be used for accurate modelling of nonlinear amplifiers. In this section, examples of applications of the measurements for modelling and in other areas are presented, as a way of proving the usefulness of the work done.

The most significative example of the use of the results obtained in this thesis is presented in Peter Jantunen's Master's Thesis [5], where modelling of the amplifier measured (i.e. ZVE-8G) was done. The Hammerstein model was chosen to characterize the frequency-dependent behavior of the amplifier. This model assumes an approach where the nonlinearity and the dynamics of the system can be separated into a nonlinear static block and a linear dynamic block.

In Jantunen's research, the Hammerstein model was implemented using a 5th-order-polynomial model for the static block and a 13th-order Finite Impulse Response (FIR) filter with a constant delay of 17 samples for the dynamic block. The polynomial coefficients were estimated with a Least Squares Estimator (LSE). On the other hand, the filter coefficients were found with the Weighted Lest Squares Estimator (WLSE) and a constant delay factor of 10^3 in order to reduce the computational complexity of the filter. The model was applied to the frequencies between 5 GHz and 7 GHz, which means a 2 GHz bandwidth inside the amplifier's operational range. Figure 7.1 shows the cascaded nonlinear static block and the linear dynamic block which represent the Hammerstein model, as well as the implementation of this model done in [5].

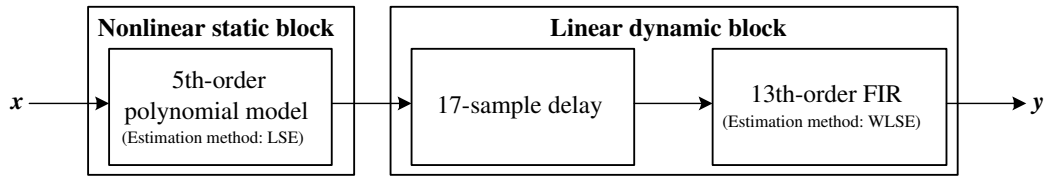

Figure 7.1: Implementation of the Hammerstein model in order to characterize the ZVE-8G amplifier.

The results of the Hammerstein model implemented were very good. Figures 7.2 and 7.3 show examples of the measured and estimated results obtained for frequency-sweep and AM-AM curves, respectively.

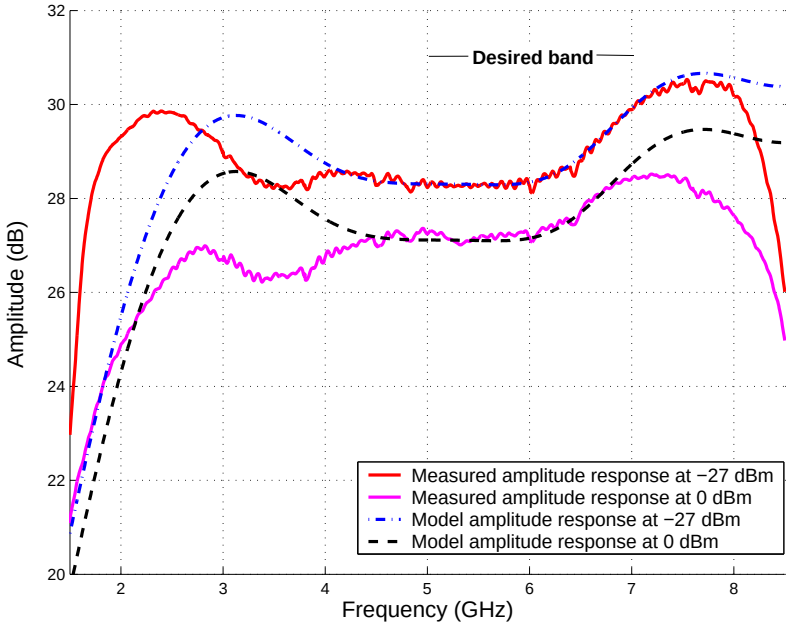

Figure 7.2: Example of measured and estimated frequency-sweep curves. [5]

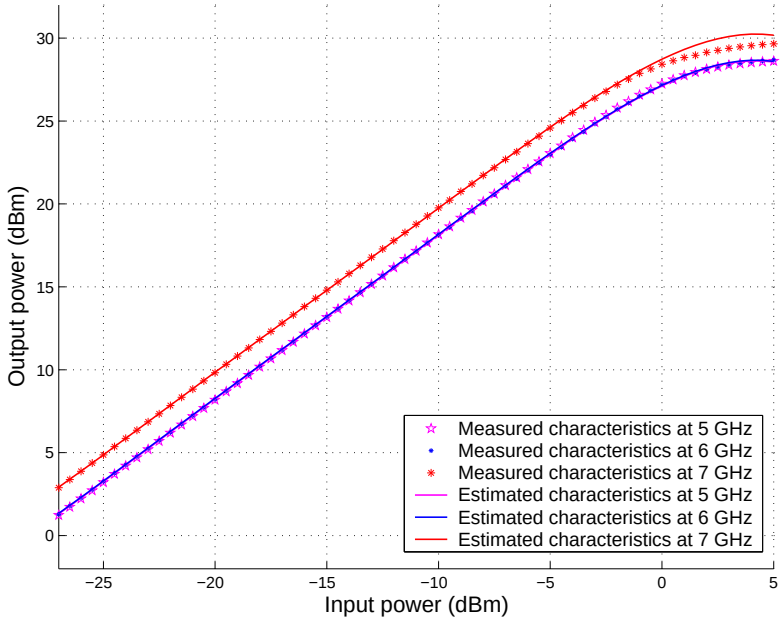

Figure 7.3: Example of measured and estimated AM-AM curves at selected frequencies inside the desired band. [93]

The amplifier nonlinearity model obtained was accurate for single-tone signals over the desired band (i.e. 5 GHz to 7 GHz) and at all power levels lower than the 1 dB compression point. Furthermore, the model obtained was used to generate a predistortion linearizer signal for the ZVE-8G amplifier [6]. This shows that the measurements done in this research are useful not only for modelling, but to generate solutions to alleviate the nonlinearity presented by the amplifier.

The amplifier modelling topic is widely researched nowadays. Consequently, there have been several approaches on the way of using measurements similar to the ones presented in this thesis. For instance, a Wiener-Hammerstein model designed based on multi-tone measurements of a broad-band RF amplifier [24]; a model for bandpass nonlinearities based on harmonic measurements [94]; or an approach of nonlinear spectral regrowth modelling based on measured continuous wave amplifier data [95].

Moreover, measurements of amplifiers are extensively used to prove in a practical way the theoretical and simulated results of linearization methods, such as a post-distortion receiver for mobile communications [96] or a third-order intermodulation reduction method in nonlinear microwave systems [97].

In general, the necessity of representing the nonlinearity of power amplifiers and linearizers is becoming overwhelming in recent wireless applications, where wide-band digital modulated signals with high Peak-to-Average Ratio (PAR), such as third-generation (3G) signals, are used [98]. Therefore, nowadays measurement applications have the common final aim of improving the efficiency of future wireless transmissions.

7.3 Summary of the chapter

In this chapter aspects to be considered after performing amplifier measurements were discussed. First, comments on the possible errors that may have occurred during the measurements performed in this thesis were given. As previously commented, high accurate measurements are a difficult task to achieve since many factors are involved in the process, from which some can be avoided or controlled but others are inherent to the setup system and to the device under test itself.

Next, the usefulness of measurements similar to the ones presented in this thesis was analyzed. Measurements of amplifiers were proven to be useful. This fact is supported by a recent example of the application of the ZVE-8G amplifier measures obtained in this research on the modelling of the amplifier. Finally, other examples of the usage of this type of measurements were commented and referred.

Chapter 8

Conclusions and future work

This chapter finalizes the work done in this thesis by presenting a brief summary of the carried out research, the conclusions obtained and recommendations for future work related to amplifier measurements.

Throughout Chapters 2 and 3, the basic theory about amplifiers was introduced, including the most common distortion parameters obtained from measurements using different input signals. Harmonic distortion appearing at frequencies multiple of the fundamental frequency is the main nonlinear effect produced by single-tone input signals. Moreover, AM-AM and AM-PM characteristic curves respectively show the output amplitude and phase behavior when varying the input signal. However, it is necessary to perform a frequency-sweep measurement, in order to represent the memory effects introduced by amplifiers. Furthermore, a two-tone input signal was used to obtained the intermodulation products in the output spectrum. The third intermodulation product present in the fundamental zone is the most important parameter obtained from a two-tone test because it is the frequency component closest to the fundamental tone and, therefore, it is difficult to filter out with simple methods. In addition, a multisine signal was chosen for measuring the effects of a nonlinear amplifier over high peak-to-average ratio signals.

Chapters 4 and 5 presented the necessary aspects to plan and perform measurements of amplifier nonlinearity. An overview of modelling and estimation methods was done in order to determine the type of measurements required to characterize

the amplifier distortion. Next, the procedure and setup systems to perform single-, two- and multi-tone signal measurements were presented. Emphasis was made on the modelling parameters to be obtained from each type of measurement.

The results obtained from performing practical measurements are presented in Chapter 6. The amplifier used is a Mini-Circuits ZVE-8G wideband high-power amplifier. Parameters such as the average gain inside the amplifier's operational range, the 1 dB compression point and the third intermodulation product were found with single-tone signal measurements, giving a positive result when compared to the expected values. A two-tone signal was generated and the intermodulation distortion ratio, among other distortion measures, was measured. Finally, a 300-tone multisine signal was generated. When feeding the amplifier with this signal the adjacent power channel ratio and the multi-tone intermodulation ratio were obtained, showing the expected behavior (i.e. higher nonlinear distortion for higher input levels).

Chapter 7 summarized aspects to be considered after performing amplifier measurements. Comments on the possible errors that may have occurred during the measurements performed and examples of the usage of the results were given. A recent example of the application of the amplifier measures obtained in this research on the modelling of the amplifier was described. Finally, complementary information needed to fulfil the objective of this research is annexed on Appendices A to D. This includes the equipment specification, setup systems and processes used, as well as the full set of results.

The objective of this thesis was to provide the basis to perform accurate measurements of power amplifiers to obtain reliable data for characterizing their nonlinearity. The objective was achieved throughout this research with theoretical and practical work. Next, the main conclusions found in this research are presented.

An extensive variety of parameters can be obtained from amplifier measurements. In general, it was observed that signals with higher number of tones represent better the distortion introduced by an amplifier. However, signals with one or two tones can give an easy-manipulable and clear approximation of the nonlinearity caused by an amplifier. For instance, it was shown how the frequency-dependent and frequency-independent behavior of the amplifier can be modelled based on the AM-AM, AM-PM and frequency-sweep curves obtained from single-tone sig-

nal measurements performed in this thesis. Therefore, it is essential to previously determine the needed parameters for a specific model, in order to better characterize an amplifier.

Moreover, it was determined that highly accurate measurements are a difficult task to achieve since many aspects are involved in the process. It was found that some of these factors can be avoided or controlled but others are inherent to the setup system and to the device under test itself. Therefore, specialized equipment and careful planning should be considered in order to avoid unnecessary errors and loss that unavoidably lead to inaccurate results.

Furthermore, the usability of the results obtained from measurements similar to the ones presented in this thesis was found to be very wide. An example of amplifier modelling based on measurements done in this research and a literature review on more applications of measurements in modelling proved this observation. In this sense, this thesis contribution is summarized into a full set of measurement results, from which diverse models can be derived.

Finally, there are many more aspects to be considered for future research. Examples for future work, including some related references, are:

- Develop more exact measuring systems. For instance, the three-tone test, which shows more accurately the effect of adjacent channels in the nonlinear distortion of an amplifier [99, 100].
- Find and perform measuring methods that characterize better the phase distortion and memory effects of amplifiers [101, 102, 103].
- Perform multi-tone noise power ratio measurements to analyze in-band distortion caused by an amplifier and make tests with noisy input signals in order to analyze the effect of amplifier distortion in carrier-to-noise ratio [104, 105, 106].
- Analyze the distortion carried by amplifiers in time-domain [107, 108, 109].
- Design a predistortion signal, based on a model designed with data obtained from this measurements and measure its performance with different input signals (single-, two- and multi-tone) [110, 111].

References

[1] Jos, R. Future developments and technology options in cellular phone power amplifiers: from power amplifier to integrated RF front-end module. In *Proceedings of the 2000 Bipolar/BiCMOS Circuits and Technology Meeting*, MN, USA, 2000. Philips Discrete Semiconductors.

[2] Ahmed, N.; et al. Finite backlog effects on downlink scheduling. Technical report, Department of Electrical and Computer Engineering. Rice University, 2003.

[3] ACTIX for decisive data. WCDMA radio link engineering basics: lessons learned from 2G IS-95 CDMA and GSM networks. White paper, 2002.

[4] Costa, E.; et al. Impact of amplifier nonlinearities on OFDM transmission system performance. *IEEE Communications Letters*, 2(2), February 1999.

[5] Jantunen, P. Modelling of nonlinear power amplifiers for wireless communications. Master's thesis, Helsinki University of Technology, Espoo, Finland, March 2004.

[6] Cheong, M.; et al. Design of pre-distorters for power amplifiers in future communications systems. In *IEEE Nordic Signal Processing Symposium, NORSIG'04*, Espoo, Finland, June 2004. http://wooster.hut.fi/publications/norsig2004/.

[7] Sedra, A.; et al. *Microelectronic circuits*. Oxford University Press, New York, USA, fourth edition, 1998.

[8] Beals, G. Biography of Thomas Alva Edison. Internet: http://www.-thomasedison.com/biog.htm, 1999.

[9] Wolff, C. Radar-basics. Travelling wave tube: physical construction and functional describing. Internet: http://mitglied.lycos.de/radargrundlagen/-top-en.html, Germany, 1996-2004.

[10] UltraRF. Application notes: high power solid state circuit design. Internet: http://www.cree.com/ftp/pub/appnote3.pdf.

[11] Van Fleteren, S. Traveling wave tube vs. solid state amplifiers. Technical report, Communications and Power Industries (formely Varian Associates), 2000.

[12] Turner, S. D. Reliability advantages of modular solid state power amplifiers compared to traveling wave tube amplifiers. Technical report, Armed Forces International, 2003.

[13] Boylestad, R. L.; et al. *Electronic devices and circuit theory.* Prentice Hall, Mexico, 6th edition, 1997.

[14] Kenington, P. B. *High-linearity RF amplifier design.* Artech House, Inc., Norwood, MA, USA, 2000.

[15] Sokal, N. O. Class-E RF power amplifiers. *QEX*, Jaunary/February 2001.

[16] Liang, C-P.; et al. Nonlinear amplifier effects in communications systems. *IEEE Transactions on Microwave Theory and Techniques*, 47(8), August 1999.

[17] Andreoli, S.; et al. Nonlinear distortions introduced by amplifier on COFDM signals. Measurements, effects and compensation techniques. In *IEEE Tyrrhenian Int. Workshop.* Itelco R&D and Instituto di Electtronica, Universita di Perugia, September 1997.

[18] Cheong, M. Y. Constant modulus algorithm based multipath channel estimation for OFDM systems with space-time block code. Master's thesis, Helsinki University of Technology, Espoo, Finland, November 2002.

[19] Bahai, A.; et al. *Multi-carrier digital communications. Theory and applications of OFDM.* Kluwer Academic / Plenum Publishers, NY, USA, 1999.

[20] Määttänen, H.-L. Nonlinear amplification of clipped-filtered multicarrier signals. Master's thesis, Helsinki University of Technology, Espoo, Finland, August 2004.

[21] Remley, K. Multisine excitation for ACPR measurements. *IEEE MTT-S Int. Microwave Symp. Dig.*, June 2003.

[22] Pedro, J.; et al. On the use of multitone techniques for assessing RF components' intermodulation distortion. *IEEE Trans. on Microwave Theory and Techniques*, 47(12), December 1999.

[23] Schreurs, D.; et al. Use of multisine signals for efficient behavioural modelling of RF circuits with short-memory effects. ARFTG 61Philadelphia, June 2003.

[24] Crama, P.; et al. Broad-band measurement and identification of a Wiener-Hammerstein model for an RF amplifier. 60th ARFTG conference digest, December 2002.

[25] Sano, M.; et al. Identification of Hammerstein-Wiener system with application to compensation for nonlinear distortion. In *Proc. SICE Ann. Conf.*, volume 3, August 2002.

[26] Schoukens,J.; et al. Simple methods and insights to deal with nonlinear distortions in FRF-measurements. *Mechanical Systems and Signal Processing*, 14(4), 2000.

[27] Braun, M.; et al. Design of minimum crest factor multisinusoidal signals for plant-friendly identification of nonlinear process systems. In *SYSID*, CA, USA, June 2000.

[28] Weiss, M.; et al. Identification of nonlinear cascade systems using paired multisine signals. *IEEE Trans. on Instrumentation and Measurement*, 47(1), February 1998.

[29] Jeruchin, M.; et al. *Simulation of communication systems: modelling, methodology and techniques.* KluwerAcademic/Plenum Publishers, NY, USA, second edition, 2000.

[30] Gutiérrez, H.; et al. Nonlinear gain compression in microwave amplifiers using generalized power-series analysis and transformation of input statistics. *IEEE Trans. Microwave Theory and Tech.*, 48(10), October 2000.

[31] Guo, Y.; et al. A novel adaptive pre-distorter using LS estimation of SSPA non-linearity in mobile OFDM systems. In *Proc. Int. Symp. on Circuits and Systems*, volume 3, May 2002.

[32] Nordsjö, A. An algorithm for adaptive predistortion of certain time-varying nonlinear high-power amplifiers. In *RADAR 2002*, October 2002.

[33] Gutiérrez, H.; et al. Spectral regrowth in microwave amplifiers using transformation of signal statistics. In *IEEE Int. Microwave Symposium Digest*, volume 3, June 1999.

[34] Vörös, J. Modeling and identification of wiener systems with two-segment nonlinearities. *IEEE Trans. Control Syst. Tech.*, 11(2), March 2003.

[35] Saleh, A. Frequency-independent and frequency-dependent nonlinear models of TWT amplifiers. *IEEE Trans. Commun.*, 29(11), November 1981.

[36] Ghorbani, A.; et al. The effect of solid state power amplifiers (SSPAs) nonlinearities on MPSK and M-QAM signal transmission. In *Proc. Int. Conf. on Digital Processing of Signals in Communications*, September 1991.

[37] Rapp, C. Effects of HPA-nonlinearity on a 4-DPSK/OFDM-signal for a digital sound broadcasting system. In *Proc. of the Second European Conference on Satellite Communications*, Lige, Belgium, October 1991.

[38] White, G.; et al. Modelling of nonlinear distortion in broadband fixed wireless access systems. *IEEE Electronics Letters.*, 39(8), April 2003.

[39] Abuelma'atti, M. T. Effect of nonmonotonicity on the intermodulation performance of A/D converters. *IEEE Trans. Commun.*, 33(8), August 1985.

[40] Abuelma'atti, M. T. Frequency-dependent nonlinear quadrature model for TWT amplifiers. *IEEE Trans. Commun.*, 32(8), August 1984.

[41] Nelles, O. *Nonlinear system identification: from classical approaches to neural network and fuzzy models*. Springer–Verlag, Berlin, Germany, 2001.

[42] Bai, E-W. Frequency domain identification of Hammerstein models. *IEEE Trans. Automatic Control*, 48(4), April 2003.

[43] Clark, C.; et al. Power amplifier characterization using a two-tone measurement technique. *IEEE Trans. Microwave Theory and Techniques*, 50(6), June 2002.

[44] Mathews, J.; et al. *Polynomial signal processing*. John Wiley & Sons, NY, USA, 2000.

[45] Lesiak, C.; et al. The existence and uniqueness of Volterra series for nonlinear systems. *IEEE Trans. Automatic Control*, 23(6), December 1978.

[46] Tummla, M.; et al. Volterra series based modeling and compensation of nonlinearities in high power amplifiers. In *Proc. Int. Conf. on Acoustics, Speech, and Signal Proc.*, volume 3, April 1997.

[47] Silva, C.P.; et al. Application of polyspectral techniques to nonlinear modeling and compensation. In *IEEE MTT-S Internationa Microwave Symposium Digest*, volume 1, AZ, USA, May 2001. Aerosp. Corp., El Segundo.

[48] Kay, S. *Fundamentals of statistical signal processing.* Prentice Hall International, Inc., NJ, USA, 1993.

[49] Friedlander, B.; et al. The exact Cramer-Rao bound for gaussian autoregressive processes. *IEEE Trans. Aerospace and Electronic Systems*, 25(1), January 1989.

[50] Peleg, S.; et al. The Cramer-Rao lower bound for signals with constant amplitude and polynomial phase. *IEEE Trans. Signal Processing*, 39(3), March 1991.

[51] Gu, H. Linearization method for finding Cramer-Rao bounds in signal processing. *IEEE Trans. Signal Processing*, 48(2), February 2000.

[52] Stuart, A.; et al. *Kendall's advanced theory of statistics: classical inference and and the linear model.* Oxford University Press, NY, USA, 6 edition, April 1998.

[53] Rohatgi, V.; et al. *An introduction to probability and statistics.* Wiley-Interscience, USA, 2 edition, October 2000.

[54] Eliason, S. *Maximum likelihood estimation : logic and practice.* SAGE Publications, USA, August 1993.

[55] Severini, T. *Likelihood methods in statistics.* Oxford University Press, NY, USA, January 2001.

[56] Gupta, N.; et al. Computational aspects of maximum likelihood estimation and reduction in sensitivity function calculations. *IEEE Trans. Automatic Control*, 19(6), December 1974.

[57] Fang, B. A more direct proof of the minimum variance property of the linear weighted least-squares estimator. *IEEE Trans. Automatic Control*, 14(6), December 1969.

[58] Besson, O.; et al. Sinusoidal signals with random amplitude: least-squares estimators and their statistical analysis. *IEEE Trans. Signal Processing*, 43(11), November 1995.

[59] Haykin, S. *Least-mean-square adaptive filters*. Wiley-Interscience, USA, September 2003.

[60] Laakso, T.; et al. Splitting the unit delay. *IEEE Signal Processing Mag.*, 13(1), January 1996.

[61] Matyas, L. *Generalized method of moments estimation*. Cambridge University Press, USA, April 1999.

[62] Powell, J. Notes On method-of-moments estimation. Internet: http://-emlab.berkeley.edu/users/powell/e241a_sp04/mmnotes.pdf. Department of Economics. University of California, Berkeley.

[63] Bar-Shalom, Y. *Estimation with applications to tracking and navigation*. Wiley-Interscience, NY, USA, June 2001.

[64] Peña, D.; et al. *A course in time series analysis*. Wiley-Interscience, USA, November 2000.

[65] Ludeman, L. *Random processes: filtering, estimation and detection*. Wiley-IEEE Press, NJ, USA, December 2002.

[66] Van Trees, H. *Detection, estimation and modulation theory, part I*. Wiley-Interscience, USA, September 2001.

[67] Duda, R. *Pattern classification*. Wiley-Interscience, USA, 2 edition, October 2000.

[68] Sundresh, T.; et al. Maximum a posteriori estimator for suppression of interchannel interference in FM receivers. *IEEE Trans. Communications*, 25(12), December 1977.

[69] Edfors, O.; et al. OFDM channel estimation by singular value decomposition. *IEEE Trans. Communications*, 46(7), July 1998.

[70] Laverghetta, T. S. *Handbook of microwave testing*. Artech, USA, 1980.

[71] Shaw, M.; et al. Characterization of a 2 GHz submicron bipolar 60 watt power transistor with single tone, multi-tone and CDMA signals. In *ARFTG 47th*, USA, 1996.

[72] Cabot, R. Comparison of nonlinear distortion measurement methods. In *Proceedings of the 11th International AES Conference*, 1992.

[73] Schreurs, D.; et al. RF behavioural modelling from multisine measurements: influence of excitation type. In *33rd. European Microwave Conference (EuMW)*, Munich, Germany, October 2003.

[74] Agilent Technologies. *Introductory operating guide to the Agilent 8780A vector signal generator*, Agilent PN 8780A-1, USA, 1986. Product Note.

[75] LeCroy Corporation, NY, USA. *Operator's manual: LW400 / LW400A/ LW400B WaveStation*, April 1999.

[76] Antenna Company Technical Support Team. Intro to SWR. Technical report, Firestik, AZ, USA, 1996.

[77] Collier, R. J.; et al. *Microwave measurements*. Peter Peregrinus Ltd., London, United Kingdom, second edition, 1989.

[78] Agilent Technologies, USA. *Agilent PNA series microwave network analyzers: data sheet*, September 2002.

[79] Agilent Technologies, USA. *Agilent 8560 EC series spectrum analyzers: data sheet*, June 2003.

[80] Lucas, J.R. Basic circuit elements. Technical report, Department of Electrical Engineering, University of Moratuwa, Sri Lanka, November 2001.

[81] Think & Tinker Ltd. The prime source for prototyping equipment and supplies: Glossary. Internet: http://www.thinktink.com/stack/volumes/-voliii/reference/glossary.asp#A, July 2004.

[82] Mini-Circuits, NY, USA. *Amplifiers, medium high power 50 kHz to 8 GHz: data sheet*.

[83] Agilent Technologies, USA. *PNA series network analyzer online help (Dec 2003)*, December 2003.

[84] Katz. E. . Harry Nyquist (biography). Internet: http://www.geocities.com/-bioelectrochemistry/nyquist.htm, November 2002.

[85] Bennett, W. R. *Electrical noise*. McGraw Hill Book Company, Inc., New York, USA, 1960.

[86] Barkley, K. Two-tone IMD measurement techniques. Seven rules to ensure the best characterization of non-linear RF components. *RF test & measurement*, June 2001.

[87] Granberg, H. Measuring the intermodulation distortion of linear amplifiers. Motorola semiconductor engineering bulletin. rf application reports, Motorola Inc., 1993.

[88] Akaiwa, Y. *Introduction to digital mobile communication*. Wiley-Interscience, NY, USA, 1st edition, January 1997.

[89] Vuolevi, J.; et al. *Distortion in RF power amplifiers*. Artech House, Inc., MA, USA, 2003.

[90] Naval Air Systems Command. Avionics Department. AIR-4.5 EW Class Desk. Naval Air Warfare Center. Weapons Division. Avionics Department. Electronic Warfare Division. Electronic warfare and radar systems engineering handbook. USA., April 1999.

[91] *Quick reference guide. Agilent Technologies 8560 E-series and EC-series spectrum analyzers*, USA, November 2000.

[92] Telegdy, A. Extending the dynamic range of RF/microwave intermodulation measurements by multiple-carrier cancellation. In *The 11th IEEE PIMRC International Symposium*, volume 1, London, UK, September 2000.

[93] Jantunen, P.; et al. Measurements and modelling of nonlinear power amplifiers. In *IEEE Nordic Signal Processing Symposium, NORSIG'04*, Espoo, Finland, June 2004. http://wooster.hut.fi/publications/norsig2004/.

[94] Behravan, A.; et al. A model for bandpass nonlinearities based on harmonic measurements. In *Proceedings of the IEEE Radio and Wireless conference*, MA, USA, August 2003.

[95] Van Moer, W.; et al. Measurement-based nonlinear modeling of spectral regrowth. *IEEE Trans. Instrumentation and Measurement*, 50(6), December 2001.

[96] Quach, L.; et al. A postdistortion receiver for mobile communications. *IEEE Trans. Vehicular Technology*, 42(4), November 1993.

[97] Hu, Y.; et al. A new method of third-order intermodulation reduction in nonlinear microwave systems. *IEEE Trans. Microwave Theory and Techniques*, 34(2), February 1986.

[98] Boumaiza, S.; et al. Realistic power-amplifiers characterization with application to baseband digital predistortion for 3G base stations. *IEEE Trans. Microwave Theory and Techniques*, 50(12), December 2002.

[99] Ma, J-G. Effects of the adjacent channels on IP3 of RF amplifiers. *Microwave and Optical Technology Letters. Wiley Periodicals, Inc.*, 35(1), October 2002.

[100] Vuolevi, J.; et al. Measurement technique for characterizing memory effects in RF power amplifiers. *IEEE Trans. Microwave Theory and Techniques*, 49(8), August 2001.

[101] Ghannouchi, F.; et al. Phase distortion measurements for saturated MESFETs loaded with arbitrary impedance terminations. In *IEEE Instrumentation and Measurement Technology Conference*, volume 1, Hamamatsu, Japan, May 1994. Dept. of Electr. & Comput. Eng., Ecole Polytech. de Montreal.

[102] Ku, H.; et al. Extraction of accurate behavioral models for power amplifiers with memory effects using two-tone measurements. In *IEEE MTT-S International Microwave Symposium Digest*, volume 1, WA, USA, June 2002.

[103] Ku, H.; et al. Quantifying memory effects in RF power amplifiers. *IEEE Trans. Microwave Theory and Techniques*, 50(12), December 2002.

[104] Upshur, J.; et al. Evaluation of linearity characterization techniques for multicarrier solid-state power amplifiers. In *IEEE MTT-S Symposium on Technologies for Wireless Applications*, BC, Canada, February 1999. COMSAT Lab. USA.

[105] Mallet, A.; et al. A new satellite repeater amplifier characterization system for large bandwidth NPR and modulated signals measurements. In *IEEE MTT-S International Microwave Symposium Digest*, volume 3, WA, USA, June 2002. Toulouse Space Center, CNES.

[106] Ku, H.; et al. Prediction of output carrier-to-interference ratios from nonlinear microwave components driven by arbitrary signals using intrinsic kernel functions. In *IEEE Radio and Wireless Conference*, CO, USA, September 2000. Sch. of Electr. & Comput. Eng., Georgia Inst. of Technol.

[107] Clark, C.; et al. Time-domain envelope measurement technique with application to wideband power amplifier modeling. *IEEE Trans. Microwave Theory and Techniques*, 46(12), December 1998.

[108] Draxler, P.; et al. Time domain characterization of power amplifiers with memory effects. In *IEEE MTT-S International Microwave Symposium Digest*. QUALCOMM Inc., June 2003.

[109] Muha, M.; et al. Accurate measurement of wideband modulated signals. *Microwave Journal*, 43(6), June 2000.

[110] Meier, I.; et al. Error-feedback for amplifier linearization. In *Proceedings of the 1998 South African Symposium on Communications and Signal Processing*, Rondebosch, South Africa, September 1998. Dept. of Electr. Eng., Stellenbosch Univ.

[111] Bösch, W.; et al. Measurement and simulation of memory effects in predistortion linearizers. *IEEE Trans. Microwave Theory and Techniques*, 37(12), December 1989.

Appendices

Appendix A

Summary of equipment specifications

A.1 Vector signal generator

Table A.1: HP/Agilent Vector Signal Generator specifications.

Brand	HP/Agilent
Model	8780A
Frequency range	10 MHz to 3 GHz
Frequency resolution	1 Hz
Level range	-100 to +4 dBm ($\geq$ 2.5 GHz)
Level accuracy	$\pm$ 2.5 dB ($\geq$ -30 dBm)
Level flatness	$<\pm$ 1 dB
Level resolution	0.1 dB
Output impedance	50Ω
Harmonics	< -35 dBc (for 2.5 GHz < f $\leq$ 3 GHz and level $\leq$ +1 dBm)
Vector modulation	
Inputs	analog I/Q
Frequency response	DC to > 350 MHz (400 MHz to 3 GHz)
Input impedance	50Ω
Temperature	0°C to +55°C (operating)

A.2 Arbitrary waveform generator

Table A.2: LeCroy Arbitrary waveform generator specifications.

Brand	LeCroy
Model	LW420
Standard function waveforms	Sine, 1 Hz - 100 MHz Square, 1 Hz - 50 MHz Triangle, 1 Hz - 25 MHz Ramp, 1 Hz - 25 MHz Pulse, (period) 20 ns - max. memory DC
Multi-tone	1-10 tones, 1 Hz - 100 MHz
Output impedance	50 Ω, ± 5%
Output voltage	10 mV - 10 V p-p
Max. output BW	100 MHz (-3 dB)
Spurious and nonharmonic distortion	< -60 dBc for frequencies $\leq$ 1 MHz for output
Max. sample rate	400 MS/second
Calibration interval	1 year
Temperature	+5°C to +35°C (full specifications) 0°C to +40°C (operating)

A.3 Network analyzer

Table A.3: Agilent Technologies microwave network analyzer specifications.

Brand	Agilent Technologies PNA Series
Model	E8363A
Frequency range	45 MHz - 40 GHz
Reflection tracking	±1.5 dB (45 MHz to 20 GHz)
Transmission tracking	±2.0 dB (2 MHz to 10 GHz)
Test port output	
Frequency resolution	1 Hz
CW accuracy	±1 ppm
Power range	-25 to +5 dBm (45 MHz to 10 GHz)
Power level accuracy	±1.5 dB (45 MHz to 10 GHz)
Power resolution	0.01 dB
Phase noise	-70 dBc (45 MHz to 10 GHz)
Harmonics	-23 dBc (for 2nd or 3rd harmonics)
Nonharmonic spurious	-50 dBc (45 MHz to 20 GHz) (at nominal output power)
Test port input	
Noise floor	<-117 dBm (2 to 10 GHz at 10-Hz IF BW) <-97 dBm (2 to 10 GHz at 1-Hz IF BW)
Receiver compression level	<0.6 dB compression at +5 dBm (45 MHz to 20 GHz)
Trace noise magnitude	<0.006 dB rms (500 MHz to 20 GHz)
Trace noise phase	<0.006° rms (500 MHz to 20 GHz)
Measured number of points	2 to 1601 points per sweep
Temperature	0°C to +40°C (operating)

A.4 Spectrum analyzer

Table A.4: Agilent Technologies spectrum analyzer specifications.

Brand	Agilent Technologies
Model	8564EC
Frequency range	9 kHz - 40 GHz
Harmonic Mixing Mode (HMM)	1 (30 Hz to 6.46 GHz) 2 (5.86 GHz to 13.2 GHz)
Frequency span Range Accuracy	 0.100 Hz to full span ±5% (span >2 MHz × HMM) ±1% (span ≤2 MHz × HMM)
Max. safe input level Average continuous power Max. DC input voltage	 +30 dBm (1 W, input att. ≥10 dB) ±0.2 Vdc (DC coupled) ±50 Vdc (AC coupled)
Displayed Average Noise Level (DANL) (0dB att, 1Hz resolution BW)	≤-145 dBm (10 MHz to 2.9 GHz) ≤-147 dBm (2.9 GHz to 6.46 GHz) ≤-143 dBm (6.46 GHz to 13.2 GHz)
1 dB gain compression	-5 dBm (10 MHz to 2.9 GHz) +0 dBm (2.9 GHz to 6.46 GHz) -3 dBm (6.46 GHz to 13.2 GHz)
Compression to noise	>145 dB (10 MHz to 2.9 GHz) >147 dB (2.9 GHz to 6.46 GHz) >140 dB(6.46 GHz to 13.2 GHz)
Signal to distortion	>111 dB (1.45 GHz to 2 GHz) >113.5 dB (2 GHz to 3.25 GHz) >111.5 dB(3.25 GHz to 6.6 GHz) >110 dB(6.6 GHz to 11 GHz)
Intermodulation	>104 dB (10 MHz to 2.9 GHz) >108 dB (2.9 GHz to 6.46 GHz) >100 dB(6.46 GHz to 13.2 GHz)
Spurious responses	<(-75 + 20 × logN) dBc
3rd order intermodulation distortion	≤-82 dBc (20 MHz to 2.9 GHz) ≤-90 dBc (2.9 GHz to 6.46 GHz) ≤-75 dBc (6.46 MHz to 26.8 GHz) (For two -30 dBm signals, ≥1 kHz apart)
Calibration interval	1 year
Warm-up time	5 minutes in ambient conditions
Temperature	0°C to +55°C (operating)

A.5 Power amplifier

Table A.5: Mini-Circuits power amplifier specifications.

Brand	Mini-Circuits
Model	ZVE-8G
Operational range	2 to 8 GHz
Minimum gain	30 dB
Max. flatness	±2.0 dB
Minimum 1 dB compression point	+30 dBm (referred to output power)
Maximum input power	+20 dBm
Noise floor	4 dB
Typical 3rd order intercept point (IP3)	+40 dBm (referred to output power)
DC power	12 V / 2 A
Typical noise figure (N_f)	4 dB
Standard connector	SMA

A.6 Attenuators

Table A.6: Midwest microwave attenuators specifications.

Brand	Midwest	Midwest
Model	ATT-0263-10-SMA-02	ATT-0263-30-SMA-02
Type	SMA miniature	SMA miniature
Nominal attenuation	10 dB	30 dB
Attenuation accuracy	±0.3 dB	±1.0 dB
Frequency range	DC to 18 GHz	DC to 18 GHz
Maximum input power	2 W (33.01 dBm)	2 W (33.01 dBm)
Interface genders	Male/Female	Male/Female
Temperature (operating)	-65°C to +125°C	-65°C to +125°C

Appendix B

Setup systems to perform measurements

B.1 Setup system to calibrate measuring devices

B.1.1 Setup system to calibrate a network analyzer

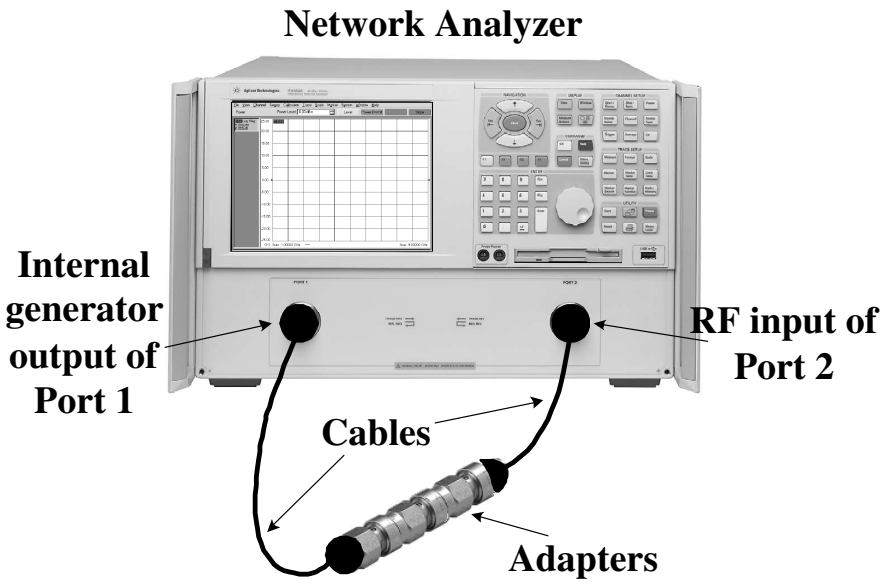

Figure B.1: Setup system for calibration of network analyzer.

B.1.2 Setup system to calibrate a spectrum analyzer

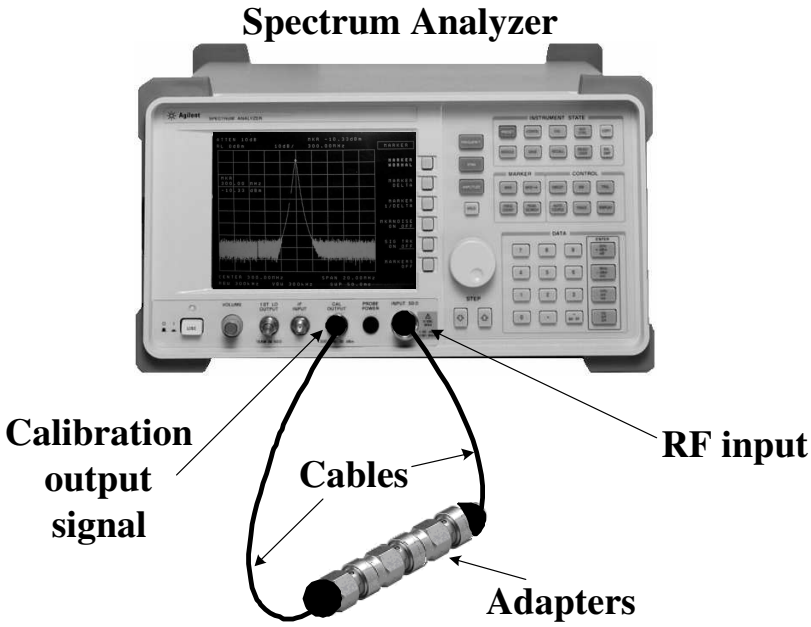

Figure B.2: Setup system for calibration of spectrum analyzer.

B.2 Setup system to perform attenuation measurements

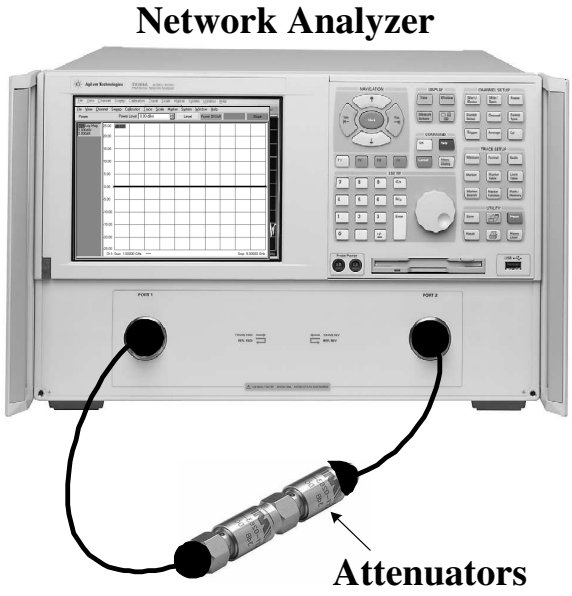

Figure B.3: Setup system for attenuation measurements.

B.3 Setup system to perform single-tone signal measurements

B.3.1 Setup system using a network analyzer

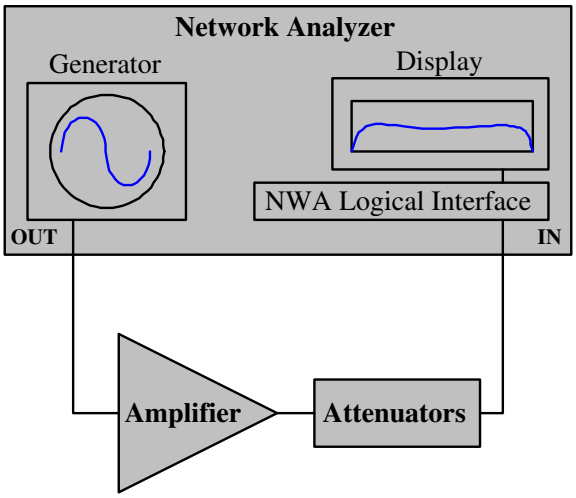

(a) Schematic representation

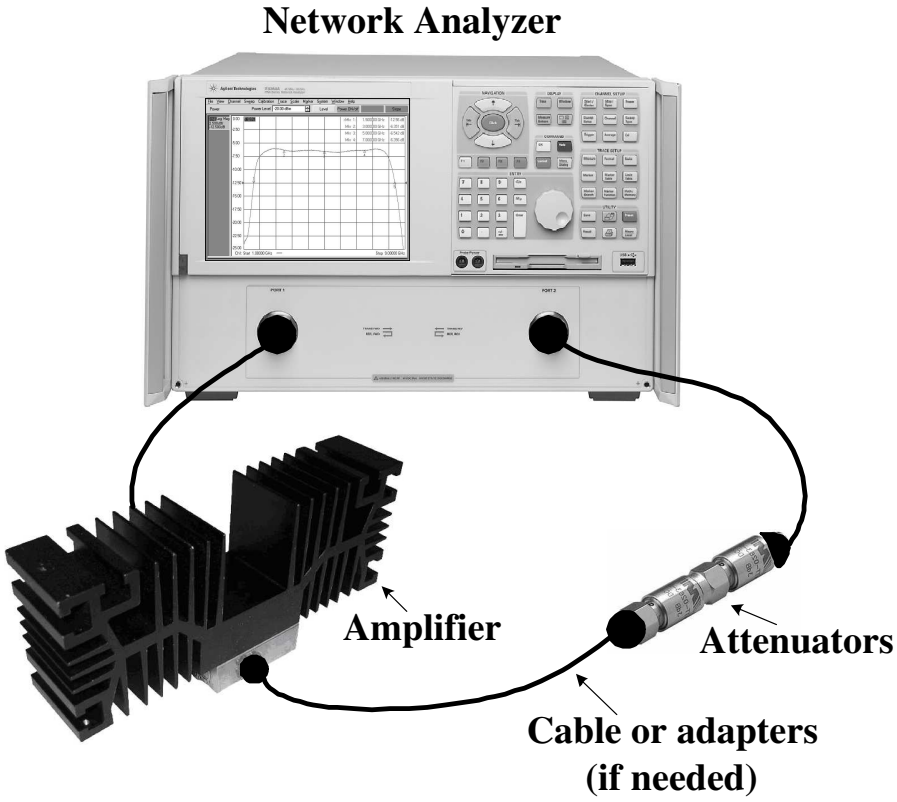

(b) Practical implementation

Figure B.4: Setup system for single-tone signal measurements of amplifiers using a network analyzer.

B.3.2 Setup system using a spectrum analyzer

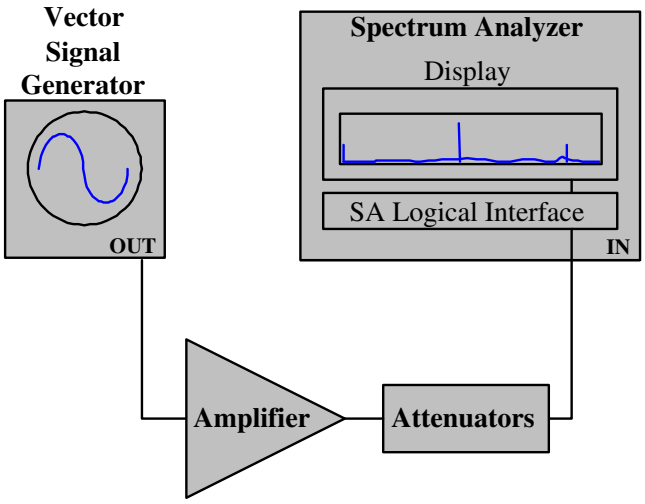

(a) Schematic representation

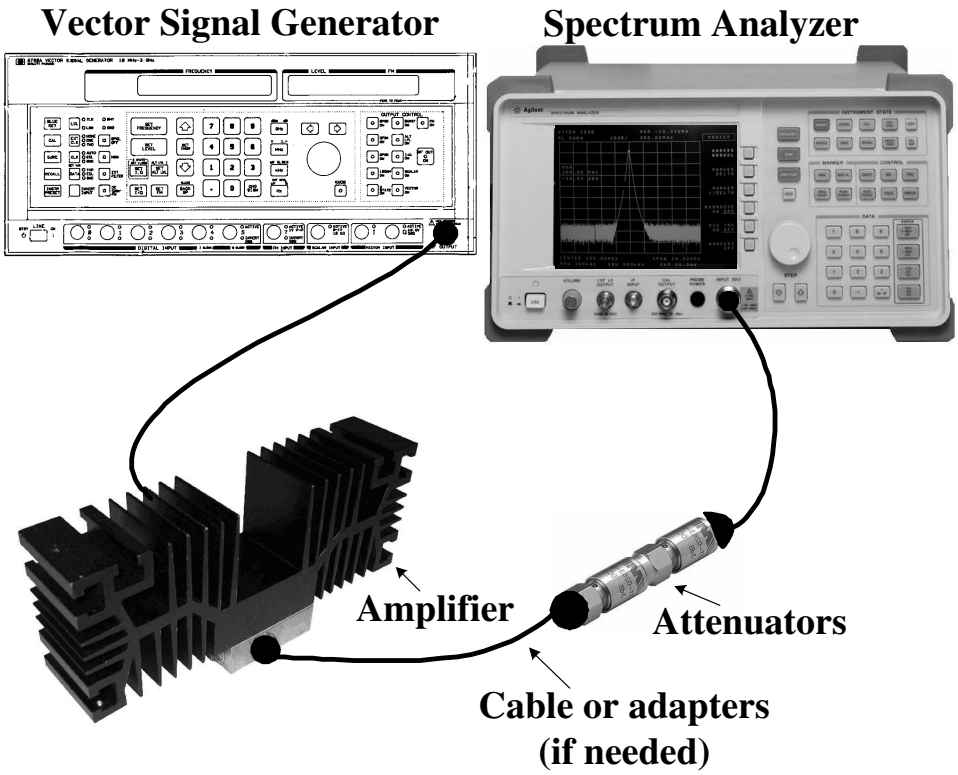

(b) Practical implementation

Figure B.5: Setup system for single-tone signal measurements of amplifiers using a spectrum analyzer.

B.4 Setup system to perform two-tone signal measurements

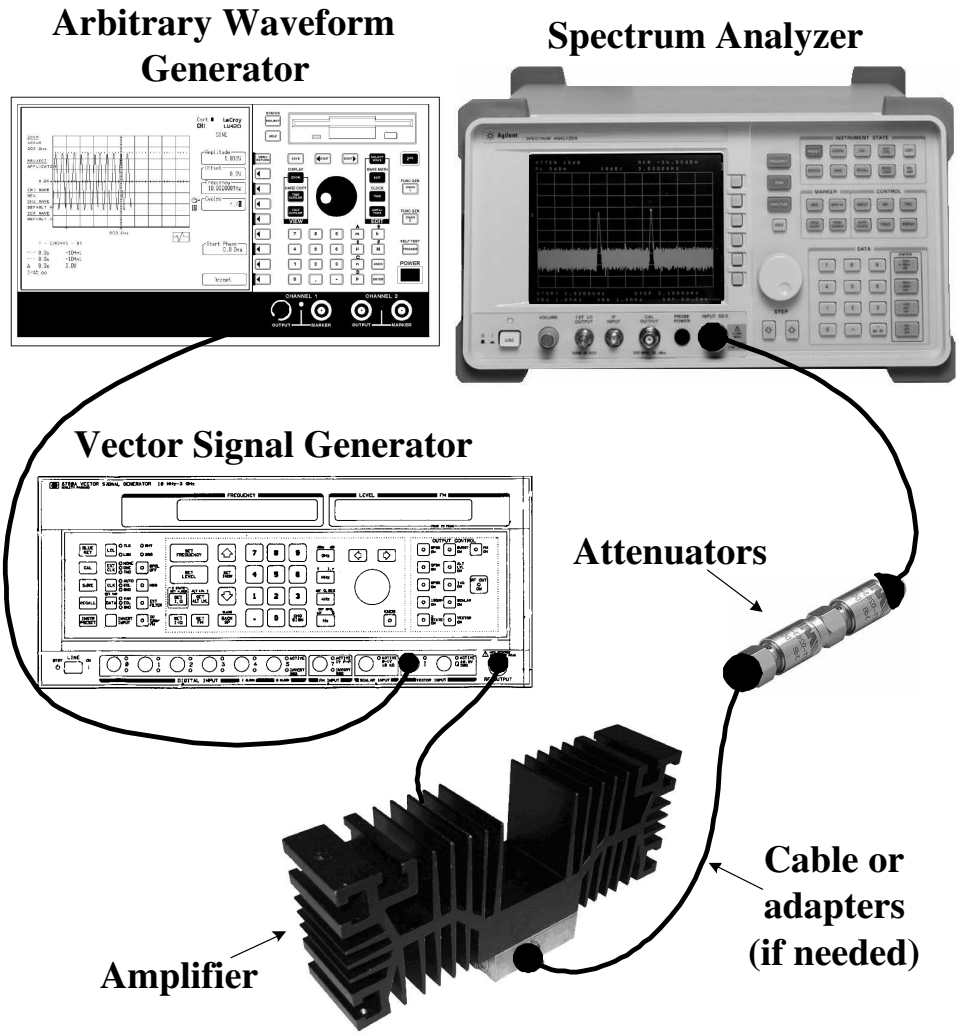

Figure B.6: Setup system for two-tone signal measurements of amplifiers.

B.5 Setup system to generate a multi-tone signal

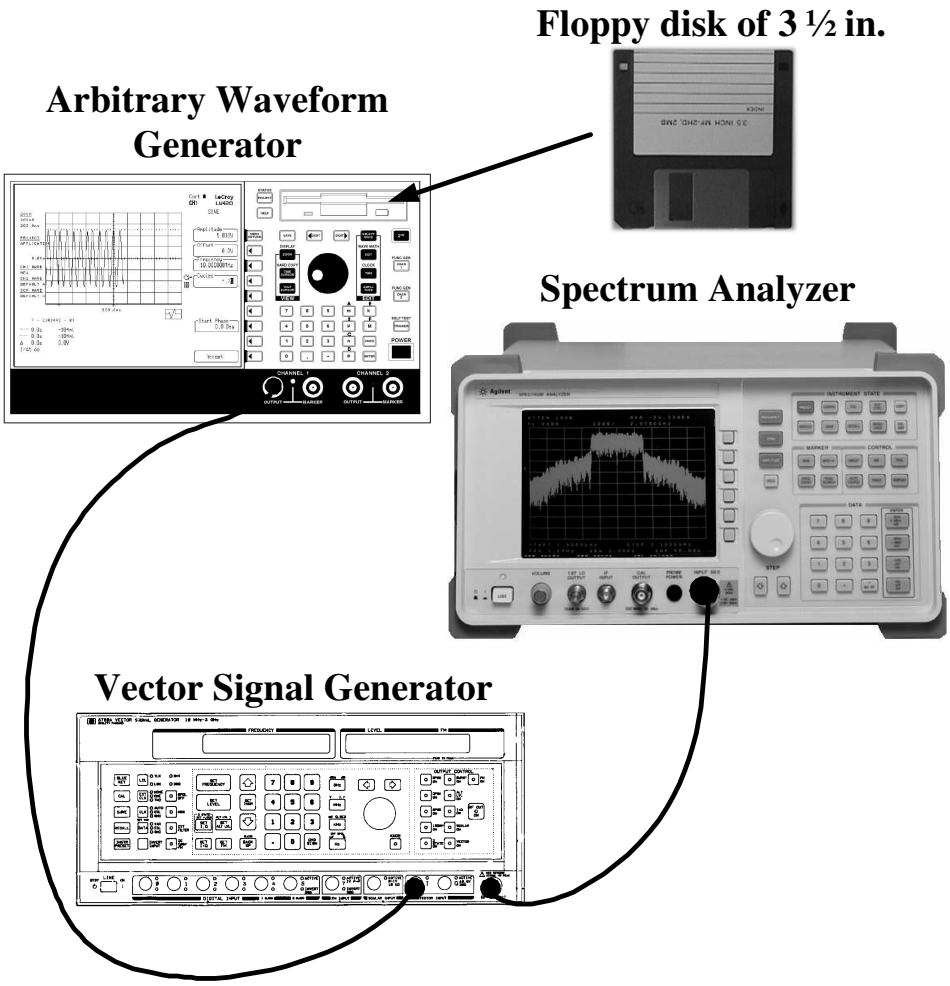

Figure B.7: Setup system for generating a multisine signal.

Appendix C

Processes to perform measurements

C.1 Process to calibrate measuring devices

C.1.1 Network analyzer calibration

1. Connect calibration system, previously shown in Figure B.1. (Include an extra connector if necessary)
2. Select from “Channel Setup” panel: Sweep Type → Power Sweep.
3. Select from “Channel Setup” panel: Power.
4. Set “Start Power” at minimum power desired.
5. Set “Stop Power” at maximum power desired.
6. Select from “Channel Setup” panel: Start.
7. Set CW Freq. at the center frequency of the amplifier’s operating range.
8. Select from “Channel Setup” panel: Sweep Type → Linear Frequency.
9. Select from “Channel Setup” panel: Start.
10. Set “Start Frequency” at minimum frequency desired.
11. Select from “Channel Setup” panel: Stop.
12. Set “Stop Frequency” at maximum frequency desired.
13. Select from “Channel Setup” panel: Power.
14. Set “Power Level” at 0 dBm.

15. Check that Power is “ON” (Power ON/off).
16. Select from the main menu bar (at the top of the screen): Sweep → Number of Points → Custom, and set for the desired number of points to be measured in the frequency span. Click OK.
17. Select from the main menu bar: Calibration, and set Interpolation “ON” (Interpolation ON/off).
18. Select from the main menu bar: Calibration → Calibration Wizard.
19. Select “Unguided Calib...” → “Use Mechanical Stds.”
20. Check the box “Create new Cal Set”. Click Next.
21. Select “THRU Response”. Click Next.
22. Click the THRU button (THRU (trans) Por...). Click OK. Click Next. (It is possible to select to save the Calibration Settings in a specific file and location in the NWA system. This file can be recalled to get the parameters just obtained from this calibration.)

The parameters for calibration currently used can be checked at any time by selecting from the main menu bar: Calibration → Cal-Set, then select the active CalSet (marked as $*$) and click “Properties”.

C.1.2 Spectrum analyzer calibration

1. Connect calibration system, previously shown in Figure B.2. (Include an extra connector if necessary)
2. Select from the main panel: Frequency.
3. Set “Center Freq” at the frequency of the calibration signal.
4. Adjust the frequency span if desired by selecting from the main panel: Span and setting “Span” as desired.
5. Select from “Calibration” panel: Cal → REF LVL ADJ.
6. Use the knob to adjust the peak of the signal to the top of grid.
7. Select “STORE REF LVL” to store the value of the amplitude correction needed (e.g. zero for no correction).
8. Press “ENTER” from the main panel.

C.2 Process to perform cables attenuation measurement with a spectrum analyzer

1. Connect calibration system, previously shown in Figure B.1. (Include an extra connector if necessary)
2. Select from the main panel: Frequency.
3. Set "Center Freq" at the frequency of the calibration signal.
4. Adjust the frequency span if desired by selecting from the main panel: Span and setting "Span" as desired.
5. Use markers for reading accuracy. Select from "Marker" panel: MKR. Use the knob to place the marker at the peak of the signal.

C.3 Process to perform attenuation measurements

1. Perform a THRU response calibration to the NWA.
2. Connect the setup system previously shown in Figure 5.3.
3. Select from "Channel Setup" panel: Sweep Type → Linear Frequency or Power sweep, depending on the desired type of results.
4. Select from "Trace Setup" panel: Scale, and adjust the scale features as desired.
5. Use markers for accurately measure specific frequencies or input levels. To do this, select from the main menu bar: Marker → Marker..., choose the preferred frequency and click ON. Click OK.

C.4 Process to perform single-tone signal measurements

C.4.1 Measurements using a network analyzer

1. Perform a THRU response calibration to the NWA.
2. Connect the setup system previously shown in Figure B.4(b).
3. Feed the amplifier with the correct amount of voltage, by using the adequate power supply.
4. Select from "Channel Setup" panel: Sweep Type → Linear Frequency or Power sweep, depending on the desired type of results.
5. Select from "Trace Setup" panel: Scale, and adjust the scale features as desired.
6. Use markers for accurately measure specific frequencies or input levels. To do this, select from the main menu bar: Marker → Marker..., choose the preferred frequency and click ON. Click OK.

C.4.2 Measurements using a spectrum analyzer

1. Check the correct calibration of the SA.
2. Connect the setup system previously shown in Figure B.5(b).
3. Turn on the vector signal generator and the spectrum analyzer.
4. Set the vector signal generator to the desired frequency and input level.
5. Press the "RF OUT ON" button of the generator and make sure that the light indicator in the button is active.
6. Feed the amplifier with the correct amount of voltage, by using the adequate power supply.
7. Select from the main panel of the SA: Frequency.
8. Set "Start Freq" at the lower limit of the desired measuring frequency range.
9. Set "Stop Freq" at the higher limit of the desired measuring frequency range.
10. Use markers for reading accuracy. Select from "Marker" panel: MKR. Use the knob to place the marker at the peak of the signal or the desired exact measuring frequency.

C.5 Process to generate a two-tone signal

1. Connect the setup system previously shown in Figure B.5, without inserting any floppy disk into the AWG.
2. Turn on the arbitrary waveform generator, the vector signal generator and the spectrum analyzer.
3. In the AWG: Press from EDIT panel: SELECT WAVE.
4. Select: NEW → NEW CH1 Wave.
5. Give a name to the new wave and select Accept.
6. Press from EDIT panel: WAVE MATH, EDIT.
7. Select: Insert Wave → Standard Waves → Sine.
8. Adjust the frequency to half of the desired tone separation.
9. Select: Accept.
10. Press from main panel: Func Gen, CHAN 1.
11. Set "Output" to ON (the CHANNEL 1 output light indicator should turn to green).
12. In the VSG: set the desired frequency and input level.
13. Press Vector and RF OUT buttons in order to turn them ON (the light indicator in each button should turn yellow).

To analyze the signal generated, connect the output of the VSG to a SA and perform a measurement following steps 7 to 10 from the process in Appendix C.4.2.

C.6 Process to perform two- and multi-tone signal measurements

1. Perform a THRU response calibration to the SA.
2. Connect the setup system previously shown in Figure B.6.
3. Follow steps 2 to 13 from the process to generate the two-tone signal to be measured (Appendix C.5).
4. Feed the amplifier with the correct amount of voltage, by using the adequate power supply.
5. Select from the main panel of the SA: Frequency.

6. Set “Start Freq” at the lower limit of the desired measuring frequency range.
7. Set “Stop Freq” at the higher limit of the desired measuring frequency range.
8. Use markers for reading accuracy. Select from “Marker” panel: MKR. Use the knob to place the marker at the peak of the signal or the desired exact measuring frequency.

C.7 Process to generate a multisine signal

1. Connect the setup system previously shown in Figure B.7.
2. Turn on the arbitrary waveform generator, the vector signal generator and the spectrum analyzer.
3. Insert the floppy disk containing the file with the multisine data into the drive of the Arbitrary Waveform Generator (AWG).
4. In the AWG: Press from main panel: PROJECT.
5. Select: Import → What → Matlab.
6. Select: Target File: Import As.
7. Give a name to the new wave and select Accept Name.
8. Make sure that the “Source File” is the desired one and select: Import (importing the file will take some time, depending on the length of the file).
9. Press from main panel: Func Gen, CHAN 1.
10. Set “Output” to ON (the CHANNEL 1 output light indicator should turn to green).
11. In the VSG: set the desired frequency and input level.
12. Press Vector and RF OUT buttons in order to turn them ON (the light indicator in each button should turn yellow).

To analyze the signal generated, connect the output of the VSG to a SA and perform a measurement following steps 7 to 10 from the process in Appendix C.4.2.

C.8 Miscellaneous processes

Saving screens in the network analyzer

1. Select from the main menu bar: File → Print to file...
2. Select the location to be saved and write a name for the file.
3. Select from the desired format. (Formats available: bitmap (.bpm), joint photographic experts group (.jpg) and portable network graphics (.png))
4. Click OK.

Saving data in a file from the network analyzer

1. Select from the main menu bar: File → Save as...
2. Select the location to be saved and write a name for the file.
3. Select Trace format (.s2p), which includes a stimulus response column plus a real value column and an imaginary value column for each of the four S-parameters.
4. Click OK.

Using averaging function in the spectrum analyzer

1. Press from control panel: BW
2. Set "VID AVG" to ON.
3. Set the desired average factor (0 to 100) by pressing the desired number of average factor in the number keypad, followed by pressing "Hz".

Appendix D

Data and plots of measurement results

D.1 Attenuation measurements

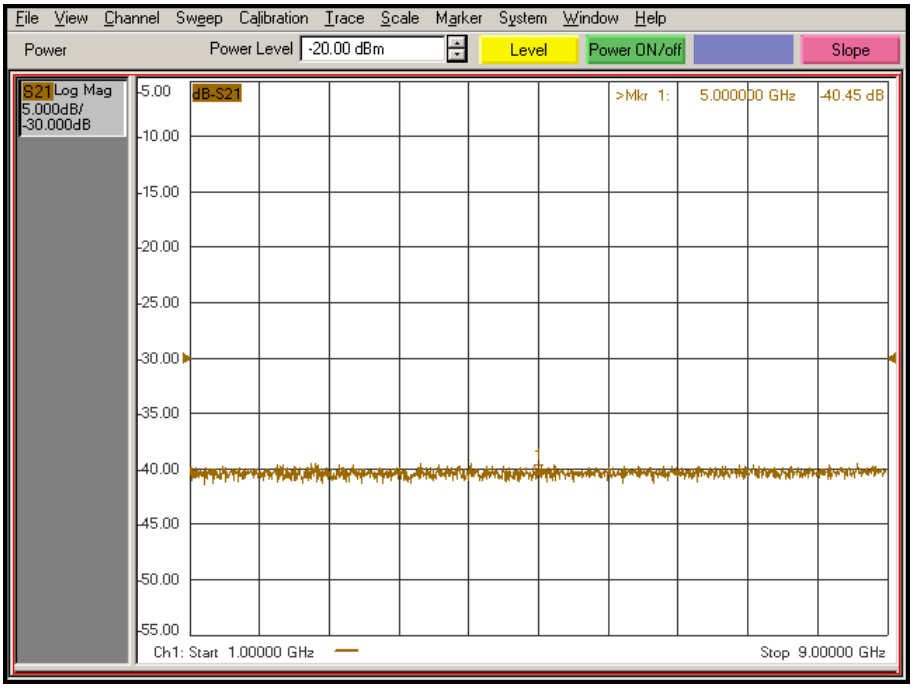

Figure D.1: Results of attenuation measurement. Frequency sweep from 1 GHz to 9 GHz at -20 dBm.

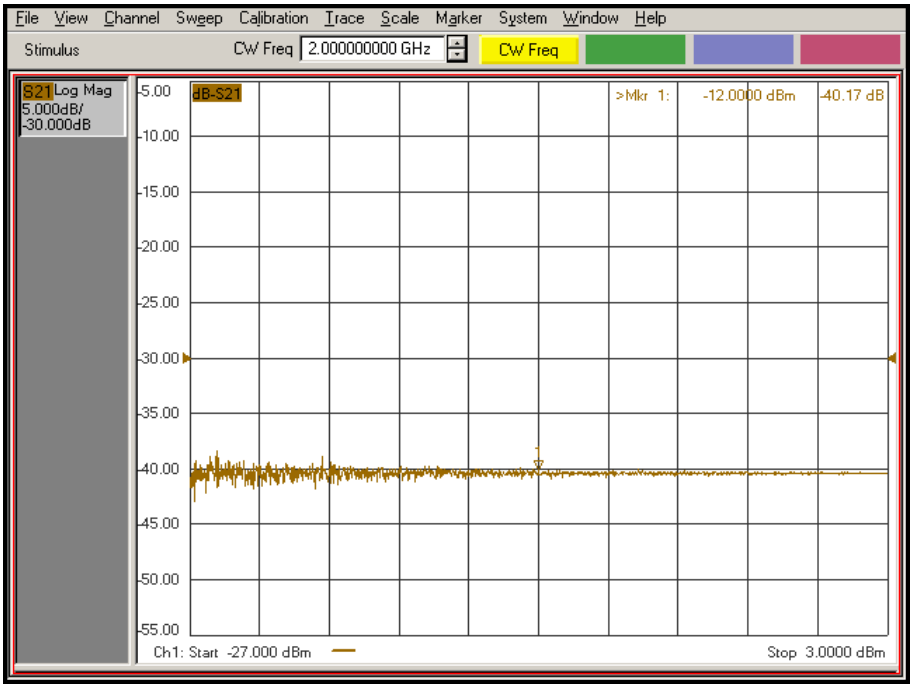

Figure D.2: Results of attenuation measurement. Power sweep from -27 dBm to +3 dBm at 2 GHz.

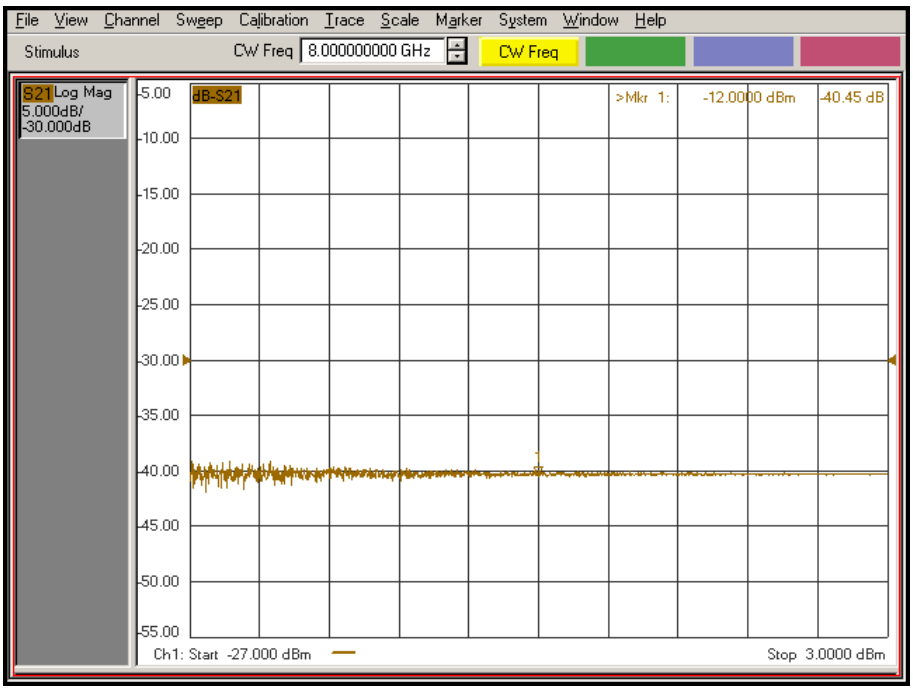

Figure D.3: Results of attenuation measurement. Power sweep from -27 dBm to +3 dBm at 8 GHz.

D.2 Single-tone signal measurements

D.2.1 Screens obtained from network analyzer

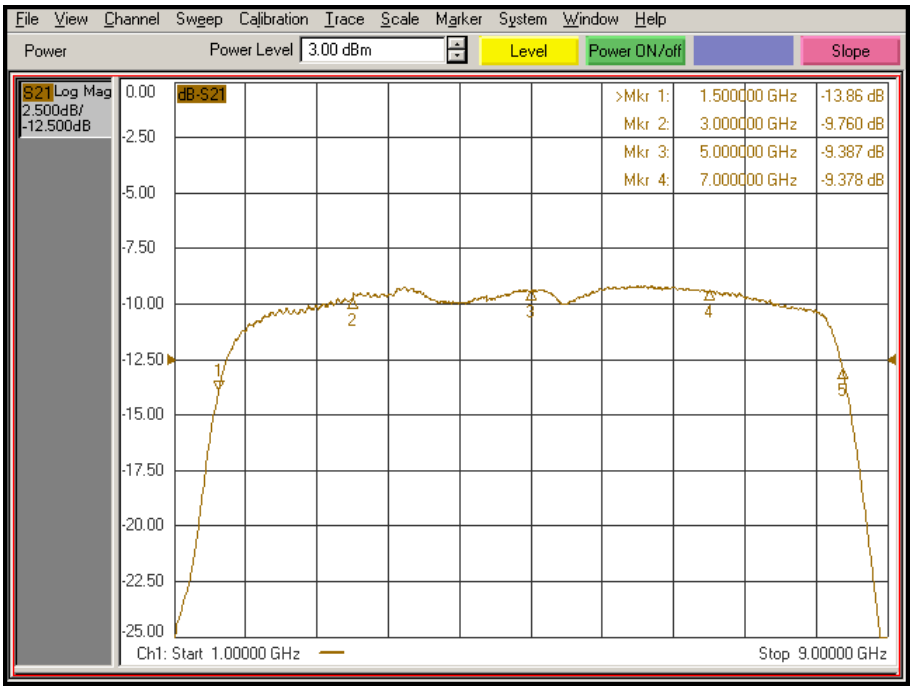

Figure D.4: Results of single-tone signal measurement to amplifier. Frequency sweep from 1 GHz to 9 GHz at +3 dBm.

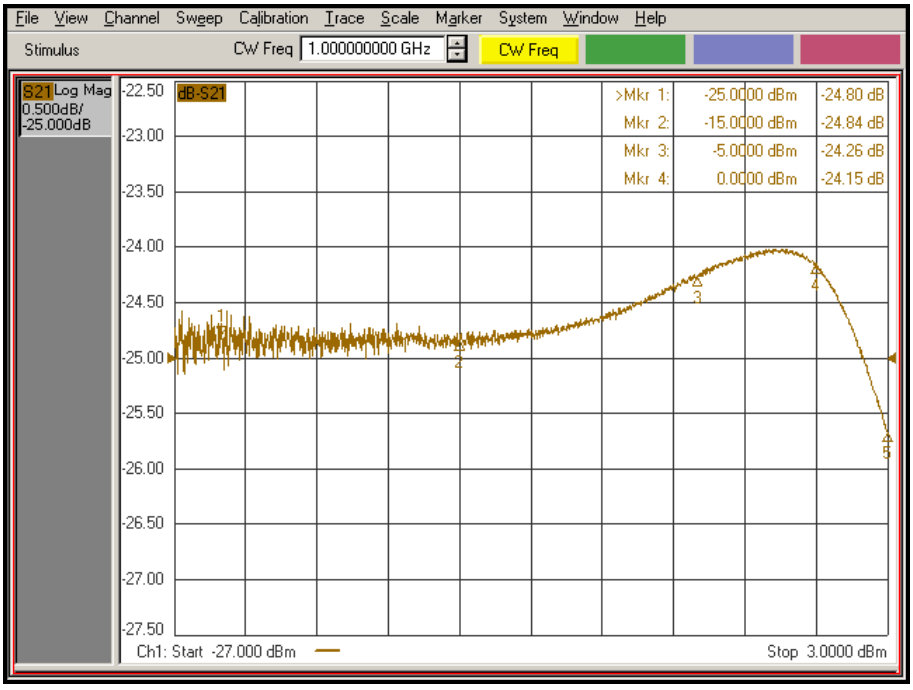

Figure D.5: Results of single-tone signal measurement to amplifier. Power sweep from -27 dBm to +3 dBm at 1 GHz.

D.2.2 Plots of frequency-sweep measurements

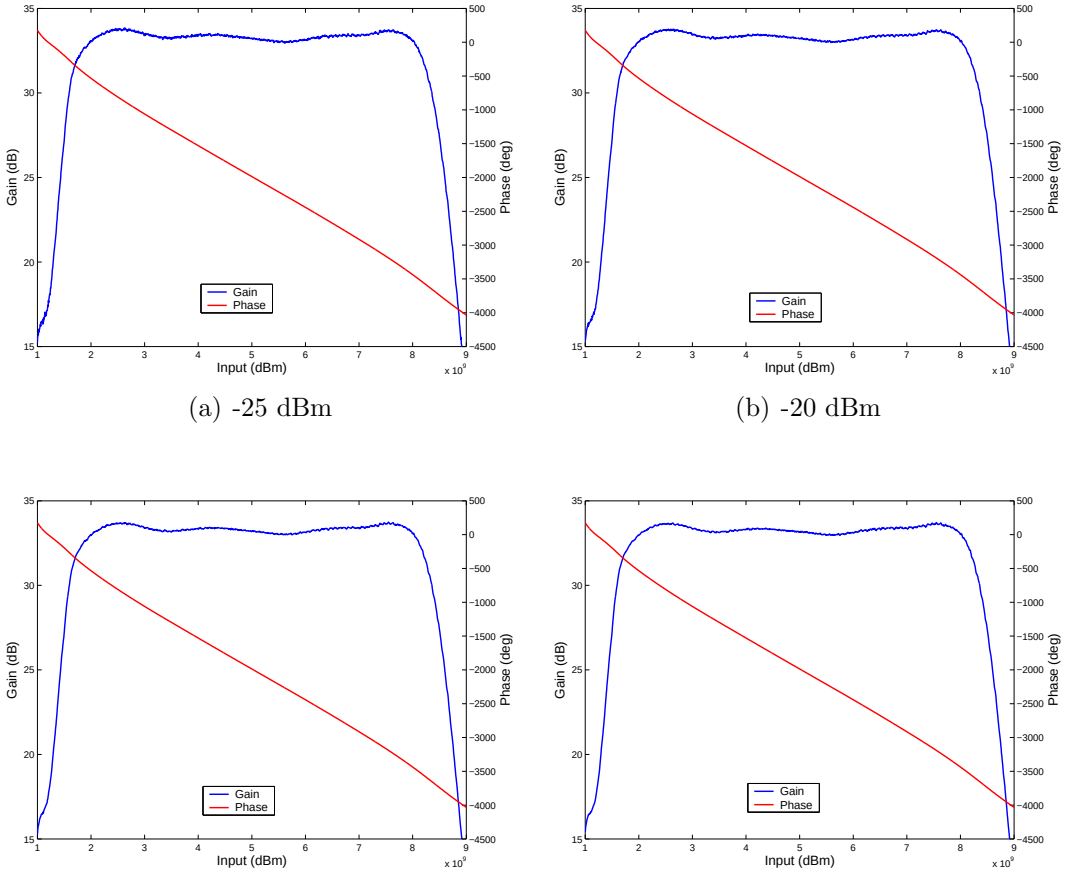

(a) -25 dBm

(b) -20 dBm

(c) -15 dBm

(d) -10 dBm

Figure D.6: Gain and phase frequency-sweep curves, result of single-tone tests performed to the ZVE-8G amplifier using the network analyzer and applying different input power levels.

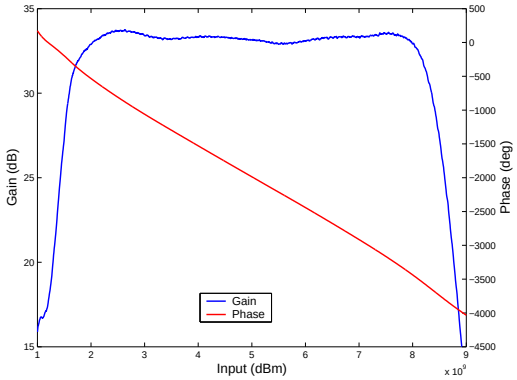

(a) -5 dBm

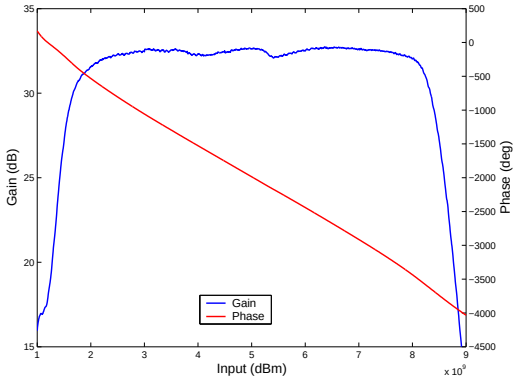

(b) 0 dBm

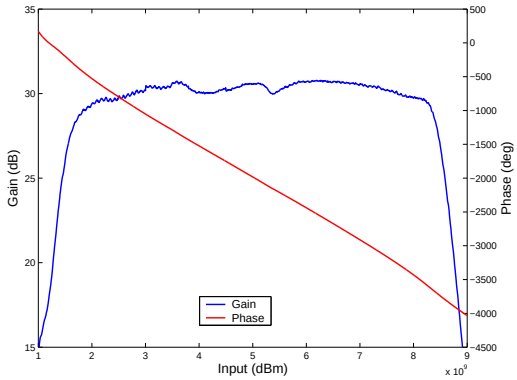

(c) +3 dBm

Figure D.7: Gain and phase frequency-sweep curves, result of single-tone tests performed to the ZVE-8G amplifier using the network analyzer and applying different input power levels.

D.2.3 Plots of power-sweep measurements

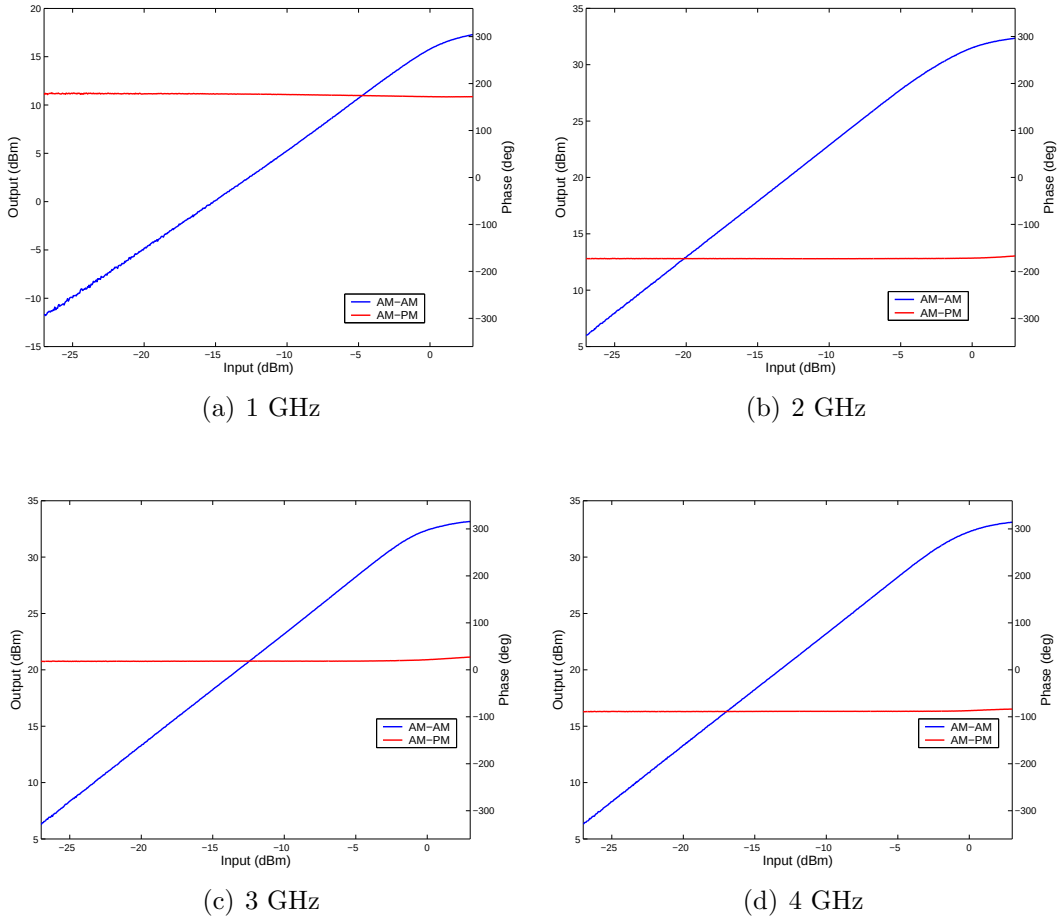

(a) 1 GHz (b) 2 GHz

(c) 3 GHz (d) 4 GHz

Figure D.8: Amplitude and phase characteristics obtained from single-tone tests performed to the ZVE-8G amplifier using the network analyzer and applying different input frequencies.

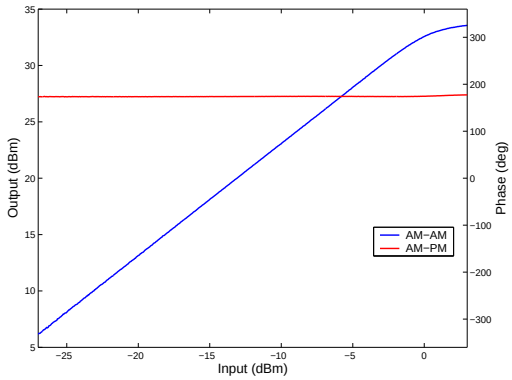

(a) 5 GHz

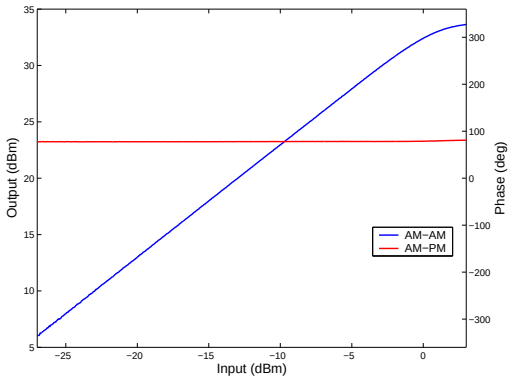

(b) 6 GHz

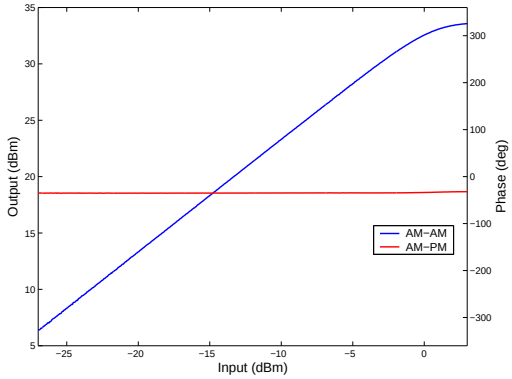

(c) 7 GHz

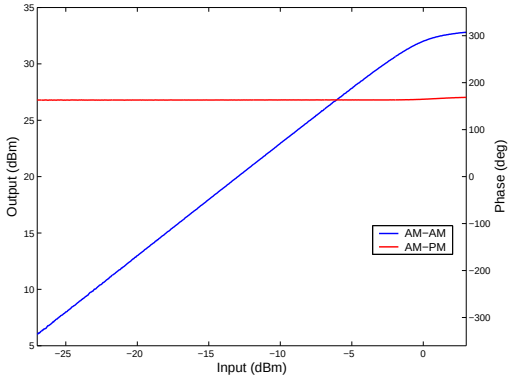

(d) 8 GHz

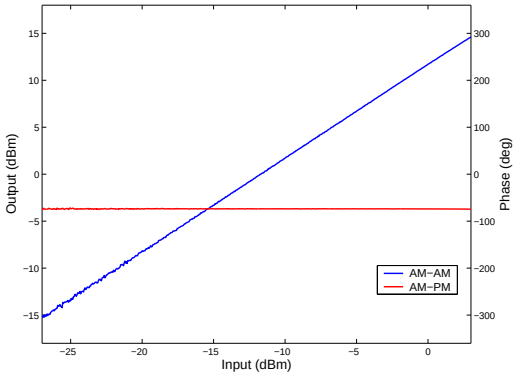

(e) 9 GHz

Figure D.9: Amplitude and phase characteristics obtained from single-tone tests performed to the ZVE-8G amplifier using the network analyzer and applying different input frequencies.

D.2.4 1 dB compression point plots

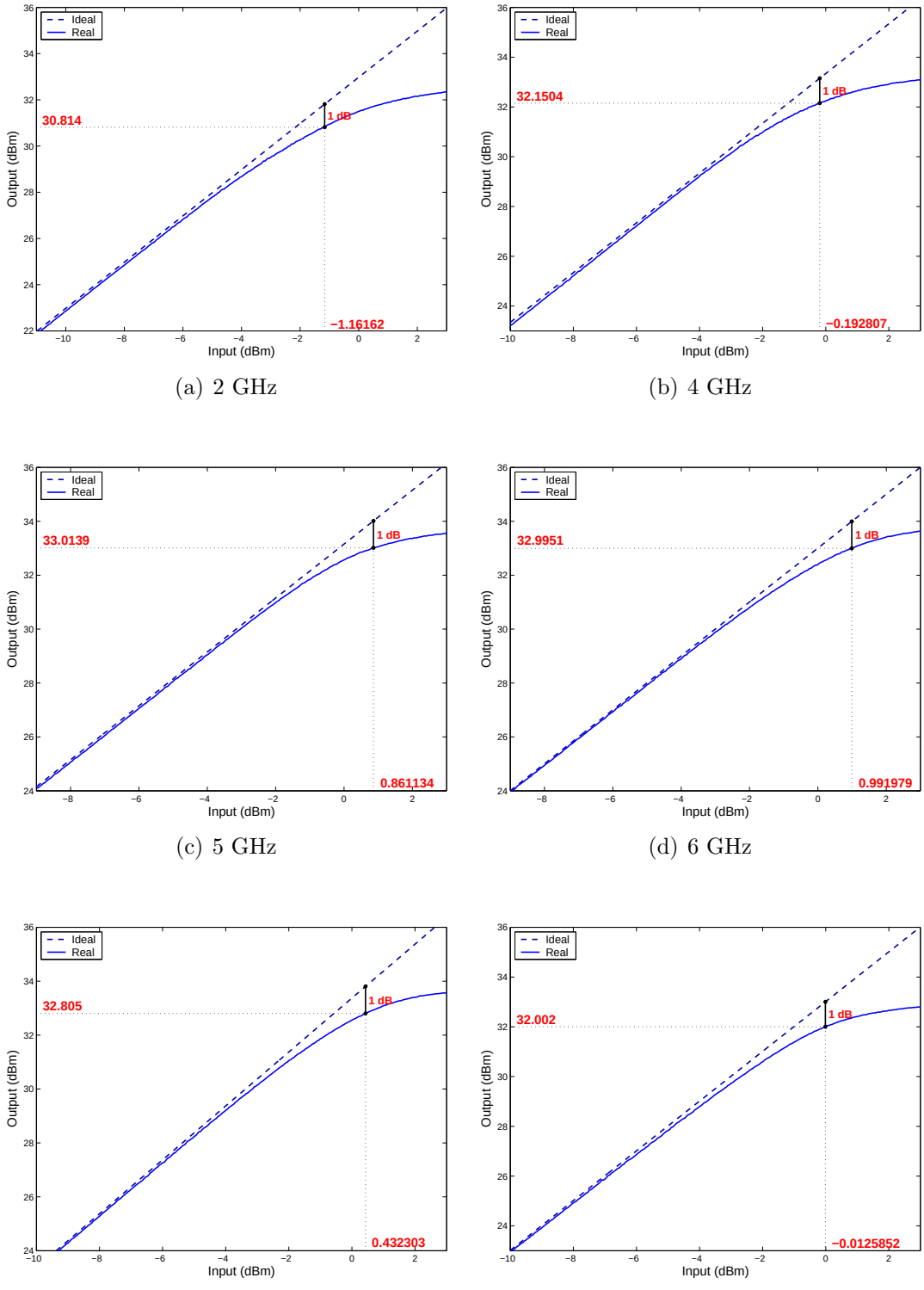

(a) 2 GHz (b) 4 GHz

(c) 5 GHz (d) 6 GHz

(e) 7 GHz (f) 8 GHz

Figure D.10: 1 dB compression point for ZVE-8G amplifier, calculated for frequencies measured inside the operational band and based on the AM-AM characteristic obtained from the corresponding power-sweep measurement performed with the network analyzer.

D.2.5 Screens obtained from spectrum analyzer

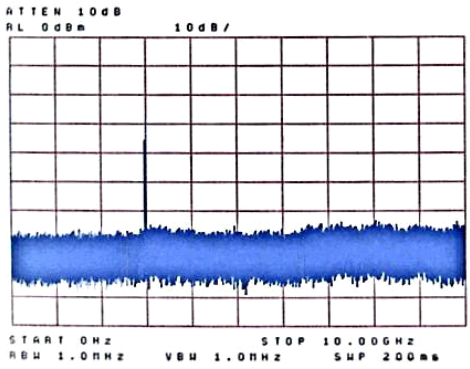

(a) Full span at -20 dBm

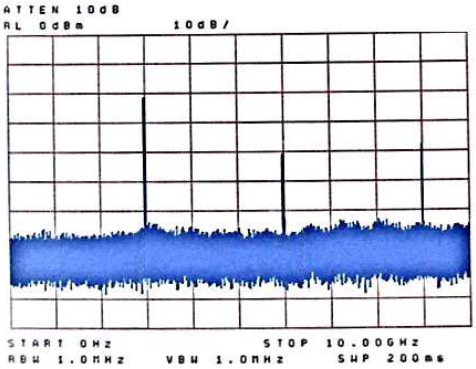

(b) Full span at 0 dBm

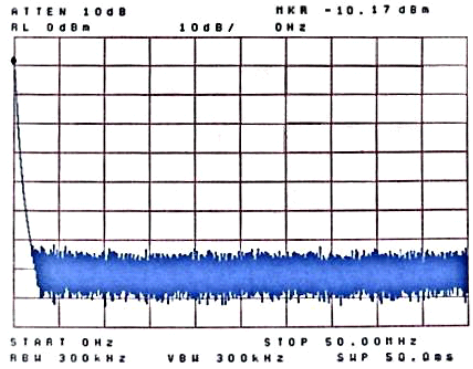

(c) DC zone at -20 dBm

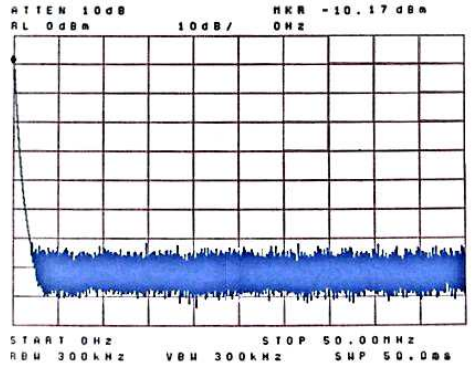

(d) DC zone at 0 dBm

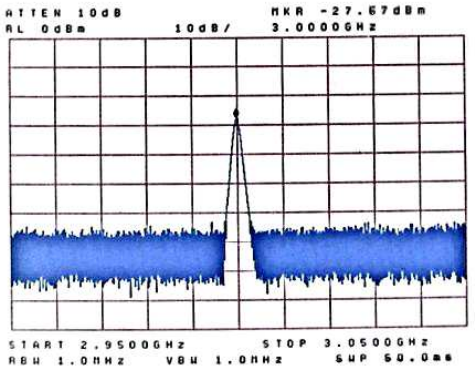

(e) Fundamental zone at -20 dBm

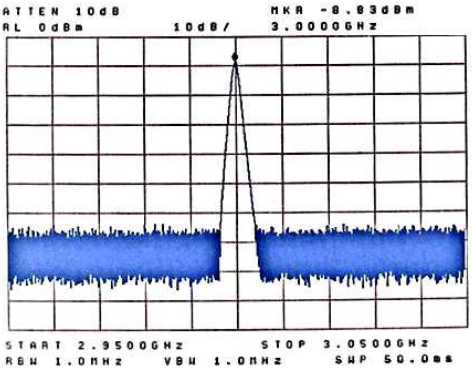

(f) Fundamental zone at 0 dBm

Figure D.11: Results of ZVE-8G amplifier single-tone signal measurements using a spectrum analyzer. The amplifier is operated at 3 GHz and at a low input level (-20 dBm) or at the DUT's 1 dB CP (0 dBm).

D.2.6 Data obtained from spectrum analyzer

Table D.1: Data obtained from spectrum analyzer when performing single-tone signal measurements. This data contains the effect of the attenuators. Therefore, to find the final results the nominal attenuation should be added.

Input level (dBm)	Output level from SA (dBm)		
	Fundamental 3 GHz	2nd harmonic 6 GHz	3rd harmonic 9 GHz
-14,00	-21,83		
-13,50	-21,50		
-13,00	-21,00		
-12,50	-20,50		
-12,00	-20,00	-57,33	
-11,50	-19,50	-56,83	
-11,00	-19,00	-56,17	
-10,50	-18,50	-55,67	
-10,00	-18,00	-55,50	-65,17
-9,50	-17,50	-55,00	-64,83
-9,00	-17,00	-54,67	-64,00
-8,50	-16,50	-54,17	-63,83
-8,00	-15,83	-53,83	-63,50
-7,50	-15,33	-53,17	-62,50
-7,00	-14,83	-52,33	-62,17
-6,50	-14,33	-51,50	-61,00
-6,00	-13,83	-50,17	-60,17
-5,50	-12,50	-49,00	-59,83
-5,00	-11,83	-47,50	-58,00
-4,50	-11,50	-46,33	-56,50
-4,00	-11,00	-44,67	-55,50
-3,50	-10,67	-43,50	-54,33
-3,00	-10,33	-42,17	-52,50
-2,50	-9,83	-41,50	-50,33
-2,00	-9,50	-41,00	-48,33
-1,50	-9,17	-40,50	-46,17
-1,00	-9,00	-40,50	-44,17
-0,50	-8,83	-40,67	-42,00
0,00	-8,50	-41,00	-39,83
0,50	-8,50	-41,00	-38,00
1,00	-8,33	-41,33	-36,17
1,50	-8,33	-41,33	-35,00
2,00	-8,17	-41,33	-34,17
2,50	-8,17	-41,33	-33,17
3,00	-8,17	-41,33	-32,50

D.2.7 Plot of fundamental, second harmonic and third harmonic curves

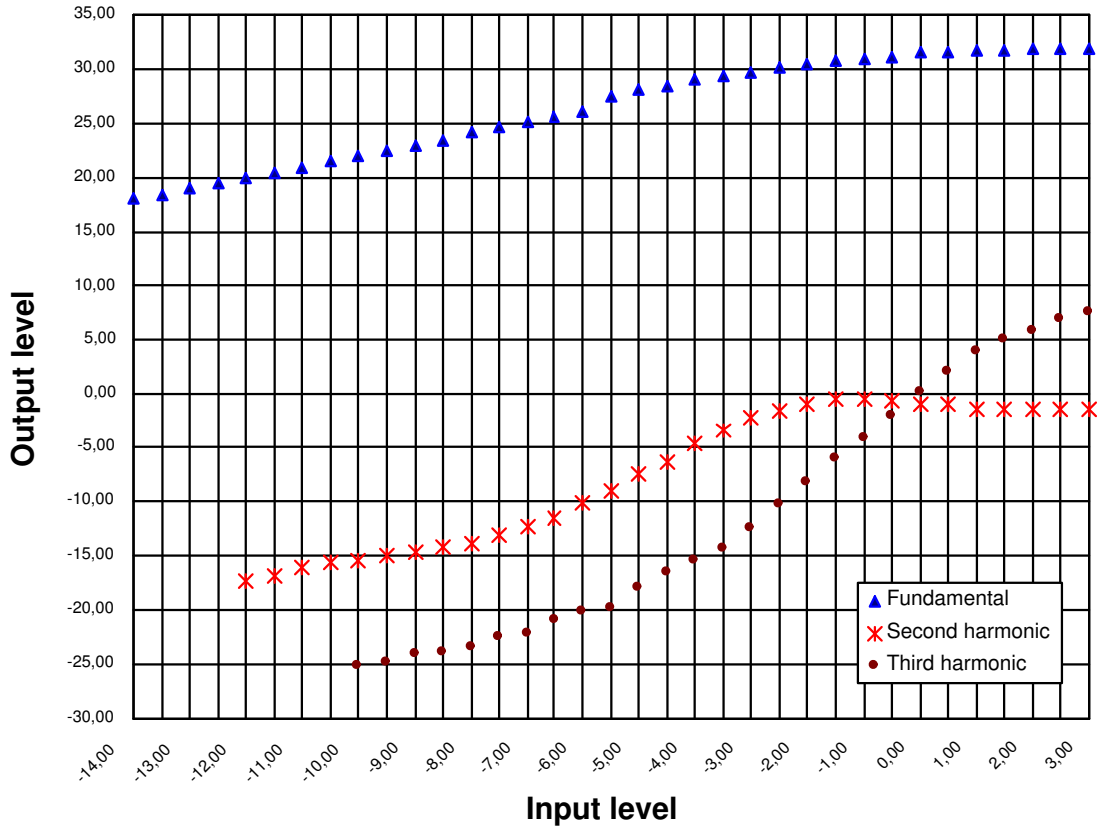

Figure D.12: Fundamental, second harmonic and third harmonic curves based on data obtained from spectrum analyzer when performing single-tone signal measurements. The data used for this plot contains the effect of the attenuators. Therefore, to find the final results the nominal attenuation should be added.

D.3 Two-tone signal measurements

D.3.1 Screens obtained from spectrum analyzer

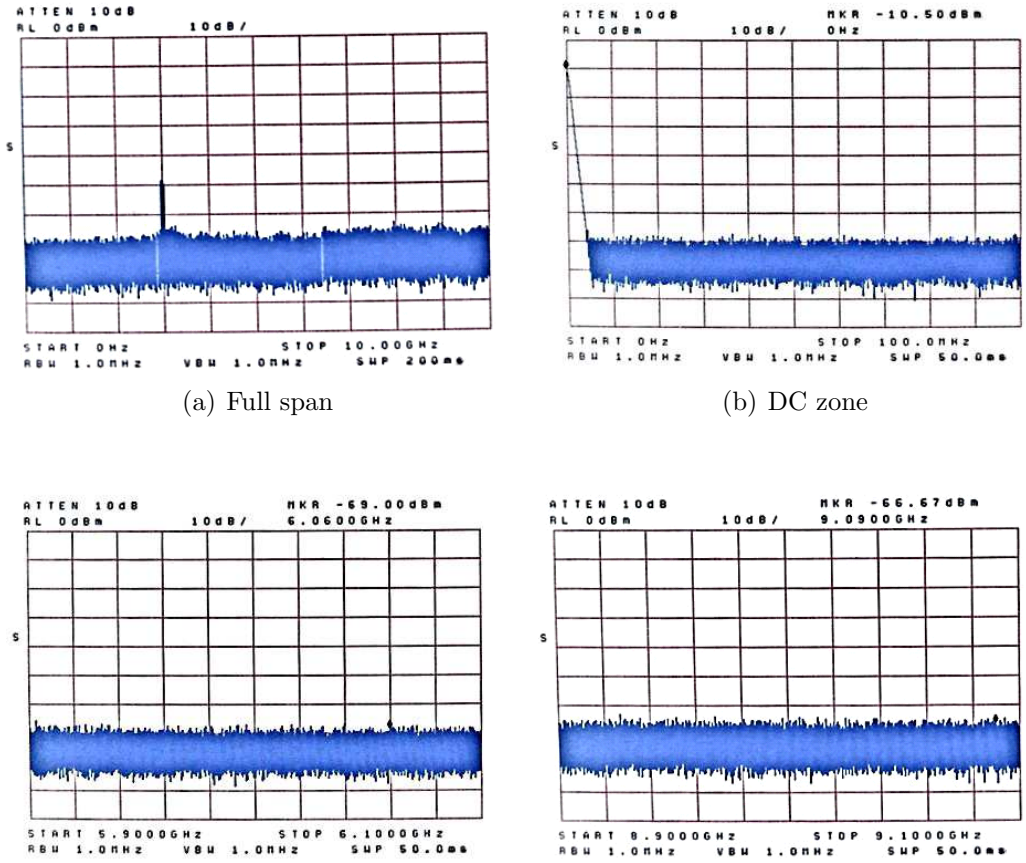

(a) Full span

(b) DC zone

(c) Second harmonic zone

(d) Third harmonic zone

Figure D.13: Measurements of the generated two-tone signal obtained with a spectrum analyzer. The two-tone signal has a center frequency of 3 GHz, tone separation of 60 MHz and it is tested at a high input power level equal to the 1 dB CP of the DUT (0 dBm).

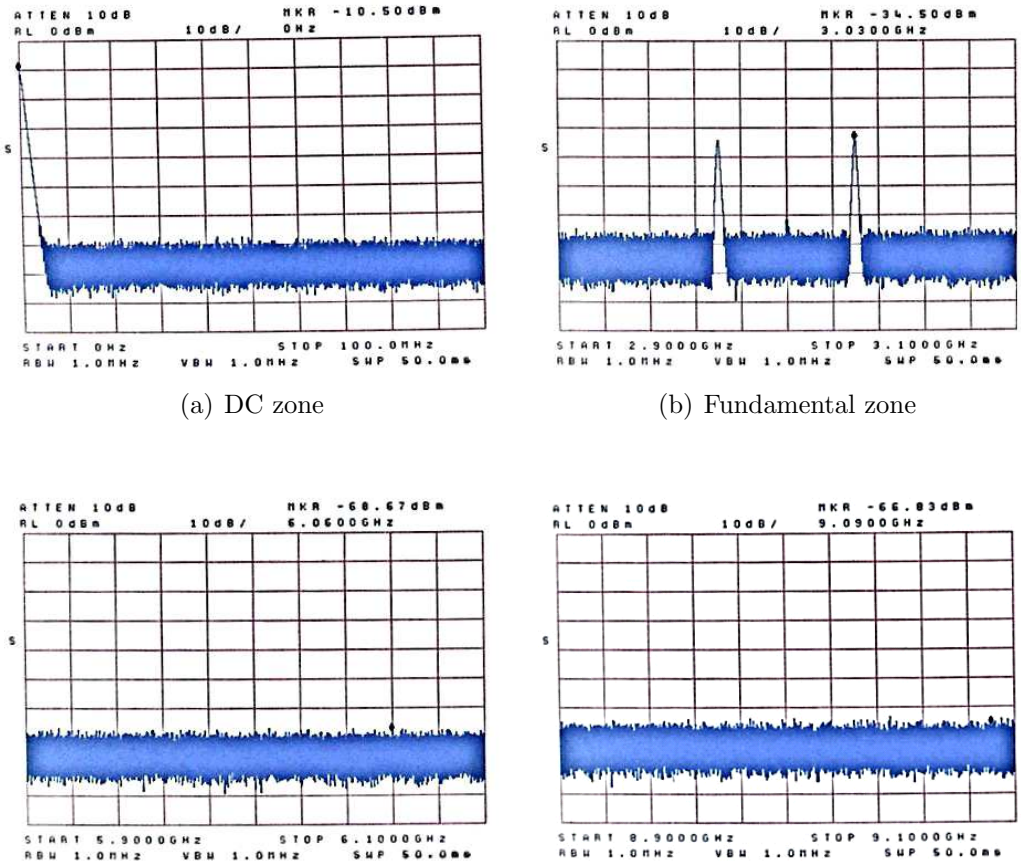

(a) DC zone

(b) Fundamental zone

(c) Second harmonic zone

(d) Third harmonic zone

Figure D.14: Results of ZVE-8G amplifier two-tone signal measurements using a spectrum analyzer. The two-tone input signal has a center frequency of 3 GHz, tone separation of 60 MHz and a low input power level equal to -20 dBm.

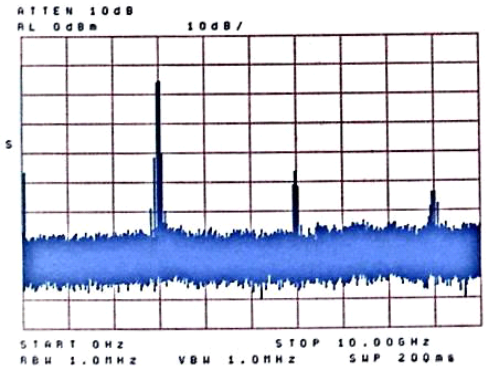

(a) Full span

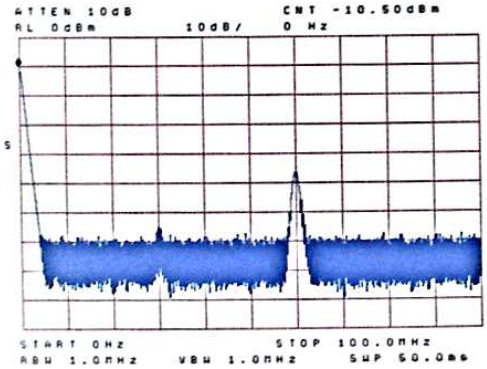

(b) DC zone

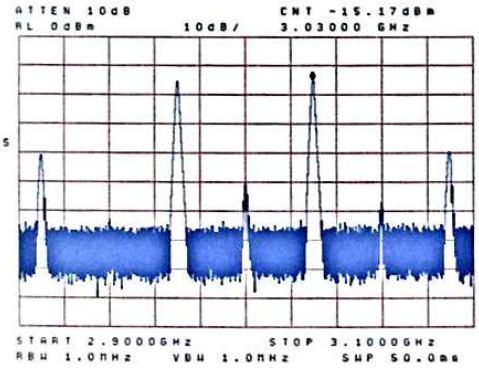

(c) Fundamental zone

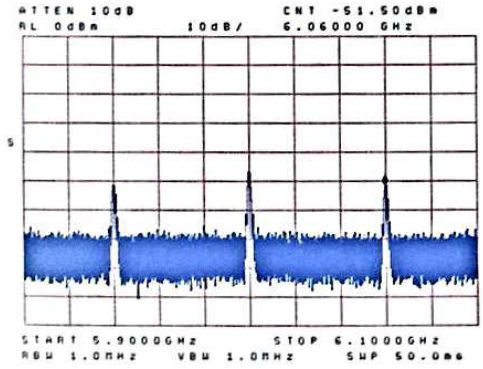

(d) Second harmonic zone

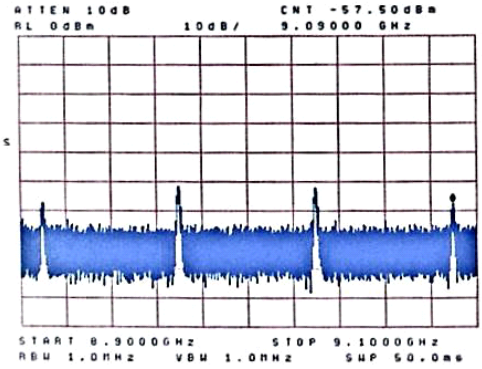

(e) Third harmonic zone

Figure D.15: Results of ZVE-8G amplifier two-tone signal measurements using a spectrum analyzer. The two-tone input signal has a center frequency of 3 GHz, tone separation of 60 MHz and an input power level equal to the DUT's 1 dB compression point input level (0 dBm).

D.3.2 Data obtained from spectrum analyzer

Table D.2: Data obtained from spectrum analyzer when performing two-tone signal measurements. This data contains the effect of the attenuators. Therefore, to find the final results the nominal attenuation should be added.

	Frequency (GHz)	Output level from SA (dBm)		
		Two-tone (1 dB CP input level)	With DUT (1 dB CP input level)	With DUT (very low input level)
DC zone				
DC component	0.00	-10,50	-10,50	-10,50
IMP2	0.06	-	-46,33	-
Fundamental zone				
Fundamental tone	3.03	-47,50	-15,17	-34,50
IMP3	3.09	-	-40,17	-
Second harmonic zone				
Second harmonic	6.06	-69,00	-51,50	-68,67
IMP2	6.00	-	-47,17	-
Third harmonic zone				
Third harmonic	9.09	-66,67	-57,50	-66,83
IMP3	9.03	-	-51,83	-

D.3.3 Plot of spectrum measurements

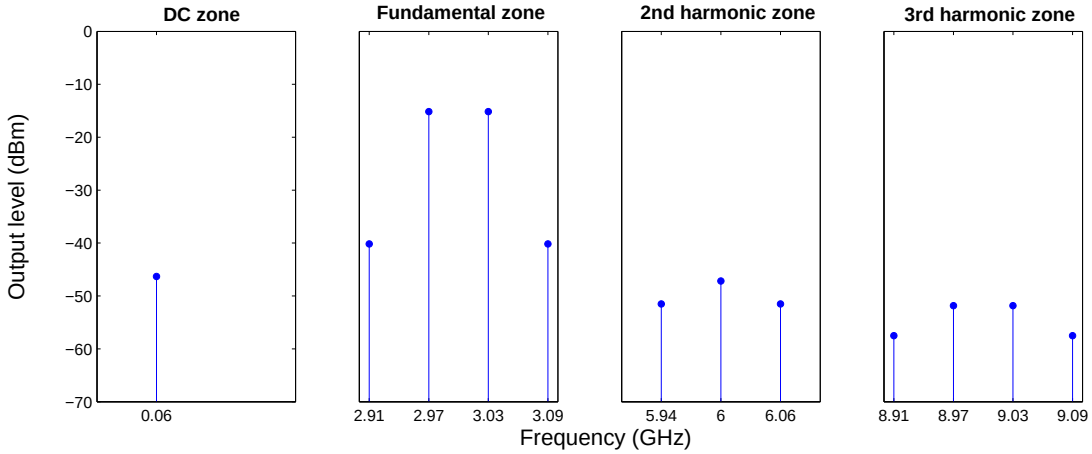

Figure D.16: Reconstructed spectrum of nonlinear amplifier based on data obtained from spectrum analyzer when performing two-tone signal measurements. The input signal has 3 GHz center frequency, 60 MHz tone separation and 0 dBm input power level (1 dB CP at 3 GHz). The data used for this plot contains the effect of the attenuators. Therefore, to find the final results the nominal attenuation should be added.

D.4 Multi-tone signal measurements

D.4.1 Screens obtained from spectrum analyzer

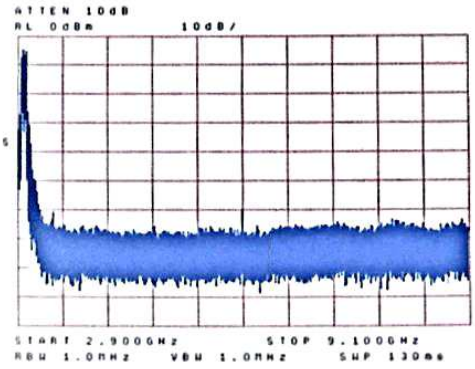

(a) Full span

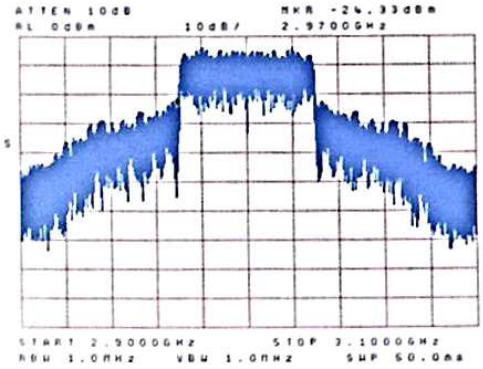

(b) Fundamental zone

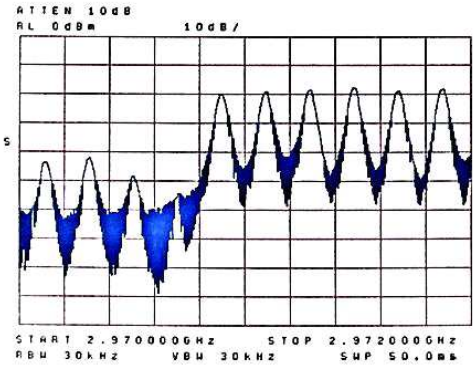

(c) Fundamental zone (zoom)

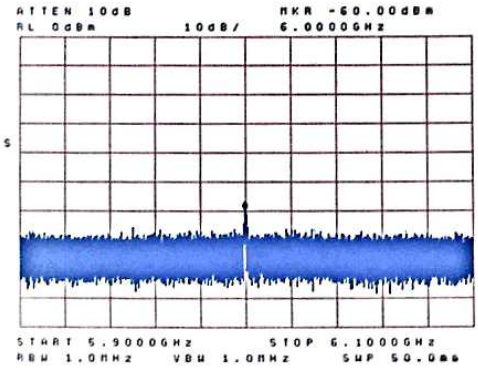

(d) Second harmonic zone

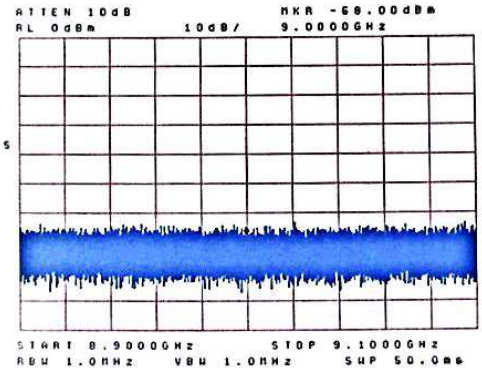

(e) Third harmonic zone

Figure D.17: Measurements of the generated multisine signal obtained with a spectrum analyzer. The multisine signal has a center frequency of 3 GHz, bandwidth of 60 MHz and it is tested at a high input power level equal to the 1 dB CP of the DUT (0 dBm).

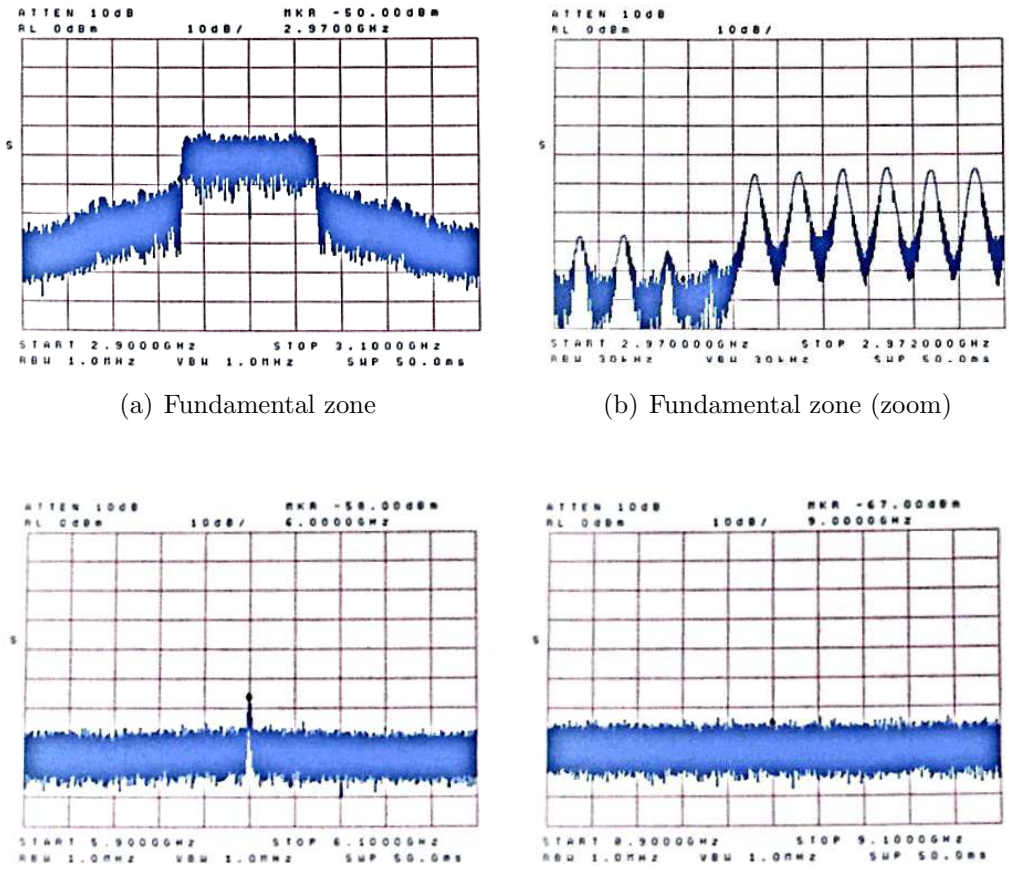

(a) Fundamental zone

(b) Fundamental zone (zoom)

(c) Second harmonic zone

(d) Third harmonic zone

Figure D.18: Results of ZVE-8G amplifier multi-tone signal measurements using a spectrum analyzer. The multisine input signal has a center frequency of 3 GHz, bandwidth of 60 MHz and a low input power level equal to -20 dBm.

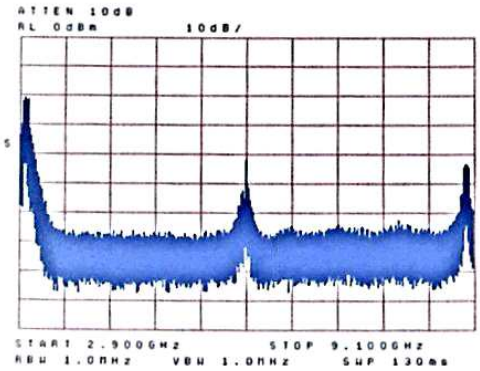

(a) Full span

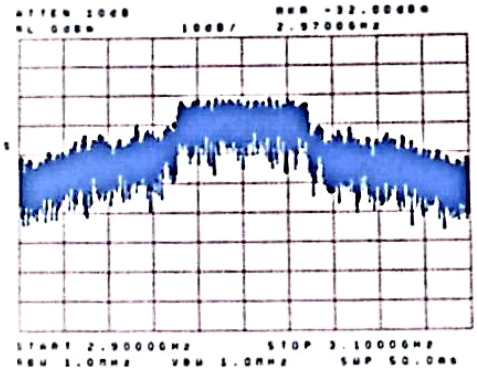

(b) Fundamental zone

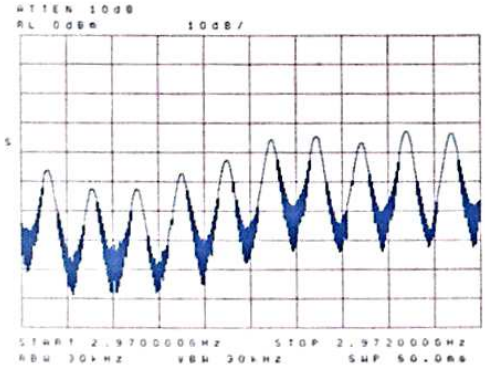

(c) Fundamental zone (zoom)

Figure D.19: Results of ZVE-8G amplifier multi-tone signal measurements using a spectrum analyzer. The multisine input signal has a center frequency of 3 GHz, bandwidth of 60 MHz and an input power level equal to the DUT's 1 dB compression point input level (0 dBm).

D.4.2 Data obtained from spectrum analyzer

Table D.3: Data obtained from spectrum analyzer when performing multi-tone signal measurements using the averaging function (average of 100 frequency-sweeps). The effect of the attenuators has been added to the results obtained. Therefore, this data does not contain the effect of the attenuators, which correspond to the final results.

	Frequency (GHz)	Output level from SA with averaging function (dBm)		
		Multi-tone (1 dB CP input level)	With DUT (1 dB CP input level)	With DUT (very low input level)
Fundamental zone				
Center Frequency	3.00	-14,17	10,00	-2,50
Offset Frequency	2.94	-42,50	-3,00	-28,00

Table D.4: Data obtained from spectrum analyzer when performing multi-tone signal measurements. The effect of the attenuators has been added to the results obtained. Therefore, this data does not contain the effect of the attenuators, which correspond to the final results.

	Frequency (GHz)	Output level (dBm)		
		Multi-tone (1 dB CP input level)	With DUT (1 dB CP input level)	With DUT (very low input level)
Fundamental zone				
Center Frequency	3.00	-7,00	17,50	6,00
Highest power (outside wanted band)	2.97	-24,33	8,00	-10,00
Second harmonic zone				
Center Frequency	6.00	-60,00	-2,17	-18,00
Third harmonic zone				
Center Frequency	9.00	-68,00	-5,50	-27,00